JOINT CONFERENCES ON ADVANCED MATERIALS

Functional and Nanostructured Materials
FNMA'11

Intermolecular and Magnetic Interactions in Matter
IMIM'11

8$^{\text{th}}$ International Workshop
on Auxetics and Related Systems
AUXETICS'11

6–9 September 2011, Szczecin, Poland

ABSTRACT BOOK

TITLE

Joint Conferences on Advanced Materials – Abstract Book:

Functional and Nanostructured Materials
FNMA'11

Intermolecular and Magnetic
Interactions in Matter
IMIM'11

8th International Workshop
on Auxetics and Related Systems
AUXETICS'11

EDITORS
Jarosław Rybicki and Krzysztof W. Wojciechowski

TECHNICAL EDITOR
Agnieszka Witkowska

TYPESETTING USING TeX
BOP s.c., www.bop.com.pl

Functional and Nanostructured Materials
FNMA'11

Intermolecular and Magnetic Interactions in Matter
IMIM'11

8th International Workshop on Auxetics and Related Systems
AUXETICS'11

ORGANISED BY

West Pomeranian University of Technology, Poland
Gdańsk University of Technology, Poland
Institute of Molecular Physics, Poznań, Poland
Poznań Supercomputing and Networking Centre, Poland
PWSZ im. St. Wojciechowskiego, Kalisz, Poland
Technical University of Lublin, Poland
University of Athens, Greece
University of Zielona Góra, Poland

IN COOPERATION WITH:

Koszalin University of Technology, Poland
Polish Physical Society

Honorary Chairmen

Sir Sam Edwards (Cambridge, England)
Joseph T. Devreese (Antwerp, Belgium)
George J. Papadopoulos (Athens, Greece)

Joint FNMA'11, IMIM'11 and AUXETICS'11 Scientific Committee

• A. Alderson (Bolton, UK) • K. Alderson (Bolton, UK) • R. Baughman (Richardson, USA) • J. Bernholc (Raleigh, USA) • S. V. Dmitriev (Ufa, Russia) • K. E. Evans (Exeter, UK) • M. Giersig (Berlin, Germany) • S. Glenis (Athens, Greece) • A. Griffin (Atlanta, USA) • J. N. Grima (Msida, Malta) • B. Grzybowski (Evanstone, USA) • N. Guskos (Athens, Greece) – Co-Chairman • W. G. Hoover (Ruby Valley, Nevada, USA) • Y. Ishibashi (Kyushu, Japan) • T. Kanaya (Kyoto, Japan) • A. A. Kornyshev (London, UK) • S. Kruchinin (Kiev, Ukraine) • R. S. Lakes (Wisconsin, USA) • V. Likodimos (Athens, Greece) • E. J. L. McInnes (Manchester, UK) • G. W. Milton (Salt Lake City, USA) • S. Mudry (Lviv, Ukraine) • H. Ohta (Kobe, Japan) • J. Olchowik (Lublin, Poland) – Co-Chairman • L. Ottaviano (L'Aquila, Italy) • V. Radmilovic (Berkeley, USA) • P. Razis (Nicosia, Cyprus) • R. Reisfeld (Jerusalem, Israel) • F. Scarpa (Bristol, UK) • C. W. Smith (Exeter, UK) • T. Tsuboi (Kyoto, Japan) • K. W. Wojciechowski (Poznań, Poland) – Co-Chairman • N. Zheludev (Southampton, UK) •

CONTENTS

LECTURES

ORAL COMMUNICATIONS

POSTERS

LECTURES

Design and modelling of mechanical and thermal responses of novel auxetic honeycomb cores for structural composites

A. Alderson[1], K. L. Alderson[1], N. Ravirala[2]

[1] *Institute for Materials Research and Innovation, University of Bolton*
Deane Road, Bolton BL3 5AB, UK

[2] *Saipem Ltd.*
Saipem House, Motspur Park, Surrey KT3 6JJ, UK

We have recently reported an extended range of auxetic (negative Poisson's ratio) cylinder-ligament honeycombs, including their in-plane and out-of-plane mechanical properties [1,2]. In this paper we will report modeling predictions of the thermal response of selected auxetic cylinder-ligament honeycombs, and also on the mechanical and thermal response of alternative 'arrowhead' auxetic honeycombs and hybrid cylinder-ligament-arrowhead honeycombs. Gradient systems (topology and properties) will also be presented.

References
[1] A. Alderson et al., *Comp. Sci. Tech.*, 70, 1042–1048 (2010)
[2] A. Lorato et al., *Comp. Sci. Tech.*, 70, 1057–1063 (2010)

The manufacture and characterisation of auxetic gradient materials

K. L. Alderson

The Institute for Materials Research and Innovation, The University of Bolton
Deane Road, Bolton BL3 5AB, UK

In order to exploit the property enhancements which arise as a result of auxetic behaviour, it is often desired that the materials produced display a combination of auxetic and conventional behaviour. This paper will report on the methods of producing such gradient structures in a range of auxetic materials. The characterisation of these materials will be discussed along with applications which require tailored Poisson's ratio and moduli.

Intraglobular structures in solutions of multiblock copolymers

M. Banaszak, K. Lewandowski

Faculty of Physics, Adam Mickiewicz University
Umultowska 85, 61-614 Poznań, Poland

Multiblock copolymer chains in implicit, nonselective solvents are studied by the Monte Carlo method, employing a parallel tempering algorithm. By varying both the reduced temperature and the compatibility between monomers, numerous intraglobular structures were obtained: diclusters (handshake, spiral, torus with core, etc.), triclusters, and n-clusters with $n > 3$ (lamellar and other), which are reminiscent of the block copolymer nanophases for spherically confined geometries. Phase diagrams were mapped for various chains. The structure factor was calculated for the selected microarchitectures. Self-assembly in those systems was interpreted in terms of competition between the minimization of the interfacial area separating different types of monomers and between the minimization of contacts between chain and solvent. The relevance of this model to protein folding is also discussed.

Multiscale simulations
of nanostructured materials and devices

J. Bernholc

North Carolina State University
Raleigh, NC 27695-7518
and Oak Ridge National Laboratories
Oak Ridge, TN 37831

Recent advances in multiscale methods and high performance computing allow for reliable first-principles predictions of complex nanostructured materials, device properties and even chemical and biological processes. This talk will discuss three topics: (i) novel energy storage mechanisms in ferroelectric polymers that enable ultrafast capacitors with very high power densities, (ii) molecular and nanoscale electronics, focusing on molecular-scale devices with negative differential resistance; and (iii) simulations of solvated biomolecules and of the role of transition metal atoms in biological processes and diseases.

Model cubic solids with auxetic behaviour

A. C. Brańka, K. W. Wojciechowski

Institute of Molecular Physics, Polish Academy of Sciences
Smoluchowskiego 17, 60-179 Poznań, Poland

In general, the Poisson's ratio (PR) depends both on the choice of the direction of the applied stretching and the transverse direction, and materials are classified as *nonauxetic*, *partially auxetic*, or *auxetic* to reflect different extents of auxetic response. Materials with negative Poisson's ratio in all directions ('auxetics') or materials possessing large PR values may have many potential applications, but they are rare in nature and their design and manufacture remains a non-trivial task.

Considerable progress in understanding auxetic behaviour has been made for materials with cubic symmetry. The aim of the presentation is to communicate recently obtained results on auxeticity for this important class of materials [1,2].

During the talk, the global maximum and global minimum Poisson's ratio surfaces, regions of different auxetic behaviour and the domains of the different extreme directions of cubic materials will be shown and discussed in terms of the elastic moduli ratios, $X = G/K$, $Y = G/W$, where K is the bulk modulus and G, W are the shear moduli. The crucial role of positive and negative pressure, P, in obtaining desired auxetic behaviour will be demonstrated.

A considerable problem in designing auxetic materials is a lack of sufficient knowledge on the connection between auxeticity and the form of the interaction between constituent objects or particles. As a step in this direction, we have investigated solids composed of spherically-symmetric particles from the point of view of their elastic properties and mechanical stability. Microscopic mechanisms which tune the cubic system to targeted different auxetic regions in the XY-plane were investigated with model solids of particles interacting via different pairwise potentials (the Lennard-Jones, the inverse-power and the tethered particle potentials). Examples of interactions and thermodynamic conditions which allow a negative Poisson's ratio to be achieved in any direction or lead to a large directional Poisson's ratio have been identified. The main results of these microscopic studies will be presented.

References
[1] A. C. Brańka, D. M. Heyes, K. W. Wojciechowski, *Auxeticity of Cubic materials*, Phys. Stat. Solidi B 246, 2063, 2009
[2] A. C. Brańka, D. M. Heyes, K. W. Wojciechowski, *Auxeticity of Cubic materials under Pressure*, Phys. Stat. Solidi B 248, 96, 2011

Inorganic crystalline nanowires with the growth and form of polymer molecules

L. Cademartiri

Department of Chemistry and Chemical Biology, Harvard University
Cambridge, Massachusetts

We are interested in determining if (and how) the topological properties of polymers can be conferred to crystals.

Much of the utility of polymer molecules comes from their unique topological properties (e.g. viscoelasticity, folding, reptation), which are a consequence of the mechanical properties of the backbone (e.g. low activation energy for rotation around single C-C bonds), and of its growth mechanism (polymerization).

We postulate that if crystals could be engineered to grow by a process kinetically similar to polymerization, they would start displaying some of the useful topological properties of polymers (e.g. globular conformation in solution), thus opening the way to a new class of inorganic materials.

The growth of both polymers and crystals proceeds via two general types of processes: (1) addition of molecules or atoms to a growing polymer or crystal facet; (2) coupling of two polymers or crystals to form a larger entity. Despite these similarities, the studies of the growth of crystals and of polymers have progressed independently of one another. Analogies between the growth of crystals and polymers have been postulated but not established.

We report on the growth kinetic of ultrathin (< 2 nm) Bi_2S_3 nanowires in solution. By combining light scattering measurements with absorption spectroscopy we are able to determine the following: (1) the length of the nanowires increases by 3 orders of magnitude in the first two hours of growth; (2) the number of nanowires decreases by 2 orders of magnitude during the same timeframe; (3) the thickness of the nanowires remains unchanged. These data are well described with a simple kinetic model that comprises only two mechanisms: an epitaxial growth (addition of monomer) and an attachment mechanism (end-to-end coupling). We determine the rate constants for both mechanisms and we compare this model to other competing models which include other mechanisms such as secondary nucleation, termination, fragmentation.

The morphology which results from this polymerization-like kinetic is analogous to that of semi-flexible polymers: it is well described as a worm-like chain characterized by a Kuhn length b of 35 nm (similar to that of double-stranded DNA) and contour length L of up to several hundred microns (longer than most synthetic polymers).

Dispersion characteristics and auxetic properties of strained graphene

S. V. Dmitriev

Institute for Metals Superplasticity Problems of RAS
Khalturins 39, 450001 Ufa, Russia

The dispersion characteristics of strained graphene were studied by molecular dynamics, using many-body interatomic potentials. We determined the following: (i) borders of the structural stability of flat graphene in three-dimensional space of the strain components ε_{xx}, ε_{yy}, ε_{xy}); (ii) elastic properties of strained graphene; (iii) sound velocities of strained graphene; (iv) phonon density of states (DOS) of strained graphene. The border of structural stability of flat graphene is also presented in the space of components of normal and shear membrane forces (T_x, T_y, T_{xy}). We find that flat graphene is structurally stable under elastic strain up to 0.3–0.4, but it becomes unstable to shear strain in the absence of tensile components of strain. Also, graphene cannot remain flat under compressive membrane forces because its bending stiffness vanishes. We employed molecular dynamics simulations to study the post-critical behavior of graphene. We demonstrate that ripples with controllable amplitude and orientation can be generated under simultaneous action of shear and tensile membrane forces. Gaps in the phonon DOS are observed when graphene is strained close to the appearance of ripples. Sound velocities of unstrained graphene do not depend on the propagation direction but application of strain makes graphene anisotropic. One of the sound velocities vanishes at the border of the structural stability of graphene meaning that vanishing of sound velocity (or corresponding elastic constant) predicts impending instability. In a wide region of strain space graphene possesses auxetic properties. A particularly interesting case is loading by negative hydrostatic pressure (tension) when graphene remains an isotropic elastic body, but, for sufficiently large pressure, it becomes auxetic, in line with theoretical prediction by Wojciechowski.

Influence of pH on the filling of porous sodium borosilicate glasses with magnetic nanoparticles of Ni/C and Fe_3O_4 dispersed in aqueous solution

M. R. Dudek[1], M. Kośmider[1], N. Guskos[2,3], B. V. Padlyak[1,4],
B. Zapotoczny[1], J. J. Kozioł[5], G. Żołnierkiewicz[3]

[1]*Institute of Physics, University of Zielona Góra*
Szafrana 4a, 65-069 Zielona Góra, Poland

[2]*Department of Solid State Physics, School of Physics*
Faculty of Sciences, University of Athens
Panepistimiopolis, 15 784 Zografos, Athens, Greece

[3]*Institute of Physics, West Pomeranian University of Technology*
Al. Piastów 48, 70-311 Szczecin, Poland

[4]*Institute of Physical Optics*
Dragomanov 23, 79-005, Lviv, Ukraine

[5]*Faculty of Biological Sciences, University of Zielona Góra*
Szafrana 1, 65-516 Zielona Góra, Poland

The insertion process of carbon-coated fcc nickel (Ni/C) nanoparticles and Fe_3O_4 nanoparticles into the pores of sodium borosilicate porous glass in aqueous solutions was investigated both theoretically and experimentally. The surface electrical charge that a magnetic nanoparticle acquired in aqueous solution was a function of pH. In this case, the pH value corresponding to the point of zero charge (PZC) becomes an important insertion parameter. As-synthesized porous glasses revealed weak super-paramagnetic properties due to the presence of ferromagnetic particles, which were adsorbed at the pores in the preparatory stage [1]. The glass also acquired charge in aqueous solution, which is one of the main obstacles to the introduction of Ni/C or Fe_3O_4 nanoparticles into the pores, from water solution. Therefore, apart from the chemical cleaning of the porous glass surface and placing the magnetic nanoparticle suspension in an ultrasonic generator, it is necessary to choose an aqueous solution with proper pH. X-band ferromagnetic resonance (FMR) spectroscopy and static magnetic susceptibility measurements of the nanoparticles embedded in the porous glass matrix were performed in order to determine the degree of filling of the pores with magnetic nanoparticles.

A theoretical model for the incorporation of magnetic nanoparticles into the porous glass was constructed. The model was based on the Langevin equation of motion for magnetic nanoparticles at a given pH value.

References

[1] N. Guskos, M. R. Dudek, B. V. Padlyak, G. Żołnierkiewicz, Yu. K. Gorelenko, E. Rysia-kiewicz-Pasek, I. Pelech, U. Narkiewicz, *Magnetic properties and FMR spectra of Ni/C nanoparticles in sodium borosilicate porous glasses* 2011 – submitted

Spin Hall effect in two-dimensional systems with Rashba spin-orbit interaction

A. Dyrdał[1], J. Barnaś[1,2], V. K. Dugaev[3]

[1] *Faculty of Physics, Adam Mickiewicz University*
Umultowska 85, 61-614 Poznań, Poland

[2] *Institute of Molecular Physics, Polish Academy of Sciences*
Smoluchowskiego 17, 60-179 Poznań, Poland

[3] *Department of Physics, Rzeszów University of Technology*
Powstańców Warszawy 6, 35-959 Rzeszów, Poland

An important feature of low dimensional systems, like two dimensional electron gas and graphene, is relatively long spin phase coherence length [1,2]. This makes such systems very promising materials for future applications in spintronics devices. However, one needs an effective method of spin current generation. One method of reaching this objective relies on spin injection from an external source of spin polarized carriers – e.g. from ferromagnetic contacts. However, the efficiency of this is rather low. Another option relies on the spin Hall effect due to spin-orbit interaction – either intrinsic or extrinsic [3–6]. A dominant spin-orbit interaction in two-dimensional systems is usually Rashba coupling. This coupling has an additional advantage over other spin-orbit interactions – its magnitude can be controlled and tuned by an external gate. Spin current generation in graphene and two dimensional electron gas via the spin Hall effect will be considered theoretically. Both intrinsic (topological) and extrinsic (due to impurities) contributions will be analyzed. Moreover, we will also consider the possibility of spin current generation due to some thermoelectric phenomena. Our theoretical considerations are based on the linear response theory (Kubo formalism) formulated in terms of the relevant Green functions.

Acknowledgements

References

[1] V. K. Dugaev, M. Inglot, E. Ya. Sherman, J. Barnaś, Phys. Rev. B 82, 121310 (2010)
[2] V. K. Dugaev, E. Ya. Sherman, J. Barnaś, Phys. Rev. B 83, 085306 (2011)
[3] C. L. Kane, E. J. Mele, Phys. Rev. Lett. 95, 226801 (2005)
[4] N. A. Synitsyn, J. E. Hill, H. Min, J. Sinova, A. H. MacDonald, Phys. Rev. Lett. 97, 106804 (2006)
[5] A. Dyrdał, V. Dugaev, J. Barnaś, Phys. Rev. B 80, 155444 (2009)
[6] A. Dyrdał, J. Barnaś, submitted

Carbon nanotubes and negative compressibility

R. Gatt[1], R. Cauchi[1], J. N. Grima[1,2]

[1] *Department of Chemistry, Faculty of Science, University of Malta*
Msida MSD 2080, Malta

[2] *Metamaterials Unit, Faculty of Science, University of Malta*
Msida MSD 2080, Malta

Carbon nanotubes received a lot of attention in the last two decades due to their exceptional mechanical, thermal and electrical properties [1]. For example, carbon nanotubes have very high Young's moduli (values higher than 1000 GPa have been measured [2]) and can also exhibit negative Poisson's ratios [3]. In this study we show through the use of molecular modelling that carbon nanotubes have also the potential of exhibiting negative linear compressibility, a property, which was found to be dependent on the type of carbon nanotube (armchair, zig-zag, and chiral) as well as on the diameter of the carbon nanotube. This anomalous linear negative compressibility behavior may be explained in terms of the large differences between the axial and radial Young's moduli of the carbon nanotubes as well as their Poisson's ratios. All this is very significant as it highlights another important property of carbon nanotubes, a property which increases the domain where carbon nanotubes may be employed, given the unique properties exhibited by negative compressibility materials [4].

References
[1] J. N. Coleman, U. Khan, W. J. Blau and Yu. K. Gun'ko, Small but strong: A review of the mechanical properties of carbon nanotube-polymer composites, *Carbon 44* (2006) 1624–1652
[2] E. W. Wong, P. E. Sheehan, C. M. Lieber, Nanobeam mechanics: elasticity, strength and toughness of nanorods and nanotubes, *Science* 277 (1997) 1971–5
[3] F. Scarpa, J. W. Narojczyk, K. W. Wojciechowski, Unusual deformation mechanisms in carbon nanotube heterojunctions (5,5)-(10,10) under tensile loading, *Physica Status Solidi (b)*, **248**, (2011) 82–87
[4] R. H. Baughman, S. Stafström, C. Cui, S. O. Pantas, Materials with negative compressibility in one or more directions, *Science* 279 (1998) 1522–1524

Recent developments in materials and structures exhibiting negative behaviour

J. N. Grima[1,2], R. Gatt[1], D. Attard[1], A. R. Casha[3], R. Cauchi[1],
Ch. Zerafa[1], R. Caruana-Gauci[1], B. Ellul[1], A. Buttigieg[1],
M. Camilleri[1], M. Zammit[1], E. Manicaro[1], E. Chetcuti[1]

[1]*Department of Chemistry, Faculty of Science, University of Malta*
Msida MSD2080, Malta

[2]*Metamaterials Unit, Faculty of Science, University of Malta*
Msida MSD2080, Malta

[3]*Mater Dei Hospital*
Msida MSD 2090, Malta

Recent developments made by the University of Malta group on materials and structures exhibiting anomalous thermo-mechanical behaviour including negative and/or zero Poisson's ratio, negative thermal expansion and/or negative compressibility are presented and discussed. These developments include the development of new and/or improved models for cellular structures such as auxetic foams and the development and/or discovery of systems and materials which exhibit negative compressibility.

From 'nanoions' to functional nanomaterials

B. A. Grzybowski

Department of Chemical and Biological Engineering and Department of Chemistry
Northwestern University

Nanoscopic objects stabilized with charged organics exhibit properties fundamentally different from either molecular or macromoleculer ions, and can combine ionic-like properties with electronic and ionic conductivity and/or photoexcitability. By careful control of electrostatic interactions, 'nanoions' of various shapes and material compositions can be assembled into functional nanomaterials including 3D supracrystals, 'layered' crystals, or extended films. Depending on the properties of the charged organics, these nanomaterials can act as chemical amplifiers, photoconductors and inverse photoconductors, or batteries. In my lecture I will discuss both the fundamental aspects of nanoscale electrostatics and electrodynamics, as well as the practical applications of 'nanoions' in chemical sensing and amplification, electronics, and energy storage.

References
[1] A. M. Kalsin, M. Fialkowski, M. Paszewski, S. K. Smoukov, K. J. M. Bishop, B. A. Grzybowski, Electrostatic self-assembly of binary nanoparticle crystals with a diamond lattice, *Science* 312, 420 (2006)
[2] H. Nakanishi, K. J. M. Bishop, B. Kowalczyk, E. A. Weiss, A. Nitzan, K. V. Tretiakov, M. M. Apodaca, R. Klajn, J. F. Stoddart, B. A. Grzybowski, Photoconductance and inverse photoconductance in films of functionalized metal nanoparticles, *Nature* 460, 371–375 (2009)

Temperature dependence of EPR spectra of modified nanocrystalline TiO_2 samples

N. Guskos[1,2], A. Guskos[2], P. Berczyński[2], J. Typek[2],
D. Dolat[3], B. Grzmil[3], A. Morawski[3]

[1] *Solid State Section, Department of Physics, University of Athens*
Panepistimiopolis, 15 784, Greece

[2] *Institute of Physics, West Pomeranian University of Technology*
Al. Piastów 48, 70-311 Szczecin, Poland

[3] *Institute of Chemical and Environmental Engineering*
West Pomeranian University of Technology
Al. Piastów 17, 70-310 Szczecin, Poland

Two samples of TiO_2, calcined at $500°C$, were prepared without and with water rinsing. Their magnetic resonance spectra were studied in the 4–300 K range and the presence of different magnetic centers was recorded. In the high temperatures range magnetic clusters of a correlated spin system were observed for a sample obtained without rinsing with water in contrast to a previously studied sample calcined at lower temperatures [1]. The EPR spectra of oxygen radicals and of titanium ions in a lower oxidation state were recorded in both samples (Figure 1). The sample subjected to water rising showed an increased concentration of trivalent titanium ions arising from the disappearance of a correlated spin system. Additionally, the relaxation processes in both samples were different. The photocatalytic properties under UV-VIS irradiation of the both studied samples showed an opposite effect than for samples calcined at lower temperatures [1].
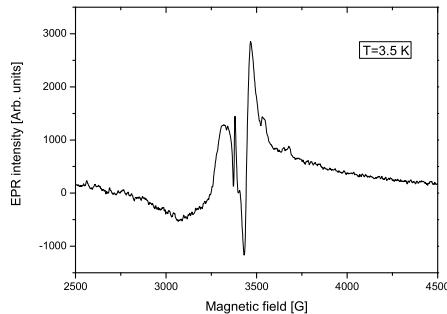
Figure 1: EPR spectrum of TiO_2 at 3.5 K

References

[1] N. Guskos, A. Guskos, P. Berczyński, J. Typek, D. Dolat, B. Grzmil, A. Morawski, submitted for publication in Materials Science and Engineering

Colloidal nanoparticles and nanostructures

M. Hilgendorff, M. Giersig

Freie University Berlin
Berlin, Germany

Nanostructured materials have attracted intense research interest in recent years since they provide the critical building blocks for nanoscience and nanotechnology and exhibit new and enhanced properties distinguishable from bulk material behaviour. In the nanoscale regime, physical parameters like ε_0, μ_0, ϱ, etc., normally defined as constants describing bulk material properties, become size dependent. In short, by tuning the size and shape of nanoscale materials new materials are produced.

For the design of novel nanostructured particles, which could be applicable for e.g. biomedical science, spintronics, or plasmonics, a technique is needed for preparing monodisperse particles, whose properties can be adjusted for desired applications by size- and shape-controlling synthesis parameters, doping, and/or surface-functionalization. Different methods have been investigated in the past to obtain small particles with desired properties. These approaches typically exploit either "top-down" design techniques, involving, for example, ball milling of bulk materials, or "bottom-up" design techniques, that rely on cluster or nanoparticle growth from precursors in gaseous or liquid phases. The latter methodology, also referred to as the wet chemical synthesis of inorganic colloidal particle fluids, is the most elegant from a chemist's point of view, and the focus of this presentation.

This Talk aims to present recent advances in the design of magnetic particles for applications in biomedicine and spintronics, i.e. streptavidin coated iron oxide nanoparticles (surface functionalization) and zinc oxide nanorods doped with cobalt and aluminum as diluted magnetic semiconductors (shape controlling, doping), respectively.

Furthermore, if time allows, plasmonic interactions between colloidal nanoparticles and nanostructured substrates, the latter prepared by use of submicron organic colloidal particles deposited as a lithographical mask on diverse substrates followed by metal evaporation and removal of the organic mask, will be presented.

Dislocation networks as active components in novel Si devices

M. Kittler

IHP
Im Technologiepark 25, 15236 Frankfurt (Oder), Germany

Joint Lab IHP/BTU Cottbus
PF 101344, 03013 Cottbus, Germany

Dislocations in Si form native nanowires exhibiting exciting properties regarding luminescence and carrier transport, for example [1,2,3]. It is shown that Si wafer direct bonding allows well-controlled formation of dislocation networks [4], giving rise to adjustable dislocation properties.

Ideas for novel Si devices utilizing dislocations as active components are presented. In particular, dislocation-based light emitters at about 1.55 μm wavelength are demonstrated, e.g. [5,6]. Moreover, concepts for Si-based thermo-electric generators using dislocations are sketched [7].

References

[1] M. Kittler, X. Yu, T. Mchedlidze, T. Arguirov, O. F. Vyvenko, W. Seifert, M. Reiche et al., *Small* 3, 964 (2007)
[2] M. Kittler, M. Reiche, *Adv. Eng. Mater.* **11**, 249 (2009)
[3] M. Reiche, M. Kittler, D. Buca, A. Hähnel, Q. T. Zhao, S. Mantl, U. Gösele, *Jpn. J. Appl. Phys.* **49**, 04DJ02-1 (2010)
[4] M. Reiche, *Mat. Sci. Forum 590*, 57 (2008)
[5] M. Kittler, M. Reiche, X. Yu, T. Arguirov, O. F. Vyvenko, W. Seifert et al., *International Electron Devices Meeting* San Francisco, USA, Dec. 2006, *IEDM Tech. Digest*, pp. 845–848 (2006)
[6] M. Kittler, T. Arguirov, T. Mchedlidze, M. Reiche, W. Seifert, M. Trushin, in, Proceedings *5th Int. Symp. on Advanced Science and Technology of Silicon Materials*, Kona, Hawaii, November 2008, pp. 55–59 (2008)
[7] M. Kittler, M. Reiche, Patent: *Thermoel. Semicond. Device*, WO 2010/084059 A2

Investigation on the use of thermal expansion mismatch to produce engineered negative stiffness metamaterial inclusions

T. Klatt[1,2], D. Shahan[1], M. R. Haberman[1,2], C. C. Seepersad[1], P. S. Wilson[1,2]

[1] *Department of Mechanical Engineering, The University of Texas of Austin*
P.O.Box 8029, Austin, Texas 78713-8029, USA

[2] *Applied Research Laboratories, The University of Texas of Austin*
P.O.Box 8029, Austin, Texas 78713-8029, USA

Theory and recent experimental data show that bistable mechanisms can be constrained to make useof their inherent negative stiffness behavior [1]. It is also known that embedding negative stiffness inclusions in a viscoelastic matrix results in overall stiffness and loss properties of the composite that exceed values attainable by combining conventional (positive stiffness) materials [2,3]. The ability to engineer microscale inclusions displaying negative stiffness is therefore of significant interest for the control of vibroacoustic energy. This work presents the results of analytical and finite element (FE) studies on several candidate constrained bistable structures that rely on thermal expansion mismatches to produce negative stiffness behavior. It considers the effect of inclusion structure, composition, orientation, and volume fraction on the overall material response using a hierarchical materials design process. First, the mechanical behavior of simple bistable structures is analyzed using analytical models to benchmark FE simulations. FE simulations are then employed to characterize the effective stiffness properties of inclusions with more complex microstructures that can be produced using specialized fabrication techniques. Finally, both strain energy FE homogenization and analytical effective medium models are employed to predict the overall response of composites containing low volume fractions of constrained negative stiffness elements. The overall viscoelastic response is compared with established complex bounds and a sensitivity analysis of inclusion parameters on the overall mechanical behavior is performed and discussed.

References
[1] L. B. Kashdan, M. R. Haberman, P. S. Wilson, C. C. Seepersad, *Constrained negative stiffness metamaterials*, Presented at the Joint 160th Meeting of the Acoustical Society of America, 7th IberoAmerican Congress on Acoustics, 17th Mexican Congress on Acoustics, Cancun, Mexico (15–19 November, 2010)
[2] R. S. Lakes, T. Lee, A. Bersie, Y. C. Wang, *Extreme damping in composite materials with negative-stiffness inclusions*, Nature, 410: 565–567 (2001)
[3] T. Jaglinski, D. Kochmann, D. S. Stone, R. S. Lakes, *Materials with viscoelastic stiffness greater than diamond*, Science, 315: 620–622 (2007)

Dynamics of nanocars and molecular rotors on surfaces: what are fundamental mechanisms?

A. Kolomeisky

Rice University
6100 Main Street, 77005-1892 Houston, United States of America

Artificial molecular motors, known as nanocars, and molecular rotors have attracted attention as potential candidates to develop new devices and materials with tailored and controlled properties. However, fundamental mechanisms of motion of these molecules at the single-molecule level are still not well understood. Experimental studies on these nanoscale objects suggest complex dynamics that depend on many factors.

We have developed a theoretical approach that combines molecular dynamics simulations and simple phenomenological models to investigate what factors control mechanisms of nanocars and molecular rotors bound to metallic surfaces. Our analysis suggests that rotational and translational dynamics is determined by the size of the molecules, by the symmetry of the surfaces and the molecules, and by interactions with the surfaces. Our theoretical predictions not only allow us to explain current experimental observations, but also suggest specific experimental tests on mechanisms and dynamics.

Physics of nano-porous supercapacitors with ionic liquids: from understanding to nano-engineering

S. Kondrat[1], A. A. Kornyshev[1], M. V. Fedorov[2], Y. Gogotsi[3]

[1] *Department of Chemistry, Faculty of Natural Sciences, Imperial College London*
SW7 2AZ, UK

[2] *Max-Planck-Institut für Mathematik in den Naturwissenschaften*
D-04103 Leipzig, Germany

[3] *A. J. Drexel Nanotechnology Institute, Drexel University*
Philadelphia, PA, USA

Room-temperature ionic liquids (RTILs), owing to their unique properties, have recently attracted much attention in various fields and found numerous industrial applications, ranging from lubricants to energy storage devices. RTILs have a wide electrochemical window and are almost non-volatile, which makes them a promising "green" alternative to conventional electrolytes.

On the other hand, recent advances in the fabrication of porous carbon-based materials have stimulated the development of electric double-layer capacitors (EDLCs, or supercapacitors) with *nano-* and *subnano*-porous carbon electrodes. Being porous, these supercapacitors make use of the high surface-to-volume ratio, and thus increase the stored energy-density significantly.

The utilization of the RTILs in nano-porous EDLCs seems to be an important breakthrough in the sustainable energy-storage technology. In this lecture we present a brief and concise overview of recent developments in this research area. Particular emphasis will be given to the underlying physical phenomena, while current and potential applications will also be discussed, and certain open questions will be pointed out.

Behavior of a dipole glass parameter in ferro-antiferroelectric solid mixtures

N. A. Korynevskii[1,2,3], V. B. Solovyan[1]

[1]*Institute for Condensed Matter Physics, National Academy of Sciences of Ukraine*
1 Svientsitskii Str., 79011 Lviv, Ukraine

[2]*Institute of Physics, University of Szczecin*
Wielkopolska 15, 70-451 Szczecin, Poland

[3]*Lviv Polytechnic National University*
S. Bandera 12, 79013 Lviv, Ukraine

We propose a new definition of a dipole glass parameter for ferro-antiferroelectric solid mixtures, which is constructed on the basis of the nearest-neighbor pair correlation functions of the interacting dipole moments. Our theoretical approach takes into account the competition between the ferroelectric and antiferroelectric coupling, and microscopically calculates the correlation functions.

It was shown that in the investigated system, at low temperatures and for intermediate concentrations, due to the frustration of the system, the long-range ordering disappeared and only the short-range correlations between the neighboring dipole particles were present. These correlations were characterized by a non-stochastic distribution. The dipole-glass phase appeared. The behavior of the dipole glass parameter and the physical properties of solid mixtures are calculated and discussed.

References
[1] S. F. Edwards, P. W. Anderson, *J. Phys. E* 5, 965 (1975)
[2] Z. Trybula, J. Kaszynski, H. Maluszynska, *Ferroelectrics* 316, 125 (2005)
[3] N. A. Korynevskii, V. B. Solovyan, *Rev. Adv. Mater. Sci.* 12, 90 (2006)
[4] N. A. Korynevskii, V. B. Solovyan, *Phase Transitions* 80, 55 (2007)
[5] N. A. Korynevskii, V. B. Solovyan, *Phisica B* 405, 2232 (2010)

Thermoelectricity in single molecular junctions

S. P. Kruchinin, V. N. Ermakov

Bogolyubov Institute for Theoretical Physics, NASU
Kiev 03143, Ukraine

The study of charge transport in molecules is of fundamental interest owing to the potential applications in molecular electronics. Scanning Tunnelling Microsopy (STM) was employed to study the thermoelectric phenomena in molecular nanosystems [1]. The concept of resonant tunneling has been used to elucidate the thermoelectrical phenomenon in molecular junctions [2].

References
[1] P. Reddy, S. Jang, R. Segelmen, A. Mayundar, Science, 315, 1568 (2007)
[2] V. N. Ermakov, S. P. Kruchinin, H. Hori, A. Fujiwara, Int. J. Mod. Phys. B, 21 1827 (2007)

Nonlinear coupler systems as *nonlinear quantum scissors* and beyond

W. Leoński[1], A. Kowalewska-Kudłaszyk[2], J. Peřina Jr.[3]

[1] *Quantum Optics and Engineering Division*
Institute of Physics, University of Zielona Góra
Prof. A. Szafrana 4a, 65-516 Zielona Góra, Poland

[2] *Department of Physics, Adam Mickiewicz University*
Umultowska 85, 61-614 Poznań, Poland

[3] *Institute of Physics of AS CR, Joint Laboratory of Optics*
17. listopadu 50a, 772 07 Olomouc, Czech Republic

Quantum nonlinear oscillators are very often used as the basis for nanoscience models. Some of them are very promising from the point of view of quantum-state engineering. Such states can be used in investigations concerning systems in quantum information theory. In particular, it has been shown that a nanoresonator with a moving mirror can be a source of various quantum electromagnetic field states [1]. As it was discussed in [2], such systems act as quantum nonlinear oscillators. Moreover, quite recently, nanoresonators and carbon nanotubes have been discussed in that context [3,4].

In this communication, we shall present systems involving two quantum nonlinear oscillators. The oscillators are coupled by linear or nonlinear processes, forming a nonlinear coupler system. In addition, the oscillators can be excited by an external electromagnetic field. Assuming that the external excitation is sufficiently weak, as compared with the nonlinearity parameters, the system behaves as *nonlinear quantum scissors* [5,6]. In consequence, despite the presence of external excitation, the evolution of the system, in fact, remains closed within the finite set of Fock states.

We show that if the nonlinear coupler system satisfies certain conditions, entangled states can be generated. In particular, we can produce Bell states that are *maximally entangled states* (MES). These states are commonly used in the investigations of quantum information theory. Moreover, nonlinear couplers discussed here can be treated as generators of *generalized Bell states* (GBS). Including certain damping processes in our models, we can observe entanglement decay. Interestingly, the vanishing effects of such entangled states can be observed in finite time. In such case, we deal with the phenomenon of *sudden death of entanglement* (SDE) [7,8]. Additionally, if entanglement reappears in the system, the effect of *sudden birth of entanglement* (SBE) [9,10] takes place.

References

[1] B. Jacobs 2007 *Phys. Rev. Lett.* **99** (11) 117203
[2] J. Bose, K. Jacobs, P. L. Knight 1997 *Phys. Rev. A* **56** (5) 4175

[3] I. Wilson-Rae, C. Galland, W. Zwerger, A. Imamoglu 2009 *arXiv:0911.133v1* [cond-mat. mes-hall]

[4] Jin-Jin Li, Wei He, Ka-Di Zhu 2011 *Phys. Rev. B* **83** (11) 115445

[5] A. Miranowicz, W. Leoński 2004 *J. Opt B* **6** (3) S43; *J. Phys B: At. Mol. Opt. Phys.* **39** (7) 1683

[6] A. Kowalewska-Kudłaszyk, W. Leoński 2006 *Phys. Rev. A* **73** (4) 042318

[7] K. Życzkowski, P. Horodecki, M. Horodecki, R. Horodecki 2001 *Phys. Rev. A* **65** (1) 012101

[8] T. Yu, J. H. Eberly 2004 *Phys. Rev. Lett.* **93** (14) 140404

[9] Z. Ficek, R. Tanaś 2006 *Phys. Rev. A* **74** (2) 024304

[10] A. Kowalewska-Kudłaszyk, W. Leoński 2009 *J. Opt. Soc. Am. B* **26** (7) 1289

Mixed auxeticity of auxetic sandwich structures

T.-Ch. Lim

School of Science & Technology, SIM University
461 Clementi Road, S 599491, Singapore

A sandwich structure in which the Poisson's ratios of the core and facesheets have opposite signs has been shown to exhibit overall conventional or auxetic behavior depending on the loading mode – axial loading or bending – for an intermediate range of relative core thicknesses [1]. In addition to these two loading modes, sandwich structures used in aerospace applications are subject to torsional loading. In this presentation, an effective Poisson's ratio for torsional loading is proposed. Results show that, depending on the loading mode and the relative core thickness, there can be up to four levels of auxeticity, namely (a) full auxeticity (FA), if the structure behaves as an auxetic under all three modes of loading; (b) high auxeticity (HA), if the structure behaves as an auxetic in two of the loading modes; (c) low auxeticity (LA), if the structure behaves as an auxetic structure in only one of the loading modes; and (d) no auxeticity (NA), if the structure behaves conventionally under all three modes of loading. These results suggest that by properly selecting the Poisson's ratios and the thickness of the cores and facesheets, the sandwich structure can be tuned to respond differently under different external loading conditions.

References
[1] T. C. Lim, Physica Status Solidi B **244**, 910–918 (2007)

Recent developments of multi-extreme terahertz EMR in Kobe

H. Ohta[1,2], S. Okubo[1], E. Ohmichi[1], T. Sakurai[3]

[1]*Molecular Photoscience Research Center, Kobe University*
1-1 Rokkodai-cho, Nada, Kobe 657-8501, Japan

[2]*Graduate School of Science, Kobe University*
1-1 Rokkodai-cho, Nada, Kobe 657-8501, Japan

[3]*Center for Supports to Research and Education Activities, Kobe University*
1-1 Rokkodai-cho, Nada, Kobe 657-8501, Japan

Recent developments of multi-extreme terahertz EMR in Kobe will be presented. Our system covers the frequency region between 0.03 and 7 THz and the temperature region between 1.8 and 300 K [1]. Moreover, our system can combine multi-extreme conditions such as a pulsed magnetic field up to 55 T [2] and high pressure up to 1.4 GPa [3]. We are also developing a highly-sensitive micro-cantilever EMR system using a torque method, which enables the EMR measurement of a μm size single crystal [4]. Some examples of terahertz EMR measurements, such as the multiferroic material CuO, will be presented.

References
[1] H. Ohta, S. Okubo, K. Kawakami, D. Fukuoka, Y. Inagaki, T. Kunimoto, Z. Hiroi, J. Phys. Soc. Jpn. 72 (2003) Supplement B 26-35; H. Ohta, M. Tomoo, S. Okubo, T. Sakurai, M. Fujisawa, T. Tomita, M. Kimata, T. Yamamoto, M. Kawauchi, K. Kindo: J. Phys.: Conf. Series 51 (2006) 611–614

[2] H. Ohta, S. Okubo, N. Souda, M. Tomoo, T. Sakurai, T. Yoshida, E. Ohmichi, M. Fujisawa, H. Tanaka, R. Kato, Appl. Magn. Reson. 35 (2009) 399–410

[3] T. Sakurai, A. Taketani, T. Tomita, S. Okubo, H. Ohta, Y. Uwatoko, Rev. Sci. Inst. 78 (2007) 065107/1–6; T. Sakurai, T. Horie, M. Tomoo, K. Kondo, N. Matsumi, S. Okubo, H. Ohta, Y. Uwatoko, K. Kudo, Y. Koike, H. Tanaka, J. Phys.: Conf. Series 215 (2010) 012184/1–4

[4] H. Ohta, M. Kimata, S. Okubo, E. Ohmichi, T. Osada, AIP Conference Proceedings 850 (2006) 1643–1644; E. Ohmichi, N. Mizuno, M. Kimata, H. Ohta, Rev. Sci. Instrum. 79 (2008) 103903/1–5; E. Ohmichi, N. Mizuno, M. Kimata, H. Ohta, T. Osada, Rev. Sci. Instrum. 80 (2009) 013904/1–5; H. Ohta, E. Ohmichi, Appl. Magn. Reson. 37 (1–4) (2010) 881–891; E. Ohmichi, N. Mizuno, S. Hirano, H. Ohta, J. Low Temp. Phys. 159 (2010) 276–279

Toward molecular-level organic auxetic polymers

W. Ren[1], C. J. Booth[2], P. Liu[2], <u>A. C. Griffin</u>[1]

[1] *School of Materials Science & Engineering, Georgia Institute of Technology Atlanta, GA 30332 USA*

[2] *work done at Department of Chemistry, University of Southern Mississippi Hattiesburg, MS 39406 USA*

As part of an ongoing program aimed at creating molecular-level organic auxetic materials, we have synthesized and examined two series of main-chain liquid crystalline linear polymers and elastomers. The key structural feature is the presence of a laterally-attached rod that, upon tensioning the polymer main chain, would rotate into a position approximately perpendicular to the stretching direction leading to lateral expansion. This site-connectivity driven rod reorientation mechanism is examined in a series of experiments: X-ray diffraction, stress/strain measurement, and strain retention measurement.

The rationale for choice of the rod chemistry, the site of attachment to the polymer main chain, and the synthetic details for construction of the macromolecular structure will be presented.

One set of polymers is a family of nematic polyesters having terphenyl or pentaphenyl as the transverse rod. The thermal and X-ray data for these materials reveals the parallel orientation of these rods to the nematic director in the quiescent nematic phase – a desirable feature of using liquid crystalline systems as potential auxetics.

Our results for the other set, siloxane-containing main chain liquid crystalline polymers and elastomers, indicate that even at 50% transverse rod incorporation, a mesophase – likely smectic – still persists. We have also found that the shorter, stiffer trisiloxane spacer group produces a higher Sc-I temperature compared to a more flexible octasiloxane unit. Copolymers of variable ratios of these spacers have Sc-I temperatures which track with composition of the end members of the series. X-ray results confirm likely smectic organization in the polymers examined here with fiber samples having SAXS intensity distributions showing molecular level orientation.

Stress/strain data including measurement of strain retention (shape memory) will be presented and interpreted in light of the orientation of the laterally-attached rod as the specimen is under tension.

Acknowledgements

Morphology and swelling dynamics of polyelectrolyte thin films: correlation with added salt concentration

T. Samanta, <u>M. Mukherjee</u>

Surface Physics Division, Saha Institute of Nuclear Physics
1/AF Bidhannagar, Kolkata 700064, India

Solution state morphology of a polyelectrolyte solution and its time evolution with and without added low-molecular-weight salt were examined using dynamic light scattering (DLS). Correlation functions obtained from a DLS study of the solutions (concentration range ~ 3–30 mg/mL) without added salt were found to vary with time, indicating time-dependent aggregation within the solution. The agglomeration time of the solution was strongly dependent on the solution concentration and decreased with a decrease in solution concentrations.

The presence of the ions of low-molecular-weight salt (NaCl, 10^{-4}–1 mol/L) in the solution led to different agglomeration behavior, possibly due to different screening of the electrostatic interaction between the polyelectrolyte chains. Agglomeration was hindered when the concentration of externally added salt ions was higher than the amount of counterions present in the solution. Higher concentration of polyelectrolyte in the solution did not favor the formation of agglomerations.

The effect of the solution morphology of polyelectrolyte chains on the morphology of the thin film surface was studied by preparing ultrathin films from different stages of solutions (below and above the agglomeration time). The surface morphology of the films showed a dependence on the salt concentration, as evidenced by tapping-mode AFM study.

Ultrathin films of pure poly (sodium 4-styrenesulfonate) (NaPSS) were prepared by the spin-coating method, and the swelling dynamics of the films were studied by X-ray reflectivity. The diffusion coefficient of the NaPSS chains was found to be orders of magnitude lower than that of a neutral polymer. The fraction of charged monomer, which determines the strength of the repulsive interaction between polymer segments, showed the confinement effect.

Swelling dynamics of the films are likely to be modified with a change in the concentration of added salt.

Carbon nanocones:
models and mechanical properties

F. Scarpa[1], J. W. Narojczyk[2], K. W. Wojciechowski[2]

[1] *Bristol Centre for Nanoscience and Quantum Information (NSQI)*
University of Bristol
BS8 1UJ Bristol, UK

[2] *Institute of Molecular Physics, Polish Academy of Sciences*
Smoluchowskiego 17, 60-179 Poznań, Poland

In this work we describe the mechanical properties of carbon nanocones subjected to tip compressive loading. The nanocones are modelled using a hybrid atomistic-continuum Finite Element approach, where the C-C Sp^2 bonds are represented by structural beam elements having equivalent mechanical properties obtained by the minimisation of the energy equivalence between the stechiometric harmonic potential (AMBER) and the strain energies associated to deep shear bending (Timoshenko) beams . We highlight the dependence of the compressive Young's modulus and equivalent Poisson's ratio of the nanocones versus the length and azimutal angle of the nanostructures. Semi-empirical relations are derived to related the mechanical properties the geometry of the nanocones.

a)   b)
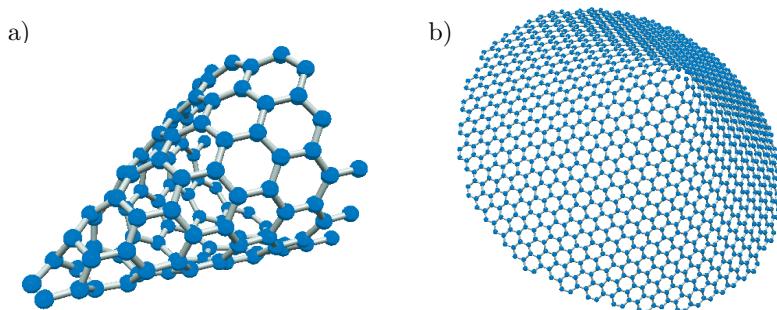
Figure 1: (a) Nanocone with length 15 Å, disclination angle $240°$ (b) Nanocone having length 30 Å, disclination angle $120°$

References
[1] F. Scarpa, S. Adhikari, A. S. Phani, Nanotechnology 20, 065709 (2009)
[2] F. Scarpa, L. Boldrin, H. X. Peng, C. D. L. Remillat, S. Adhikari, Applied Physics Letters 97, 151903 (3 pp) (2010)
[3] F. Scarpa, J. W. Narojczyk, K. W. Wojciechowski, Phys. Stat. Solidi (b) 248, 82 (2011)

Numerical study of negative refraction and focusing of ultrasonic lamb waves by a thickness change in an isotropic plate

F. Schubert, J. Schreiber

Fraunhofer-Institute for Non-Destructive Testing, Dresden Branch (IZFP-D)
Maria-Reiche-Strasse 2, 01109 Dresden, Germany

Recently, a Veselago lens for elastic Lamb waves, exhibiting negative refraction and focusing in a free plate with a step change in thickness has been demonstrated experimentally for the first time (S. Bramhavar et al., Physical Review B 83, 014106, 2011). In the present paper, this extraordinary result in a very simple mechanical system is numerically investigated in detail using the 3D Elastodynamic Finite Integration Technique (EFIT). We study the refraction of Lamb waves at a plane interface consisting of an abrupt thickness change between two different plate regions. While one of the regions supports a backward-propagating (negative group velocity) mode, the other plate region supports a forward-propagating (positive group velocity) mode at exactly the same frequency and wave number. We demonstrate negative refraction and focusing by means of time-resolved wavefront snapshots, paying particular attention to the wave pattern in the immediate vicinity of the interface. Additionally, we investigate the influence of different geometrical transitions between the thin and the thick part of the plate. Our results confirm that guided ultrasonic waves provide a powerful test bed for negative-index physics and offer interesting new possibilities for imaging applications in nondestructive evaluation.

Mathematically determined auxetic cellular structures fabricated by selective electron beam melting

J. Schwerdtfeger[1], F. Schury[2], M. Stingl[2], R. F. Singer[3], C. Körner[3]

[1] *Institute of Advanced Materials and Processes (ZMP), University of Erlangen-Nuremberg*
Dr.-Mack-Str. 81, 90762 Fürth, Germany

[2] *Institute of Applied Mathematics 2 (AM2), University of Erlangen-Nuremberg*
Martensstr. 3, 91052 Erlangen, Germany

[3] *Institute of Material Science and Technology of Metals (WTM)*
University of Erlangen-Nuremberg
Martensstr. 5, 91058 Erlangen, Germany

In additive manufacturing, structures are built up layer by layer, enabling complete control over material distribution in each layer. The approach allows a large degree of freedom in terms of the design of structures. In the context of designed cellular structures, this translates into a high degree of control over the mesoscopic geometry and, consequently, over their physical properties (e.g. mechanical). This allows, for example, to impart the auxetic behaviour into cellular structures [1]. In this work, we combine the imaging capabilities of rapid prototyping with mathematical optimization procedures, used in order to determine new auxetic structures. Topological optimization allows us to identify unit cells with properties matching a prescribed compliance tensor. However, the resulting unit cells are often too complex for traditional manufacturing routes, whereas additive manufacturing has the potential for producing even. Here, we present examples of such topologically optimised auxetic
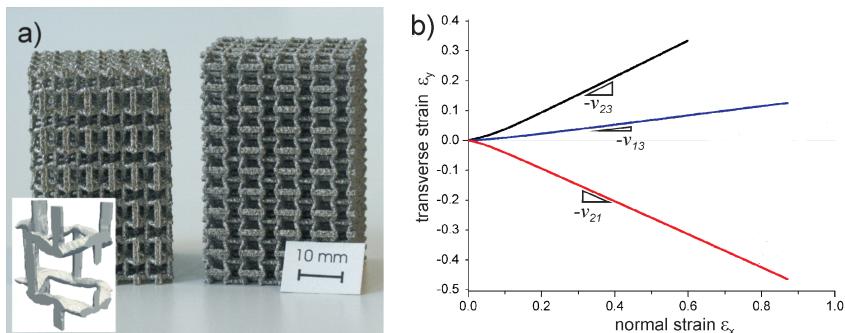
Figure 1: a) Example of a unit cell obtained by optimisation and its physical realisation in Ti-6Al-4V; b) Poisson's ratio of the structure, determined by mechanical testing

structures (Figure 1), as well as numerical and experimental results of their mechanical characterisation. We also discuss the potential of additive manufacturing in the context of other unusual properties of cellular materials.

References

[1] J. Schwerdtfeger, P. Heinl, R. F. Singer, C. Körner, *Phys. stat. sol. (b)* 247, no. 2, p. 269–272 (2010)

Structure of homopolymers and copolymers adsorbed on homogenous and patterned surfaces

A. Sikorski, M. Pawłowska, L. Oldziejewski

Department of Chemistry, University of Warsaw
Pasteura 1, 02-093 Warsaw, Poland

Computer simulations of idealized models of macromolecules at interfaces were performed by means of the Monte Carlo method. The coarse-grained models chains were approximated as sequences of beads and were embedded to a [310] hybrid lattice. We studied the following chain internal architectures: linear, star-branched and cyclic [1]. Each polymer chain was built of two kinds of beads: hydrophobic (H) and hydrophilic (P). Some sequences of beads like homopolymers, random copolymers, alternating copolymers and block copolymers were studied. The polymer beads interacted with a long-distance contact potential and were placed near an impenetrable and attractive surface. The properties of the model system were determined using a Replica Exchange Monte Carlo algorithm. The influence of the temperature, the strength of the adsorption, the sequence of beads and the macromolecular architecture on the properties of chains were studied. The highest degree of adsorption was found for cyclic macromolecules while it was comparable for linear and star-branched chains [2]. It was shown that the most pronounced influence of the adsorbing surface on the chain's structure was observed for alternating copolymers polymers. The changes of the polymer film structure in the presence of repulsive patterns were also presented and discussed [3].

Acknowledgements

References

[1] Rybicka J and Sikorski A 2010 *Macromol. Theory Simul.* **19** 135
[2] Eisenriegler E 1993 *Polymers near Surfaces*, World Scientific, Signapore
[3] Adamczyk P, Romiszowski P and Sikorski A 2009 *Catal. Lett.* **128** 130

Static response of a hexagonal chiral lattice

A. Spadoni

Institute of Mechanical Engineering, École Polytechnique Fédérale de Lausanne (EPFL)
EPFL STI IGM LOMI ME B2 444 (Bâtiment ME)
Station 9, CH-1015 Lausanne, Switzerland

The objective of this talk is to introduce a new micropolar model derived in order to improve the existing continuum models with respect to the static behavior of auxetic structural networks. The chiral lattice is an example of an auxetic structure, made of rings connected by ligaments. This configuration exhibits unusual static behavior dominated by a Poisson's ratio predicted to be exactly −1. While this in itself is a rather remarkable characteristic, promising significant shear resistance, it prevents the employment of continuum models of classical elasticity from exploring the possible applications of this structural system. In order to remove this singularity, the response of a macrocell that includes all topologically distinct components was studied by employing a micropolar continuum representation of the strain energy density. This formulation includes microrotations as independent degrees of freedom and results in a refined representation of the behavior of the chiral lattice. At least three findings emerge from this analysis. Auxetic structures whose internal components are subject to bending deformations are stiffer in shear than similar configurations with a positive Poisson's ratio. This remarkable stiffness was found to be bounded by that of structural configurations dominated by axial deformations of their internal components. Finally, Poisson's ratio exhibits boundary-layer behavior in transitioning from negative values (close to −1) to 0.33 in the case of a triangular lattice.

Acoustic and mechanical system with negative power transmission

T. Stręk, W. Parnasow

Institute of Applied Mechanics, Poznań University of Technology
Piotrowo 3, 60-965 Poznań, Poland

External boundaries of acoustic devices can channel sound propagation, and in certain cases create a build-up or attenuation of acoustic energy in a confined space. We demonstrate the viability of proposed efficient practical numerical method (based on FEM) for the calculation of the attenuation of sound power transmission through ducts by showing how it consistently predicts results in agreement with experiment.

One can observe the mechanical behaviour of the medium of the duct at lower frequencies (high transmission loss, high attenuation) and wave behaviour at higher frequencies (small or zero attenuation). For certain incident waves, one can observe negative transmission "loss" (power build-up).

We proved that mechanical vibrations of the medium reduce the possibility of the transmission of acoustic energy in duct systems. Radiation impedance of the duct was also calculated. The model of a mechanical system with negative power transmission was proposed and analysed.

Acoustic power transmission and impedance – for the ideal case, where there is no ambient velocity and the viscosity and thermal conduction are neglected, the energy density in the considered domain at a given time is described by:

$$W = \frac{1}{2}\left(\rho v^2 + \frac{p^2}{\rho c^2}\right). \tag{1}$$

The first term in the above expression for the energy density is recognized as the acoustic kinetic energy per unit volume, and the second term is identified as the potential energy per unit volume due to the compression of the fluid.

Frequency-dependent sound transmission loss (TL) is a useful tool for measuring the acoustic performance which depends only on the device. TL is defined as the ratio of the sound power incident on the inlet of the device to that leaving the device at the outlet. Transmission loss is given by:

$$\mathrm{TL} = 10\log\frac{W_{\mathrm{in}}}{W_{\mathrm{out}}}, \tag{2}$$

where W_{in} denotes the incoming power at the inlet of the duct, W_{out} denotes the transmitted (outgoing) power at the outlet. The incoming and transmitted sound power, respectively, is given by:

$$W_{\mathrm{in}} = \int_S \frac{p_0^2}{2\rho c}dS, \quad W_{\mathrm{out}} = \int_S \frac{|p|^2}{2\rho c}dS, \tag{3}$$

where p_0 is the applied amplitude of the pressure source and S is the area of the boundary, where waves are incoming to and outgoing from the duct. The power of the incoming sound is expressed by the amplitude of the applied pressure source, and not by the pressure at the inlet. The calculated sound power at the inlet is the sum of the sound power from the source, sound power reflected from the pipe inlet, pipe outlet and pipe boundaries.

One can derive the average complex acoustic impedance over the outlet of a cylindrical duct as an integral in cylindrical coordinates:

$$Z_R = \frac{1}{S} \iint_S \frac{p}{v_n} dS = \frac{1}{\pi a^2} \int_0^{2\pi} \int_0^a r \cdot \left[\mathrm{Re}\left(\frac{p}{v_n}\right) + j\mathrm{Im}\left(\frac{p}{v_n}\right) \right] dr d\varphi = \frac{2}{a^2} \int_0^a r \cdot \hat{z}(r) dr, \quad (4)$$

where S is the area of the surface and $v_n = n \cdot v$ is the outward normal component of the velocity on the surface. The outlet of the duct is the radiating surface, where the radiation impedance is a function of the frequency and cylindrical coordinate r.

Mechanical impedance is a measure of how much a structure resists motion, when subjected to a given force. It relates forces with velocities in a mechanical system. The mechanical impedance of a point in a structure is the ratio of the force applied to the point to the resulting velocity at that point. It is a function of the frequency of the applied force and can vary greatly with frequency. At resonance frequencies, the mechanical impedance is lower, i.e. a smaller force is required to cause a structure to move at a given velocity.

Due to the mechanical behaviour of the medium of the duct, a mechanical model is proposed, where the system is comprised of masses and springs.
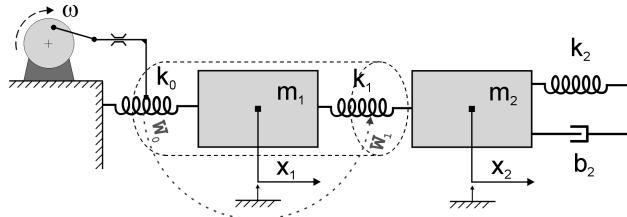
Figure 1: Mechanical model of system

Transmission loss of a mass-spring system can be defined as:

$$\mathrm{TL}_{\mathrm{mech}} = 10 \log \frac{W_0}{W_1} = 10 \log \frac{k_0}{k_1} + 20 \log \left| \frac{X_{01}}{X_{02} - X_{01}} \right|, \quad (5)$$

where X_{01} and X_{02} describe the amplitudes of motion of the two masses in a mechanical system.

If we assume that $k_0 = k_1$, we can write the above formula for the power transmission as:

$$\mathrm{TL}_{\mathrm{mech}} = 20 \log \frac{k_1/k_2}{(\omega/\omega_{02})^2 - 1} - 1 = 20 \log \left(\frac{1}{\Omega^2} - 1 \right), \quad (6)$$

where $\omega_{02} = \sqrt{k_2/m_2}$ is the frequency of the second part of the system and $\Omega = \sqrt{(\omega/\omega_{02})^2 - 1/(k_1/k_2)}$ is the reduced frequency of the system for $\omega > \omega_{02}$.

a)

b)
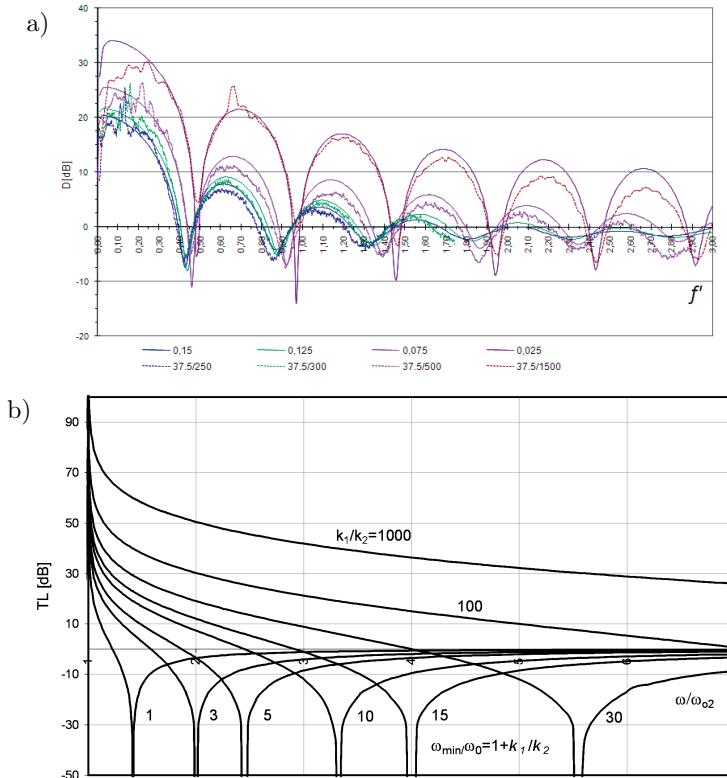
Figure 2: Power transsmision loss: a) acoustic systems (numerical and experimental results); b) mechanical systems

Power transmission can be negative both for acoustic systems (Figure 2 a) and mechanical systems (Figure 2 b). A negative power transmission loss corresponds to an increase in the power of the considered systems for a certain band of frequencies of a potential (e.g. harmonic force in a mechanical system and acoustic pressure in an acoustic system). Devices or materials with negative properties find use in the design of acoustic metamaterials (e.g. phononic crystals). Moreover, it was proved that mechanical vibrations of the medium reduce the possibility of acoustic energy transmission in duct systems.

References

[1] T. D. Rossing (Ed.) 2007 *Handbook of Acoustic*, Springer, LLC New York
[2] T. Strek 2010 Finite Element Modelling of Sound Transmission Loss in Reflective Pipe, in: Finite Element Analysis, David Moratal (Ed.), pp. 663–684, ISBN: 978-953-307-123-7, Sciyo
[3] M. Utsumi 2001 Sound Transmission in Circular Ducts of Continuously Varying Cross-Sectional Area, *Journal of Sound and Vibration*, 242(2), pp. 369–376
[4] G. P. Wilson, W. W. Soroka 1965 Approximation to the Diffraction of Sound by a Circular Aperture in a Rigid Wall of Finite Thickness, *The Journal of The Acoustical Society of America*, 37(2), pp. 286–297

[5] Lee Fok, Muralidhar Ambati, Xiang Zhang 2008 Acoustic Metamaterials, MRS BUL-LETIN, Vol 33, 2008

[6] Huang, C. T. Sun 2009, Wave attenuation mechanism in an acoustic metamaterial with negative effective mass density, *New Journal of Physics* 11 (2009) 013003 (15pp), doi:10.1088/1367-2630/11/1/013003

[7] H. H. Huang, C. T. Sun, G. L. Huang 2009 On the negative effective mass density in acoustic metamaterials, *Int. J. Engineering Science* 47 (2009) 610–617

[8] Comsol Multphisycs User's Guide 2007 *Modeling Guide and Model Library. Acoustic Module Model*, Documentation Set, Comsol AB

Polymorphism in a dynamical self-assembled system driven by minimum energy dissipation rate

K. V. Tretiakov

Institute of Molecular Physics, Polish Academy of Sciences
M. Smoluchowskiego 17/19, 60-179 Poznań, Poland

Self-assembly (SA) [1,2] is a process in which discrete components organize spontaneously into ordered and/or functional super-structures [1]. Here, we present both an experimental and a numerical study of dynamic self-assembly (DySA) in a system of millimeter-sized magnetic disks at a liquid-air interface, subject to a rotating, external magnetic field [3,4]. In the experiment, we observed polymorphism at DySA and we collected the statistical data on the frequency of occurrence of different patterns. Numerical simulations were used to describe a DySA system [5,6,7]. Our model not only correctly mimics the dynamical behavior and the symmetry of the aggregates at various Reynolds numbers, but also reproduces the frequencies with which the polymorphic patterns occur experimentally. The calculation of energy dissipation rates in a prototypical DySA system allowed us to explain the frequency with which the polymorphic patterns occur from the point of view of non-equilibrium thermodynamics. We found that most realized structures had low energy dissipation rates. As the realization of any given pattern depends on its energy dissipation rate and the principle of minimum dissipation rate of energy is equivalent to the principle of minimum entropy production rate, we can say that nature favors structures (patterns) with minimum entropy production rate.

References

[1] G. M. Whitesides, B. Grzybowski, *Science* 295, 2418–2421 (2002)

[2] M. Fialkowski, K. J. M. Bishop, R. Klajn, S. K. Smoukov, C. J. Campbell, B. A. Grzybowski, *J. Phys. Chem. B* 110, 2482–2496 (2006)

[3] B. A. Grzybowski, H. A. Stone, G. M. Whitesides, Dynamic self-assembly of magnetized, millimetre-sized objects rotating at a liquid-air interface, *Nature* 405, 1033–1036 (2000)

[4] B. A. Grzybowski, H. A. Stone, G. M. Whitesides, Dynamics of self-assembly of magnetized disks rotating at the liquid-air interface, *Proc. Natl. Acad. Sci. USA* 99, 4147–4151 (2002)

[5] E. Climent, K. Yeo, M. R. Maxey, G. E. Karniadakis, Dynamic self-assembly of spinning particles, *Journal of Fluids Engineering-Transactions of the Asme* 129, 379–387 (2007)

[6] K. V. Tretiakov, K. J. M. Bishop, B. A. Grzybowski, On the dependence between forces and dissipation rates mediating Dynamic Self-Assembly, *Soft. Matter* 5, 1279–1284 (2009)

[7] K. V. Tretiakov, K. J. M. Bishop, B. A. Grzybowski, Additivity of the excess energy dissipation rate in a dynamically self-assembled system, *J. Phys. Chem. B* 113, 7574–7578 (2009)

White organic light-emitting diodes for flat-panel lighting

T. Tsuboi

Faculty of Engineering, Kyoto Sangyo University
Kamigamo, Kita-ku, Kyoto 603-8555, Japan

White organic light-emitting diodes (OLEDs) are interesting due to their application in flat-panel displays and solid-state lighting sources. OLED displays consume far less energy than conventional LCD and plasma panel displays. OLED lighting is not only energy-efficient, but also lightweight and flexible. There are several methods for fabricating white OLEDs. One of these consists in connecting three primary-color (red, green, and blue) OLED devices. Another method comprises a single OLED device, from which white emission is obtained. The latter method is preferable, since the fabrication is more cost-efficient than in the case of the former method. In a single OLED system, three different layer structures are conceivable. The first one comprises red, green, and blue emitting layers, the second – two layers emitting complementary colors, whereas the third one comprises a single emitting layer which gives rise to white emission. This type of OLED is the most cost-efficient, because its layer structure is simple. We fabricated these three types of OLEDs, using various emitting materials, such as small molecules and polymers. Simultaneously, we developed materials generating white emission, e.g. a small molecule with a ligand emitting a different color, and a fluorene copolymer with a red-emitting iridium complex in the main chain. We present the electroluminescence (EL) characteristics (EL spectra, external quantum efficiency, power efficiency, etc.) of these white OLEDs with different layer structures, including the high luminance of 16800 cd/m^2 achieved at a low operating voltage of 3.8 V. We also present the photophysics of organic materials used in the fabrication of white OLEDs.

Solitary wave propagation in a plate made of an auxetic material – numerical experiment

A. Uściłowska[1], B. Maruszewski[1], K. W. Wojciechowski[2]

[1] *Institute of Applied Mechanics, Poznań University of Technology*
Piotrowo 3, 60-965 Poznań, Poland

[2] *Institute of Molecular Physics, Polish Academy of Sciences*
Smoluchowskiego 17, 60-179 Poznań, Poland

Solitary wave propagation is studied numerically in plates with positive Poisson's ratios (common materials) and those with negative Poisson's ratios (auxetic materials) to analyse the influence of material characteristics on the propagation of such waves.

Propagation of solitary waves in a plate constitutes an initial-boundary value problem, described by a partial differential equation of the fourth order [1]. In general, its solution cannot be expressed in the form of an analytic function and has to be found by numerical calculations. In this study, it is assumed that the wave is a well localized, bell-shaped strain which moves preserving its shape. The detailed algorithm of the used numerical procedure is described in [2]. The procedure is based on the method of fundamental solutions (see e.g. [3,4]), which is one of meshless methods. The last decades saw a rise in the popularity of these methods [5–13], owing to the fact that they possess certain advantages compared to mesh methods or other numerical procedures. Their main advantage is the fact that there is no need to construct any particular mesh in order to perform calculations (as is the case in mesh procedures). (Mesh generation is a time-consuming procedure and the mesh occupies a significant amount of computer memory. Obviously, meshless methods avoid these disadvantages.) Meshless methods base just on sets of points, which may be placed regularly or be disordered – in a form of a 'cloud of points'. The other advantage of the applied procedure is that the fundamental solutions, which are known for most popular operators appearing in the equations of mechanics, strength theory, fluid mechanics etc., are used as the basis functions [5–13]. (In other methods for solving initial-boundary value problems, one needs to find the basis functions, usually by trial and error. Of course, such a procedure is time consuming.)

For solving the problem considered in this study, we used the procedure of solution of the boundary value problem for the biharmonic operator with boundary conditions, the solution for which is described in the literature, for example in [14]. A numerical experiment was performed to confirm the convergence and accuracy of the proposed numerical algorithm. After validating the method, we studied the influence of the Poisson's ratio on solitary wave propagation in plates. Not only some common materials were considered but also various auxetics. Results of the experiments will be discussed during the lecture.

References

[1] G. C. Medeiros, P. W. Partridge, J. O. Brandao, The method of fundamental solutions with dual reciprocity for some problems in elasticity, Engineering Analysis with Boundary Elements 28, 453–461, 2004

[2] A. Uściłowska, The method of fundamental solutions for solving problem of a wave propagation in a plate made with auxetic material, 3rd International Conference and the 7th International Workshop on Auxetics and Related Systems, 19–23 July, 2010, Malta&Gozo, 2010. Book of abstracts, ISBN 978-83-930549-1-6

[3] V. D. Kupradze, M. A. Aleksidze, The method of functional equations for the approximate solution of certain boundary value problems, USSR Comput. Meth. Math. Phys. 4, 82–126, 1964

[4] A. Poullikkas, A. Karageorghis, G. Georgiou, Methods of fundamental solutions for harmonic and biharmonic boundary value problems, Computational Mechanics 21, 416–423, 1998

[5] A. Bogomolny, Fundamental solutions method for elliptic value problems, SIAM Journal on Numerical Analysis 22, 644–59, 1985

[6] R. A. Bialecki, U. Herding, O. Kohler, G. Kuhn, Weakly singular 2D quadratures for some fundamental solutions, Engineering Analysis with Boundary Elements 18, 333–336, 1996

[7] H. J. Choe, On the fundamental solutions to Stokes equations, Journal of Differential Equations, 153, 313–337, 1999

[8] A. H.-D. Cheng, Particular solutions of Laplacian, Helmholtz-type, and polyharmonic operators involving higher order radial basis functions, Engineering Analysis with Boundary Elements 24, 531–538, 2000

[9] T. Ushijima, F. Chiba, Error estimates for a fundamental solution method applied to reduced wave problems in a domain exterior to a disc, Journal of Computational and Applied Mathematics 159, 137–148, 2003

[10] J. T. Chen, I. L. Chen, K. H. Chen, Y. T. Lee, Y. T. Yeh, A meshless method for free vibration analysis of circular and rectangular clamped plates using radial basis function, Engineering Analysis with Boundary Elements 28, 535–545, 2004

[11] K. Weihrauch, N. Zhong, An algoritm for computing fundamental solutions, Electronic Notes in Theoretical Computer Science 120, 201–215, 2005

[12] F. Bernal, M. Kindelan, RBF meshless modeling of non-Newtonian Hele-Shaw flow, Engineering Analysis with Boundary Elements 31, 863–874, 2007

[13] Y. S. Smyrlis, A. Karageorghis, Efficient implementation of the MFS: the three scenarios, Journal of Computers and Applied Mathematics 227, 83–92, 2009

[14] A. Uściłowska, Implementation of meshless method for a problem of a plate large deflection, Chapter 12 of Computational Modelling and Advanced Simulations, Computational Methods in Applied Sciences, Edited by J. Murin, V. Kompis, V. Kutis. Springer Sciences+Business Media B. V. 2011

Simple models of anomalous mechanical properties

K. W. Wojciechowski

Institute of Molecular Physics, Polish Academy of Sciences
M. Smoluchowskiego 17, 60-179 Poznań, Poland

Models with anomalous elastic properties, like negative Poisson's ratio, negative compliance and/or negative thermal coefficient, which have been solved analytically, by computer simulations with particle methods or by finite element methods will be presented and discussed to illustrate various microscopic mechanisms responsible for the negative properties.

ORAL COMMUNICATIONS

Modelling of the mechanical properties
of single-crystalline silica frameworks

A. Alderson, K. L. Alderson, Y. T. Yao

Institute for Materials Research and Innovation, University of Bolton
Deane Road, Bolton BL3 5AB, UK

Analytical models based on the deformation of connected 3D tetrahedra and 2D squares/rectangles frameworks have previously been developed to understand the deformation mechanisms responsible for the auxetic behaviour in the α-cristobalite and α-quartz polymorphs of crystalline silica. In this paper, we report the further development of the analytical tetrahedral models to predict the Young's moduli of these frameworks. The dependency of the moduli on the various parameters (bond strength, bond angle bending, geometry etc.) are investigated and predictions using established values of these parameters from experiment and/or force fields are made and compared to the experimentally determined Young's moduli.

Negative differential mobility within nanophotonic devices

E. A. Anagnostakis

Hellenic Air Force Academy
Dekeleia, Greece

A crucial feature permeating nanophotonics semiconductor-device functionality is the appearance of negative differential mobility (NDM) of the two-dimensional carrier-gas against some proper external regulator (materialising as instantaneous cumulative photonic intake) allowing for gradual controlled modification of the nanointerfacial environment. In this work, several instances, in our two-decade principal research, of both experimental observation and conceptual prediction concerning nanophotonics NDM are reconsidered and critically discussed towards outlining a global interpretation of an intersubband-transition mechanism plausibly accountable for the phenomenon.

Thermal testing of auxetic composites

S. Aziz[1], M. Forite[2], B. Kandola[1], A. Alderson[1], <u>K. L. Alderson</u>[1]

[1]*Institute of Materials Research and Innovation, The University of Bolton Deane Road, Bolton BL3 5AB, UK*

[2]*ITECH 87 chemin des Mouilles, 69134 ECULLY cedex, France*

Auxetic materials are those which have a negative Poisson's ratio. There are a number of materials which can be produced in this form, but only angle-ply composite laminates can currently be produced using conventional starting materials and conventional processing routes. The key to producing an auxetic composite is in the stacking sequence of the individual layers alone. The Auxetic Materials Group at Bolton have performed detailed testing of auxetic carbon fibre composite laminates under indentation and impact loading and have assessed the fracture toughness of these materials. In all cases, the auxetic laminates have improved properties over conventional composites. One area which we have not examined fully to date is the thermal testing of auxetic composites and this project investigates this area in conjunction with Prof Baljinder Kandola of the Fire Materials Research Group, also at the University of Bolton. The paper will report thermal analysis and post test characterisation of auxetic carbon fibre composites in comparison with conventional carbon fibre composites, studying both in-plane and out-of-plane negative Poisson's ratio laminates.

Half-metallic properties of the electron band structure of zinc-blende Cd$_{1-x}$Cr$_x$Te ($x = 0.5$)

M. Bester[1], J. Konior[2], M. Kuźma[1]

[1] *Institute of Physics, University of Rzeszów*
Rejtana 16A, 35-959 Rzeszów, Poland

[2] *Institute of Physics, Jagiellonian University*
Reymonta 4, 30-059 Kraków, Poland

Half-metallic ferromagnets with a crystal structure compatible with important III-V or II-VI semiconductors are desirable for spintronic applications. Among the most promising materials for half-metallic ferromagnets are 3d transition-metal chalcogenides, particularly Cr$_{1-x}$Te with a Curie temperature in the range of 180–340 K, depending on composition. However, the stable structure of these compounds is hexagonal of NiAs type. Recently, Cr$_{1-x}$Te has been widely investigated in first-principles theoretical studies, since its hypothetic unstable ferromagnetic cubic zinc-blende (ZB) phase demonstrates half-metallic properties with an energy gap of 2.90 eV, which preserves almost 100% spin polarization. In this paper, we propose to stabilize this unusual structure by doping with Cd atoms. We calculated the band structure of cubic Cd$_{1-x}$Cr$_x$Te ($x = 0.5$) solid solution using the linearized-augmented-plane-wave (LAPW) method with the local-density approximation for the exchange and correlation potentials. Densities of states and magnetic moments were calculated. The results were compared to the band structure of pure CdTe and CrTe components. We conclude that the main features of ZB CrTe band structure are preserved in the band structure of Cd$_{1-x}$Cr$_x$Te, even for high concentrations of Cd atoms.

Investigation of $KGd(WO_4)_2$ single crystal EPR spectra recorded at different temperatures

T. Bodziony[1], S. M. Kaczmarek[1], T. Skibiński[1],
J. Hanuza[2], L. Macalik[2]

[1]*Institute of Physics, West Pomeranian University of Technology*
Al. Piastów 17, 70-310 Szczecin, Poland

[2]*Institute of Low Temperature and Structure Measurements, PAS*
P. Nr 1414, 50-950 Wrocław, Poland

The results of EPR measurements of a double tungstate $KGd(WO_4)_2$ (KGW) single crystal are presented for the first time. The changes in the EPR spectra are examined as a function of temperature. The EPR spectra reveal a complex structure (see Figure 1). Additionally, the temperature dependence of the EPR spectra of a KGW single crystal is very interesting. We used a few Lorentz shaped curves to fit the EPR spectra, assuming that these curves originated from several magnetically inequivalent paramagnetic centres. It seems that there are many different paramagnetic centres in a $KGd(WO_4)_2$ (KGW) single crystal. These centres behave differently with a change of temperature. An analysis of the temperature dependence gives a deeper insight into the structure and environment of paramagnetic Gd^{3+} centres in a $KGd(WO_4)_2$ single crystal.
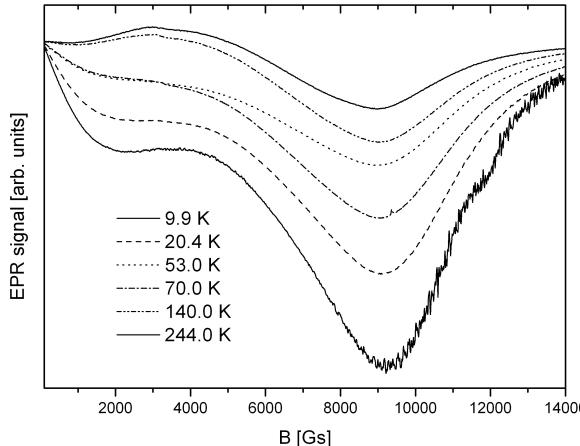
Figure 1: EPR spectra of $KGd(WO_4)_2$ single crystal in different temperatures

Synthesis of carbon and silica nanostructures supporting titanium oxide for photocatalysis

K. Cendrowski, X. Chen, B. Zielińska,
R. J. Kaleńczuk, E. Borowiak-Paleń

Center of Knowledge Based Nanomaterials and Technologies
Institute of Chemical and Environment Engineering
West Pomeranian University of Technology
Pułaskiego 10, 70-322 Szczecin, Poland

The recent publication on improvement of the photocatalytic activity of titanium dioxide supported on carbon or silica structures has focused our attention on supporting nanocrystalline titanium oxide on hollow carbon mesoporous nanospheres, multiwalled carbon nanotubes, silica nanotubes, silica/carbon nanotubes and mesoporous silica nanospheres. In this contribution we present the route of synthesis of these kinds of molecular nanostructures. The preliminary photocatalytic properties of the samples indicated enhancement of their activity in comparison to the reference titania. We tested two reactions: phenol decomposition and hydrogen generation.

The samples morphology was investigated by means of high resolution transmission electron microscopy (HR-TEM). The phase composition of the materials was studied via X-Ray diffraction. Raman spectroscopy was used to check the vibronic properties of the samples.

Classification of cubic auxetics

R. V. Goldstein, V. A. Gorodtsov, D. S. Lisovenko

A. Yu. Ishlinsky Institute for Problems in Mechanics RAS
Russia, Moscow

Among the crystals of different crystalline systems, the negative Poisson's ratio most often occurs in cubic crystals [1,2]. We identified all cubic crystals with negative Poisson's ratio ("cubic auxetics"), the elastic properties of which are given in the well-known book series of Landolt-Börnstein [3]. For anisotropic materials, elastic properties such as Poisson's ratio (the ratio of deformation due to transverse compression to the longitudinal extension) depend on the orientation of the deformable sample and several compliance moduli. Using Euler's angles φ, θ, ψ for the description of orientation in the case of cubic crystals, which are characterized by three matrix compliance coefficients s_{11}, s_{12}, s_{44} such dependence can be represented as

$$\frac{\nu}{E} = -\frac{\Delta}{2}\left[N(\varphi,\theta,\psi) - \Pi\right], \quad \Pi \equiv -\frac{2s_{12}}{\Delta},$$

$$N(\varphi,\theta,\psi) \equiv \left\{3\cos^2\theta\cos^2\psi + (\cos\theta\cos 2\varphi\cos\psi - \sin 2\varphi\sin\psi)^2\right\}\sin^2\theta.$$

Here E – Young's modulus, which is always positive, $\Delta = s_{11} - s_{12} - s_{44}/2$ – a linear combination of all compliances (the dimensional parameter of anisotropy), Π – a dimensionless combination of these three coefficients, $N(\varphi,\theta,\psi)$ – a periodic function of the angular variables with periods $T_\varphi = \pi/2$, $T_\theta = 2\pi$, $T_\psi = \pi$, for which $0 \leqslant N(\varphi,\theta,\psi) \leqslant 1$.

The analysis revealed that an overwhelming number of auxetics shows a change of sign of Poisson's ratio under changes of the orientation of the deformed crystalline sample. Such auxetics are termed "moderate auxetics". In accordance with previous formulas, the "boundary of auxeticity" $\nu(\varphi,\theta,\psi) = 0$ takes the form

$$N(\varphi,\theta,\psi) = \Pi.$$

Thus, this boundary depends only on one dimensionless characteristic of crystalline elasticity, Π. Because of lower and upper limitations on the function $N(\varphi,\theta,\psi)$, the equation for this boundary can be solved only if we have constraints on the elastic properties of the form

$$0 < \Pi \equiv -\frac{2s_{12}}{\Delta} < 1. \tag{1}$$

Positivity of the dimensionless ratio Π requires the opposite sign of the compliance modulus s_{12} and of the anisotropy parameter Δ for moderate cubic auxetics. Experimental data for the compliance coefficients in [3] permit to distinguish two subclasses of moderate cubic auxetics with $\Delta > 0$, $s_{12} < 0$ and $\Delta < 0$, $s_{12} > 0$. Hundreds of cubic

auxetics belong to the first subclass (with $\Delta > 0$, $s_{12} < 0$). Among them, we mention monocrystals of Li, Na, K, Yb, Rb, Cs, Ca, Sr, Th, Pb, Ce, Co, Cu, Ag, Tl, Ni, Fe, Pd, Au, FePd, InTl, CuAlNi, $CuAuZn_2$, $NiCrO_4$, AuZn, FeAl, CuSn, CuAu, CuMn, CuNi, CuZn, FeNi, FeCrNi, AgAu, AgZn, ZnS. Another subclass (with $\Delta < 0$, $s_{12} > 0$) is much more limited. It includes about ten auxetics (e.g., crystals of UTe, ReO_3, SmB_6, USb, USe, TmSe).

As a result of detailed analysis, it was found that the nature of the auxetic surfaces $\nu(\varphi, \theta, \psi) = 0$ strongly varies with the dimensionless parameter Π. The critical value of this parameter is defined as

$$\Pi_c \approx 0.75.$$

As this parameter varies, there is substantial restructuring of the topological type of the surface. When the following inequalities $1 > \Pi > \Pi_c$ hold, the auxetic boundaries represent collections of closed surfaces. For smaller values of the dimensionless parameter ($\Pi_c > \Pi > 0$) they take the form of pairs of "unclosed surfaces". This is illustrated in Figure 1. Euler angles characterizing the orientation of the crystals are plotted along the axes of the Cartesian coordinate system. For clarity, the angular cells $T_\varphi = \pi/2$, $T_\theta = 2\pi$, $T_\psi = \pi$ are shifted by $-\pi/6$ along the φ axis and by $-\pi/4$ along the ψ axis.
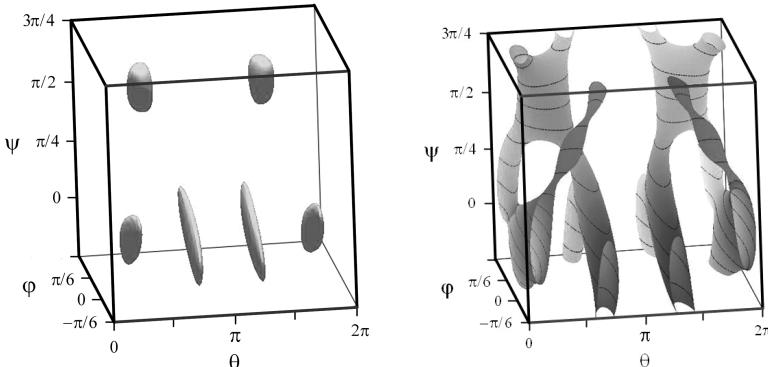
Figure 1: View of the auxetic surfaces $\nu(\varphi, \theta, \psi) = 0$ for $\Pi = 0.9 > \Pi_c \approx 0.75$ (left) and for $\Pi = 0.7 < \Pi_c \approx 0.75$ (right)

The position of the regions in which the Poisson ratio is negative depends on the sign of the dimensional parameter of anisotropy Δ. For $\Delta > 0$, these zones are located within the closed boundaries of auxeticity. Otherwise, the reverse has place.

Auxetics with dimensionless complex which does not satisfy the inequalities (1) deserve particular attention. For such "absolute auxetics", the Poisson's ratio is negative for all crystalline orientations. In this case, the separating auxetic surface $\nu(\varphi, \theta, \psi) = 0$ is absent. Three candidates for the role of an absolute cubic auxetic were found, namely, barium Ba (with $\Pi < 0$) and two solid solutions of samarium Sm (with $\Pi > 1$).

The obrtained extensive lists of moderate auxetics and the three absolute auxetics should not be considered final. They are based on the analysis of experimental data, which do not always have sufficiently high accuracy (see [3]).

Acknowledgements

References

[1] R. V. Goldstein, V. A. Gorodtsov, D. S. Lisovenko, Auxetic mechanics of crystalline materials. Mechanics of Solids, 2010, V. 45, N 4, P. 529–545

[2] R. V. Goldstein, V. A. Gorodtsov, D. S. Lisovenko, About negativity of the Poisson ratio for anisotropic materials. Doklady Physics, 2009, V. 54, N 12, P. 546–548

[3] Landolt-Börstein. Group III Condensed Matter. Berlin: Springer, 1992, V. 29a, P. 11–188

Improved analytical models for hexagonal honeycombs

J. N. Grima[1,2], D. Attard[2], B. Ellul[2], R. Gatt[2]

[1] *Metamaterials Unit, Faculty of Science, University of Malta*
Msida MSD 2080, Malta

[2] *Department of Chemistry, Faculty of Science, University of Malta*
Msida MSD 2080, Malta

Cellular structures, in particular hexagonal honeycombs have been the subject of numerous studies in view of their extensive use in many practical applications. In particular, there have been various studies which relate the mechanical properties of honeycombs to the geometrical parameters used to describe the structure of such honeycombs. Despite several improvements over the first established models [1,2,3], finite element simulations on honeycombs having ribs with realistic thickness-to-length ratios suggest that the Poisson's ratios and Young's moduli for such systems differ from those predicted by current models, sometimes to a very significant extent. In view of this, in the work presented here the deformed structures are analysed in detail in an attempt to gain insight into how and the extent to which the aspect ratio of the ligaments and their mode of connection (i.e. re-entrant or non re-entrant) affects deformation in hexagonal honeycombs. Following these observations, a modified analytical model that takes into consideration the finite thickness of the ligaments is proposed.

References
[1] F. K. Abd El-Sayed, R. Jones, I. W. Burgess, Composites, 10 (1979) 209–214
[2] L. J. Gibson, M. F. Ashby, G. S. Schajer, C. I. Robertson, Proceedings of the Royal Society A, 382 (1982) 25–42
[3] I. G. Masters, K. E. Evans, Composite Structures, 35 (1996) 403–422

Negative thermal expansion in space frame trusses

T.-Ch. Lim

School of Science & Technology, SIM University
461 Clementi Road, S 599491, Singapore

2D periodic networks consisting of three sets of rods made of different materials are known to exhibit adjustable thermal expansion. It has been shown that triangles, one side of which is made of a different material than the remaining two sides, can exhibit negative thermal expansion (NTE) [1–3]. A generalized study of a triangular network for various combinations of different rod lengths and coefficients of thermal expansion (CTE) further supports the high adjustability of the thermal expansion of this network, spanning both negative and positive values [4]. This presentation considers a 3D periodic network consisting of six sets of rods arranged in a tetrahedron, known as space frame trusses in the civil engineering context, as an extension of the 2D network. Various combinations of rod lengths and CTEs leading to overall negative CTEs of the space frame trusses are presented.

References

[1] L. J. Vandeperre, A. Howlett, W. J. Clegg, *Application of negative thermal expansion to optical fibres*, in CIMTEC 2002: International Conference on Modern Materials and Technologies (Florence, Italy, 2002), vol. 4, 945

[2] L. J. Vandeperre, W. J. Clegg, *Tailoring strains through microstructural design*, in Materials and Devices for Smart Systems, Vol. 785, edited by Y. Furuya, E. Quandt, Q. Zhang, K. Inoue, (Materials Research Society, Warrendale, PA, 2004), 389–394

[3] C. W. Smith, W. Miller, D. S. Mackenzie, K. E. Evans, *Mechanism for negative thermal expansion and its links to negative Poisson's ratio*, presented at the 2nd International Workshop on Auxetic and Related Systems, Poznań, Poland (2005)

[4] J. N. Grima, P. S. Farrugia, R. Gatt, V. Zammit, *A system with adjustable positive or negative thermal expansion*, Proceedings of the Royal Society A 463, 1585–1596 (2007)

Selective oxidation of single-walled carbon nanotubes via long term thermal treatment

P. Łukaszczuk[1], E. Borowiak-Paleń[1], R. J. Kaleńczuk[1],
M. H. Rümmeli[2]

[1] *Institute of Chemical and Environment Engineering*
West Pomeranian University of Technology
Pułaskiego 10, 70-322 Szczecin, Poland

[2] *Leibniz Institute for Solid State and Materials Research Dresden*
Helmholtzstr. 20, 01069 Dresden, Germany

A study on selective oxidation of raw single walled carbon nanotubes (SWCNT) treated by long time oxidation in open air will be presented in this contribution. The as-produced SWCNT consists of a mixture of semiconducting and metallic nanotubes and fractionation is highly required to broaden their applications. Therefore, the aim of this research is to enrich a bulk SWCNT sample in one particular electronic type. Thermal oxidation gives a simple route to reach this goal on a large scale. Other fractionation techniques such as dielectrophoresis, density gradient ultracentrifugation or gel chromatography are very efficient, however the scaling up of these processes is very limited. The obtained single fractions of SWCNTs can be applied for flexible print on electronics, semiconducting SWCNT after modification (n-type and p-type doping) can form diodes or simple transistors, when metallic SWCNT will act as a contact for these active components.

The samples were characterized by means of high resolution transmission electron microscopy, micro-Raman and optical absorption spectroscopy.

Influence of heating temperature on luminescent properties of microwave-hydrothermal synthesized ZrO_2:Tb,Y

U. Narkiewicz[1], J. Kaszewski[1], I. Pełech[1],
S. Yatsunenko[2], M. Godlewski[2]

[1]*Institute of Chemical and Environmental Engineering*
West Pomeranian University of Technology
Pułaskiego 10, 70-322 Szczecin, Poland

[2]*Institute of Physics of the Polish Academy of Sciences*
al. Lotników 32/46, 02-668 Warsaw, Poland

Many factors are known to influence the luminescence phenomenon, e.g. composition, density of lattice defects, purity of initial materials, preparation method, temperature, humidity, atmosphere, presence of water and foreign ions [1]. The heating process affects many phenomena in materials, including structural changes, grain growth, dopant diffusion and water behavior [2]. We present the influence of heating temperature on the luminescent properties of a material exhibiting a narrow grain size distribution, which could find application in optoelectronic devices. Powders were prepared via the microwave hydrothermal route. The residue was precipitated from water solution of metal nitrates at pH 10. The microwave-hydrothermal process was conducted under a pressure of 55 atm for 20 minutes. The obtained powders were dried and heated in an air atmosphere. The temperature of heating varied from 200 to 1000°C. The content of yttrium varied from 0 to 10%, whereas terbium concentration was 0.5%. Luminescent properties were investigated in all powders in order to find the most intense emission. The grain size of heated powders varied from 5 to 30 nm and depended on the concentration of yttrium. Stabilization was found to be inefficient in the powders with low concentration of yttrium, heated at high temperatures. After a critical grain size was reached, a phase transition occurred, like in materials synthesized by calcination.

References
[1] A. A. Bol, A. Meijerink 2001 *Phys. Status Solidi B* **224** (1) 291
[2] K. Prasad, D. V. Pinjari, A. B. Pandit, S. T. Mhaske 2011 *Ultrason. Sonochem.* **18** (5) 1128

Elastic properties and Poisson's ratio of disordered static solids

J. W. Narojczyk[1,2], K. W. Wojciechowski[2]

[1]*Institute of Molecular Physics, Polish Academy of Sciences*
Smoluchowskiego 17, 60-179 Poznań, Poland

[2]*President St. Wojciechowski PWSZ*
Nowy Świat 4, 62-800 Kalisz, Poland

Recent computer simulations of elastic properties of two- and three-dimensional static systems with n-inverse-power interactions are reviewed. In particular, based on the study of atomic and molecular models, the influence of various forms of structural disorder on Poisson's ratio will be discussed.

Size polydispersity of the particles forming a solid is typically responsible for an increase of the (average) Poisson's ratio [1–5]. Moreover, for such systems as 2D discs [1], 2D trimers [2], 3D spheres [3] and 3D dimers [4], the Poisson's ratio tends to its extreme positive value in the limit of hard interactions. In the case of anisotropic models, it is possible to decrease the value of the Poisson's ratio, even below -1 (which is the lower limit for isotropic systems [2]), by proper selection of the shape of the particles. In such systems, the negative value of Poisson's ratio is retained even in the presence of atomic size polydispersity [5].

Although atomic size polydispersity leads to an increase of the Poisson's ratio in the limit of hard interactions, anisotropic systems of cubic symmetry have been found that exhibit, in some directions, a decrease of the Poisson's ratio driven by an increase of structural disorder. The three-dimensional sphere [3] and dimer [4] models are examples of such systems. In the case of the latter system, i.e. a degenerate crystalline structure of cubic symmetry [4], the size polydispersity leads to a decrease of Poisson's ratio in a certain direction for large values of the exponent n, which was not observed previously in any of studied models. This is a promising result in the context of manufacturing mechanically stable (partial) auxetics of cubic symmetry.

References

[1] J. W. Narojczyk, K. W. Wojciechowski, *J. Non Cryst. Sol.* **352**: 4292–4298 (2006)
[2] J. W. Narojczyk, K. W. Wojciechowski, *Phys. Stat. Sol. B.* **244**: 943–954 (2007)
[3] J. W. Narojczyk, K. W. Wojciechowski, *Phys. Stat. Sol. B.* **245**: 606–613 (2008)
[4] J. W. Narojczyk, K. W. Wojciechowski, *J. Non Cryst. Sol.* 356: 2026–2032 (2010)
[5] J. W. Narojczyk, A. Alderson, A. R. Imre, F. Scarpa, K. W. Wojciechowski, *J. Non Cryst. Sol.* 354: 4242–4248 (2008)

Synthesis and spectroscopy of LiCaBO$_3$ glasses doped with manganese and copper

B. V. Padlyak[1,2], A. Drzewiecki[2], V. T. Adamiv[1], Ya. V. Burak[1], I. M. Teslyuk[1]

[1]*Institute of Physical Optics*
Dragomanov Str. 23, 79-005 Lviv, Ukraine

[2]*Division of Spectroscopy of Functional Materials*
Institute of Physics, University of Zielona Góra
Prof. Szafrana 4a, 65-516 Zielona Góra, Poland

Series of new glasses with an LiCaBO$_3$ composition, doped with Mn and Cu (LiCaBO$_3$:Mn and LiCaBO$_3$:Cu) were obtained and their electron paramagnetic resonance (EPR) and optical spectra were investigated and analyzed. The LiCaBO$_3$:Mn and LiCaBO$_3$:Cu glasses of high optical quality were obtained from corresponding polycrystalline compounds by fast cooling of their melts. The melts were heated more than 100 K higher that the melting temperatures of the LiCaBO$_3$ compound ($T_{\mathrm{melt}} = 1103$ K) to exceed the glass transition point. Lithium and calcium carbonates (Li$_2$CO$_3$ and CaCO$_3$) and boric acid (H$_3$BO$_3$) of high chemical purity were used for solid state synthesis of the LiCaBO3 compound. Mn and Cu impurities were added to the melt compositions in the form of MnO$_2$ and CuO oxides in the amounts of 0.5 and 1.0 mol.%.

On the basis of an EPR spectra analysis it was shown that the Mn and Cu impurities were incorporated into the LiCaBO$_3$ glass network as Mn^{2+} (3d^5, ^{6}S$_{5/2}$) and Cu^{2+} (3d^9, ^{2}D$_{5/2}$) paramagnetic ions. The observed EPR spectra of the Mn^{2+} and Cu^{2+} centers in the LiCaBO3 glasses were characteristic for glassy (or vitreous) compounds and were closely similar to the corresponding EPR spectra of the Mn- and Cu-doped glasses with Li$_2$B$_4$O$_7$ and KLiB$_4$O$_7$ compositions, investigated by us earlier [1–3].

The EPR spectra, observed in the LiCaBO$_3$:Mn glasses, were attributed to the isolated Mn^{2+} ions with a broad distribution of crystal field parameters and small clusters of Mn^{2+} ions in trigonally distorted octahedral sites of the glass network. The positions of the Mn^{2+} EPR lines in the LiCaBO$_3$:Mn glasses were almost independent of temperature in the 77–300 K range and their intensities increased with the increasing amount of the Mn impurity. The EPR spectra parameters of Mn^{2+} centers (isotropic g-factors and hyperfine constants of the ^{55}Mn isotopes as well as peak-to-peak derivative linewidths of hyperfine components) in the LiCaBO$_3$:Mn glasses were determined at $T = 300$ K.

It was shown by optical spectroscopy that the Mn impurity was incorporated into the LiCaBO$_3$ glass network simultaneously as Mn^{2+} (3d^5) and Mn^{3+} (3d^4) ions. All the observed transitions of the Mn^{2+} and Mn^{3+} centers in the optical absorption, emission, and luminescence excitation spectra of the LiCaBO$_3$:Mn glasses were identified.

In particular, a broad optical absorption band with a maximum near 470 nm was related to the $^5E_g \rightarrow {}^5T_{2g}$ spin-allowed transition of the Mn3$^+$ centers in octahedral sites and the intense absorption at $\lambda < 350$ nm was assigned to the $Mn^{3+} \rightarrow O^{2-}$ charge-transfer band. A complex intense emission band, peaked around 600 nm, belonged to $^4T_{1g} \rightarrow {}^6A_{1g}$ transition of the Mn^{2+} centers in octahedral sites of the LiCaBO$_3$ glass structure. The luminescence kinetics of the Mn^{2+} emission bands in the LiCaBO$_3$:Cu glasses, containing 0.5 and 1.0 mol.% of MnO were investigated and their lifetime values were determined at $T = 300$ K.

The observed EPR spectra of the Cu^{2+} centers in the LiCaBO$_3$:Cu glasses were assigned to the isolated Cu^{2+} centers in the octahedral sites of the glass network. The positions of the Cu^{2+} EPR lines in the LiCaBO$_3$:Mn glasses were independent of temperature in the 77–300 K range and their intensities increased with the increasing Cu impurity amount. The EPR spectra parameters of Cu^{2+} centers (axial g – factors and hyperfine constants of the ^{63}Cu and ^{65}Cu isotopes as well as peak-to-peak derivative linewidths of hyperfine components) in the LiCaBO$_3$:Cu glasses were determined at $T = 300$ K. The optical spectroscopy of the LiCaBO3:Cu glasses showed that the Cu impurity was incorporated into the LiCaBO$_3$ glass network simultaneously as Cu^{2+} (3d^9) and Cu$^+$ (3d^{10}) ions. A characteristic broad absorption band, peaked about 750 nm, was assigned to the $^2B_{1g} \rightarrow {}^2B_{2g}$ transition of the Cu^{2+} centers in the octahedral sites of the LiCaBO$_3$ glass network. An intense absorption in the UV region ($\lambda < 350$ nm) was assigned to the $Cu^{2+} \rightarrow O^{2-}$ charge-transfer band. Complex broad emission bands around 450 nm were observed in the photoluminescence spectra of the LiCaBO$_3$:Cu glasses. The emission bands belonged to the parity- and spin-forbidden 3d^{9}4s $\rightarrow$ 3d^{10} transition from the triplet state of the Cu$^+$ centers with different local environments or their distortion. The luminescence kinetics of the Cu$^+$ emission bands in the LiCaBO$_3$:Cu glasses, containing 0.5 and 1.0 mol.% of CuO$_2$ was investigated and its lifetime values were determined at $T = 300$ K.

The EPR and optical spectra and their parameters in the LiCaBO$_3$:Mn and LiCaBO$_3$:Cu glasses were analyzed in comparison with the corresponding spectra and parameters for Li$_2$B$_4$O$_7$:Mn, KLiB$_4$O$_7$:Mn, Li$_2$B$_4$O$_7$:Cu, and KLiB$_4$O$_7$:Cu glasses, containing 0.4 and 1.6 mol.% of MnO$_2$ [1–3]. Possible local structures of Mn^{2+}, Mn^{3+}, Cu^{2+}, and Cu$^+$ impurity centers in the LiCaBO$_3$ glass network are discussed on the basis of the obtained and referenced spectroscopic and structural data for different borate glasses and their crystalline analogies.

Acknowledgements

References
[1] B. V. Padlyak, W. Wojtowicz, V. T. Adamiv, Ya. V. Burak, I. M. Teslyuk 2010 Acta Phys. Pol. A 117 (1) 122
[2] B. V. Padlyak, W. Ryba-Romanowski, R. Lisiecki, O. Smyrnov, A. Drzewiecki, Ya. Burak, V. Adamiv, I. Teslyuk 2010 J. Non-Cryst. Solids 356 2033
[3] B. V. Padlyak, A. Drzewiecki, O. Smyrnov O 2010 Current Topics of Biophysics 33 (suppl. A) 171

Scattering of an electron in a plane by a perpendicular magnetic field in there resides a one dimensional attracive parabolic potential

G. J. Papadopoulos

Department of Physics, Solid State Section, University of Athens
Panepistimiopolis, Zografos 157 84, Athens, Greece

The charge distribution for an electron constrained in a plane in which resides a one-dimensional attractive parabolic potential, and under the influence of a constant magnetic field perpendicular to the plane is treated in the case whereby the particle's initial wave function constitutes a wave packet locating the particle at a given position in the plane and carrying an initial momentum. There follows a picture consiting of instances of the evolving charge distribution in the course of time. The distribution starts from a concentrated form associated with the initial wave packet and continuously smears out retaining, however, the form of a wave hill extending along and partially accross a line turning about the moving projection of the hill crest. The evolution in time of the crest projection coordinates onto the plane of motion show periodicity determined by a combination of the cylotron together with the parabolic potential frequency. The corresponding trajectory of the crest projection differs from the classical particle's one, but significantly enough, by certain adjustment in the initial momentum either in the quantal or classical case the two trajectories can coincide.

In situ synthesis and characteristics of polymer nanocomposites based on poly (ethylene terephthalate) and exfoliated graphite

S. Paszkiewicz[1], A. Szymczyk[2], Z. Spitalsky[3], J. Mosnacek[3],
M. Soccio[4], T. A. Ezquerra[4], Z. Rosłaniec[1]

[1] *Institute of Materials Science and Engineering*
West Pomeranian University of Technology
Al. Piastów 17, 70-310 Szczecin, Poland

[2] *Institute of Physics, West Pomeranian University of Technology*
Al. Piastów 17, 70-310 Szczecin, Poland

[3] *Polymer Institute, SAS*
Dubravska cesta 9, 84541 Bratislava 45, Slovakia

[4] *Instituto de Estructura de la Materia*
CSIC Serrano 121, Madrid 28006, Spain

Graphite is a 2-dimensional carbon material which is naturally abundant. In graphite, sp2-hybridized carbons are covalently bonded in a hexagonal manner, forming individual graphene sheets bound together by van der Waals forces. Graphite has been used in many industrial applications, such as lubricants [1] and high-temperature gaskets [2]. Recently, it has received attention due to its superior in-plane properties [3,4]. It competes with carbon nanotubes in many ways. Its in-plane stiffness is as high as that of carbon nanotubes ($E \sim 1$ TPa), [4–6] and its electrical ($\sigma \sim 10^6$ (ohm cm)$^{-1}$) [7–9] and thermal conductivity (~ 400 W m^{-1} K^{-1}) [10] are also exceptional. The potentially high aspect ratio of single graphene sheets indicates that graphene can greatly improve mechanical and gas barrier properties if it is well dispersed in the polymer matrix.

In this work, we report an efficient method for the preparation of poly(ethylene terephthatale)/expanded graphite (PET/EG) nanocomposites by in situ polymerization of PET in the presence of exfoliated graphite. By adjusting the feed ratio of PET to EG, various composites with a graphite content of 0.025–0.4 wt% were obtained. The effect of the presence of exfoliated graphite in the PET matrix on the electrical, thermal and mechanical properties was studied by dielectric spectroscopy, differential scanning calorimetry (DSC), dynamic mechanical thermal analysis (DMTA), thermogravimetric analysis (TGA) and tensile testing. The morphologies of the nanocomposites were examined using both SEM and TEM. Our studies showed that the electrical conductivity and thermal stability of PET were notably enhanced by the introduction of EG. The value of the electrical percolation threshold was 0.05 wt% (EG). The

crystallization behaviour of PET/EG nanocomposites was not significantly influenced by the presence of graphite in the PET matrix.

Acknowledgements

References

[1] A. V. Tamashuasky, In National Lubricating Grease Institute 72nd Annual Meeting, San Antonio, TX, 2005

[2] D. D. L. Chung, J. Mater. Sci. 1987, 22, 4190

[3] L. T. Drzal, H. Fukushima, Polym. Prepr. (Am. Chem. Soc., DiV. Polym. Chem.) 2001, 42, 42

[4] H. Fukushima, L. T. Drzal, Annu. Tech. Conf.sSoc. Plast. Eng. 2003, 2230

[5] B. T. Kelly, Physics of Graphite; Applied Science: London, 1981

[6] L. S. Schadler, S. C. Giannaris, P. M. Ajayan, Appl. Phys. Lett. 1998, 73, 3842

[7] K. S. Novoselov, A. K. Geim, S. V. Morozov, D. Jiang, Y. Zhang, S. V. Dubonos, I. V. Grigorieva, A. A. Firsov, Science 2004, 306, 666

[8] Y. Zhang, Y.-W. Tan, H. L. Stormer, P. Kim, Nature (London) 2005, 438, 201

[9] T. Tsuzuku, Carbon 1979, 17, 293

[10] A. W. Smith, N. S. Rasor, Phys. ReV. 1956, 104, 885

Auxeticity of materials with shape preserving inclusions: studies of two-dimensional models

A. A. Pozniak[1], K. W. Wojciechowski[2]

[1] *Institute of Physics, Poznań University of Technology*
Nieszawska 13A, 60-965 Poznań, Poland

[2] *Institute of Molecular Physics, Polish Academy of Sciences*
Smoluchowskiego 17, 60-179 Poznań, Poland

Common materials exhibit a positive Poisson's ratio (PR) [1], i.e. they shrink when stretched. Mechanically stable models [2] and thermodynamically stable phases of model molecules [3] exhibiting negative Poisson's ratio, i.e. expanding laterally when stretched, have been known for more than two decades. Materials with negative Poisson's ratio, first manufactured in 1987 [4] and termed auxetics [5], have since attracted increasing interest [6].

For stable isotropic materials, PR cannot be lower than -1. Materials that satisfy this condition, further referred to as *perfect auxetics*, preserve their shape when stretched. Although such materials are not known in nature, as yet, some model structures exhibiting this unusual property have been described in the literature [2,7–10]. By applying finite pieces of these materials ('particles') as inclusions in matrices of common materials, one can obtain composites exhibiting effective auxetic behaviour.

We present results of our recent analytic investigations and computer simulations of two-dimensional model composites containing pieces of the structures described in refs. [7,10], which can be easily manufactured (at least on a macroscopic level). Such perfectly auxetic 'particles' (PAPs) can be built of circles, squares, or other rigid bodies with 'holes' in which non-bendable rods (of diameters only slightly smaller than the diameters of the holes) are placed [10]. The rods connecting the rigid bodies play the role of constraints which keep the shape of any cluster intact when its volume changes. In this presentation, our attention will be focused on composites containing small PAPs, like trimers, tetramers and hexamers. Both isotropic and anisotropic composites will be discussed.

Acknowledgements

References
[1] L. D. Landau, E. M. Lifshitz, Theory of elasticity, 3rd Edition, Oxford (1986)
[2] R. F. Almgren, Journal of Elasticity **15**, 427 (1985)
[3] K. W. Wojciechowski, Molecular Physics **61**, 1247 (1987)
[4] R. S. Lakes, Science **235**, 1038 (1987)

[5] K. E. Evans, Endeavour **15**, 170 (1991)

[6] K. L. Alderson, A. Alderson, K. W. Wojciechowski, Physica Status Solidi B**248**, 28 (2011); see also references there

[7] K. W. Wojciechowski, A. C. Brańka, Molecular Physics Reports **6**, 71 (1994)

[8] J. N. Grima, K. E. Evans, Journal of Materials Science Letters **19**, 1563 (2000)

[9] Y. Ishibashi, M. Iwata, Journal of the Physical Society of Japan **69**, 2702 (2000)

[10] R. S. Lakes, K. W. Wojciechowski, Physica Status Solidi B **245**, 545 (2008)

Origin of prepeak in liquid Al-based alloys

O. S. Roik, V. P. Kazimirov, O. V. Samsonnikov,
V. E. Sokol'skii, S. M. Galushko

Chemical Department, National Taras Shevchenko University of Kyiv
64 Volodymyrska str., Kyiv, UA-01033, Ukraine

Binary and ternary liquid alloys of aluminum with 3d-, 4d-transition metals (TM) demonstrate a specific feature of the structure factor which is known as a prepeak, i.e. an additional peak at low values of the diffraction vector, at the left part of the main peak. It is observed for various liquids and amorphous solids. In the literature devoted to the structure of glasses it is also called the first sharp diffraction peak. However, in liquids the prepeak is not sharp and usually it is observed as a small shoulder on the left slope of the main peak. The existence of the prepeak is related to the presence of an intermediate-range order in the system, i.e. a certain structural organization of atoms, being beyond the nearest coordination sphere.

The present paper is devoted to examination of the prepeak origin in binary and ternary liquid alloys of aluminum with 3d-metals. Liquid Al-TM (TM = Mn, Co, Ni, Cu) [1], Al-Ni-TM (TM = Fe, Ni) [2], Al-Cu-TM (TM = Fe, Co, Ni) [3] alloys were investigated by X-ray diffraction (MoK – radiation) and the reverse Monte Carlo simulation. An analysis of the RMC models was performed using the Voronoi-Delaunay method. The prepeaks at $12 < Q/\mathrm{nm}^{-1} < 20$ were found in the total structure factor of liquid Al-rich alloys of all the investigated binary and ternary systems. The intensity of the prepeaks decreased considerably with an increase in temperature. We found that the prepeak in the total $S(Q)$ originated from the unique bonding between the TM-TM pair, as could be confirmed by the corresponding Faber-Ziman partial structure factors, $S_{\mathrm{TMTM}}(Q)$. The functions obtained from partial pair distributions showed that R_1(Al-TM) was the shortest nearest-neighbors distance that denoted a strong interaction between Al and TM atoms and the presence of a chemical short-range order (CSRO) in the melts. The high amplitude of the second peak in the $g_{\mathrm{TMTM}}(r)$ along with the shortest R_1(Al-TM) indicated that the TM atoms were located in the second coordination sphere of a portion of the TM atoms, thus suggesting a repulsion of TM-TM first neighbors. The Bhatia-Thornton partial structure factors were calculated as well. The shoulder on left side of the first peak of the $S_{CC}(Q)$ was placed in the region of the prepeak of the total $S(Q)$ which confirmed the correlation between the CSRO and the prepeak.

It was demonstrated by an analysis of structure models using the Voronoi-Delaunay method that the topological ordering was accompanied by a chemical short-range order in the case of binary and ternary Al-rich alloys with 3d-transition metals. This led to the emergence of dense-packed polytetrahedral clusters, where the TM atoms were localized at a distance of 0.4–0.5 nm in pentagon rings. The presence of dense-packed polytetrahedral clusters with a specific chemical-short-order contributed to the appearance of quasicrystal phases and their crystalline approximants.

References

[1] O. S. Roik, O. V. Samsonnikov, V. P. Kazimirov, V. E. Sokolskii, S. M. Galushko 2010 J. Mol. Liq. 151 42

[2] O. S. Roik, O. V. Samsonnikov, V. P. Kazimirov, V. E. Sokolskii 2010 Z. Naturforsch A. 65 123

[3] O. S. Roik, S. M. Galushko, O. V. Samsonnikov, V. P. Kazimirov, V. E. Sokolskii 2011 J. Non-Cryst. Solids 357 1147

Developments in medical devices having auxetic properties

M. Sanami, K. L. Alderson, A. Alderson

Institute for Materials Research and Innovation, University of Bolton
Deane Road, Bolton BL3 5AB, UK

At Auxetics 2010 in Malta we presented a poster describing preliminary Finite Element analyses of hip implant devices in which the stems exhibited auxetic properties. In this talk, further progress on hip implant devices and other biomedical device applications in which the auxetic effect can be usefully exploited will be presented. The presentation will include FE modelling and, where appropriate and available, comparison with experimental testing of demonstrator materials and devices.

Separation of various types of carbon nanotube mixutres into single- and multi-walled fractions via physicochemical methods

B. Scheibe, E. Borowiak-Paleń, R. J. Kaleńczuk

Institute of Chemical and Environment Engineering
West Pomeranian University of Technology
Pulaskiego 10, 70-322 Szczecin, Poland

This work presents separation of carbon nanotubes (CNTs) according to the number of walls. A mixture of CNTs containing single- and multi-walled carbon nanotubes was synthesized via an alcohol assisted chemical vapor deposition process (CVD). The raw material was purified from residual catalysts particles and amorphous carbon via hydrochloric acid treatment and annealing, respectively. Afterwards, the structural defects were removed by high temperature annealing under vacuum conditions. In order to prepare a mixture CNTs for the separation process, the van der Waals interactions were weakened by introduction of hydroxyl groups via a nitric acid oxidation process followed by sodium borohydrate reduction. Then, the mixture of CNTs was dispersed in a 2% sodium deoxycholate (DOC) solution in an ultra-sonication bath. The functionalized sample was separated according to the number of walls via the gradient agarose gel electrophoresis (GAGE) method and the density gradient ultracentrifugation (DGU) technique. At each step of purification the sample was investigated via Thermogravimetric Analysis (TGA) and Raman spectroscopy. After the separation procedures the samples were analyzed via Raman spectroscopy and High Resolution Transmission Electron Microscopy (HR-TEM).

Novel ice structures in carbon nanopores: pressure enhancement effect of confinement

M. Śliwińska-Bartkowiak[1], M. Jażdżewska[1], L. Huang[2], K. Gubbins[2]

[1] *Faculty of Physics, A. Mickiewicz University*
61-614 Poznań, Poland

[2] *Department of Chemical and Biomolecular Engineering*
North Carolina State University
Raleigh, NC, 27695, USA

Water confined in a nanoscale environment exhibits unique properties and has been the subject of much attention. There are at least 16 ice polymorphs of bulk water. The phase diagram of ice exhibits many different crystal forms, depending on local molecular correlations that influence the ordered arrangement of hydrogen-bonded configurations. Some of these forms are found only at pressures above 100 MPa (e.g. ice VII, VIII, IX, X and XI) and/or at temperatures below about 170 K (e.g. ice Ic, IX, XI), while some (e.g. cubic ice Ic) are metastable in the bulk.

We report experimental results on the structure and melting behavior of ice confined in multi-walled carbon nanotubes and ordered mesoporous carbon CMK-3, which is the carbon replica of a SBA-15 silica template. The silica template has cylindrical mesopores with micropores connecting the walls of neighboring mesopores. The structure of the carbon replica material CMK-3 consists of carbon rods connected by smaller side-branches, with quasi cylindrical mesopores of average pore size 4.9 nm and micropores of 0.6 nm. Neutron diffraction and differential scanning calorimetry have been used to determine the structure of the confined ice and the solid-liquid transition temperature. The results are compared with the behavior of water in multi-walled carbon nanotubes of inner diameters of 2.4 nm and 4 nm studied by the same methods. For D2O in CMK-3 we find evidence of the existence of nanocrystals of cubic ice and ice IX; the diffraction results also suggest the presence of ice VIII, although this is less conclusive. We find evidence of cubic ice in the case of the carbon nanotubes. For bulk water these crystal forms only occur at temperatures below 170 K in the case of cubic ice, and at pressures of hundreds or thousands of MPa in the case of ice VIII and IX. These phases appear to be stabilized by the confinement [1,2].

References

[1] M. Śliwińska-Bartkowiak, M. Jażdżewska, L. L. Huang, K. E. Gubbins, Phys. Chem. Chem. Phys., 2008, 10, 4957
[2] M. Jażdżewska, M. Śliwińska-Bartkowiak, A. I. Beskovnyy, S. G. Vasilovskiy, S. W. Ting, K. Y. Chan, L. Huang, K. E. Gubbins, Phys. Chem. Chem. Phys., **13**, 2011, 9008

Preparation of TiO$_2$/Graphene nanocomposite and its photocatalytic activity

M. Wojtoniszak, B. Zielińska, R. J. Kaleńczuk, E. Borowiak-Paleń

Centre of Knowledge Based Nanomaterials and Technologies
Institute of Chemical and Environment Engineering
West Pomeranian University of Technology
Poland

Graphene has attracted great interest since its discovery in 2004. Owing to its unique properties it is expected to be applicable in many fields such as nanoelectronics, sensors, nanocomposites and nanomedicine. Furthermore, the interest has broadened to the field of photocatalysis, recently. Here, we report a synthesis of TiO$_2$/graphene composite, where TiO$_2$ were deposited on few-layer graphene. The photocatalytic activity of the material was investigated by looking at the yield of phenol decomposition and hydrogen generation. Graphene and TiO$_2$/graphene were characterized with High Resolution Transmission Electron Microscopy (HR-TEM), Raman spectroscopy, X-ray Diffraction (XRD), Thermogravimetric Analysis (TGA) and Infrared spectroscopy (IR).

References

[1] A. Nowicki, M. Right, S. J. Dylan 2003 *J. Non-Cryst. Solids* **253** (2) 342

Low-temperature ordering effects in copolymer melts from lattice Monte Carlo simulation

S. Wołoszczuk, M. Banaszak

Faculty of Physics, Adam Mickiewicz University
Umultowska 85, 61-614 Poznań, Poland

Lattice computer simulations of block copolymer melts are reported. Low-temperature lamellar ordering was determined on the basis of translation and rotational diffusion, calculated for a variety of reduced temperatures. We present and discuss the results obtained for both diblock and triblock copolymer melts. Moreover, we consider the mechanical properties of triblocks by analyzing the bridging fraction as a function of the reduced temperature.

POSTERS

Negative Poisson's ratio
in smectic-C liquid crystal elastomers

J. Adams, A. Brown

Department of Physics, Faculty of Engineering & Physical Sciences
University of Surrey
GU2 7XH, United Kingdom

Models of smectic-C liquid crystal elastomers predict that it can display soft elasticity, in which the shape of the elastomer changes at no energy cost. The amplitude of the soft mode and the accompanying shears are dependent on the orientation of the layer normal and the director with respect to the stretch axis. We demonstrate that in some geometries the director is forced to rotate perpendicular to the stretch axis, causing lateral expansion of the sample; a negative Poisson's ratio. Current models do not include the effect of imperfections that must be present in the physical sample. We investigate the effect of a simple model of these imperfections on the soft modes in monodomain smectic-C elastomers in a variety of geometries. When stretching parallel to the layer normal (with imposed strain) the elastomer has a negative stiffness once the director starts to rotate. We show that this is a result of the negative Poisson's ratio in this geometry through a simple scalar model.

Stress-strain state of axisymmetric structures made of highly anisotropic composite material with auxetic properties

J. A. Baimova, S. V. Dmitriev

Institute for Metals Superplasticity Problems of RAS
Khalturins 39, 450001 Ufa, Russia

Developments in structural engineering design and technology necessitate the production of new high-performance materials. One advantage of composite materials is that they exhibit the highest qualities of their constituents and even certain qualities that none of their constituents possess. For example, composites reinforced with auxetic fibers can be made from conventional materials [1]. Currently, auxetic composite materials are attracting significant interest [2].

Materials exhibiting extreme elastic properties are closer to the boundary of thermodynamic stability than conventional materials. Large anisotropy, which triggers auxetic behavior, is a very common feature of fiber-reinforced composites. Thus, it is crucial to investigate the behavior of structural elements made of composite materials lying near the boundary of thermodynamic stability.

In the present study, we build on the work discussed in [3] and, using the finite element method, we analyze the stress-strain state of axisymmetric structures made of highly anisotropic composite materials exhibiting auxetic properties. We demonstrate the peculiarities of the stress and strain distribution in relatively thin-walled axisymmetric structures made of a highly anisotropic material. One of the counterintuitive manifestations of the auxetic properties of the material is the rapid change in the stress in the thickness direction.

References

[1] K. L. Alderson, V. R. Simkins, V. L. Coenen, P. J. Davies, A. Alderson, K. E. Evans, How to make auxetic fiber reinforced composites. Phys. Stat. Sol. (b) **242**, 509–518 (2005)

[2] K. W. Wojciechowski, A. Alderson, A. Branka, K. L. Alderson (eds.) Auxetics and related systems. Phys. Stat. Sol. (b) **242**, (2005)

[3] S. V. Dmitriev, N. Yoshikawa, R. R. Mulyukov, Rapid change of stresses in thickness direction in long orthotropic tube under internal pressure and axial load. Acta Mech. **211**, 323–336 (2010)

Morphology of nanostructured hard coatings made of S-phase

J. Baranowska, S. Fryska

Institute of Materials Science and Engineering, West Pomeranian University of Technology
Al. Piastów 17, 70-310 Szczecin, Poland

The paper presents the results of investigations on the morphology of S-phase hard coatings obtained by reactive magnetron sputtering. The coatings were produced using different process parameters (various substrate temperature, total and nitrogen partial pressure). Coatings 300–500 nm in thickness were obtained and they had a columnar structure. Grains ranging from a few to tens of nanometers in size were obtained depending on the deposition parameters (Figure 1). Depending on the process parameters it was possible to obtain coatings with a strong [200] or [111]
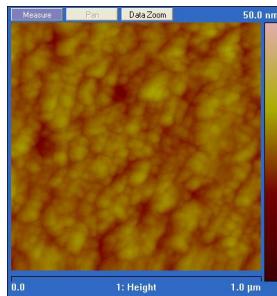
Figure 1: Grains structure on coating surface revealed by AFM
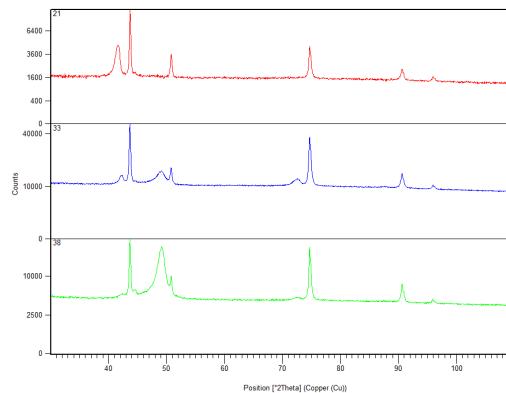
Figure 2: Examples of diffraction patterns for coatings with different texture; XRD

texture as well as coatings built of randomly oriented grains (Figure 2), which can be crucial for their mechanical properties.

The grain size was evaluated using AFM studies and XRD analysis. The latter was used to deremine the phase composition as well. The coatings structure was investigated by means of scanning electron microscopy.

Poisson's ratios of the cubic ion crystals

V. Belomestnykh, E. Soboleva

Yurga Institute of Technology of the National Research Tomsk, Polytechnical University
Leningradskaya st., 26, 652050, Yurga, Russia

The elastic properties of ionic monocrystals are studied rather intensively, however, their anisotropic Poisson's ratios practically have not been studied systematically. This work partially fills that gap, as it is devoted to calculations of Poisson's ratios along basic crystallographic directions of simple (in terms of composition and structure) ionic monocrystals with four types of lattices ($B1$, $B2$, $B3$, $NaClO_3$) under standard conditions, and varying temperature (LiF, NaCN) and pressure (CuCl).

Volume elasticity moduli and four Poisson's ratios along three special crystallographic directions of the monocrystals of studied ionic compositions are shown in Table 1. We note that the isothermal value B for $NaClO_3$ (marked with ***) exhibits a threefold decrease as compared to the adiabatic value for sodium chlorate. Data provided by Voigt show that over a period of at least 35 years ($NaClO_3$* in 1893; $NaClO_3$** in 1910; $NaClO_3$*** in 1928) [1,2] he returned to his experiments studying the elastic properties of the sodium chlorate monocrystal and obtained evidence that $c_{12} < 0$ for this substance. A recent study [3] has found out that for $NaClO_3$ c_{12} becomes negative in dynamic experiments as well, but not under room temperature as in Voigt's experiments – it becomes negative in dynamic experiments under the

Table 1: Volume elasticity modules and Poisson's ratios in cubic monocrystals

Substance	B (GPa)	$\rho_{\langle 100 \rangle}$	$\rho_{\langle 110,001 \rangle}$	$\rho_{\langle 110,1\bar{1}0 \rangle}$	$\rho_{\langle 111 \rangle}$
LiF	61.78	0.270	0.383	-0.039	0.118
NaCl	24.74	0.212	0.172	0.361	0.280
AgCl	44.12	0.376	0.232	0.614	0.432
NaCN	18.06	0.363	0.031	0.945	0.491
CsCl	18.25	0.202	0.142	0.438	0.309
TlCl	23.54	0.276	0.197	0.484	0.354
NH_4Cl	17.78	0.156	0.088	0.524	0.331
CuCl	39.29	0.444	0.856	-0.070	0.345
CuBr	38.83	0.436	0.792	-0.024	0.340
CuI	35.51	0.406	0.707	-0.036	0.281
$NaClO_3$	26.00	0.225	0.173	0.404	0.304
$NaBrO_3$	30.18	0.238	0.204	0.346	0.286
$NaClO_3$*	6.83	-0.511	-0.318	0.059	-0.059
$NaClO_3$**	7.68	-0.477	-0.284	0.121	-0.013
$NaClO_3$***	7.83	-0.476	-0.284	0.121	-0.013

temperature of about 260 K and 525 K. Such difference in the sign of the c_{12} constant in static and dynamic experiments for the monocrystal of this substance is not clear and requires further study. Anisotropic Poisson's ratios appeared to be negative for the direction $\langle 110 \rangle$ in the crystals of LiF, CuCl, CuBr and CuI. Absolute large positive Poisson's ratios are found for sodium cyanide ($\rho_{\langle 110,1\bar{1}0 \rangle} = 0.945$) and cuprous chloride ($\rho_{\langle 110,001 \rangle} = 0.856$). Three anisotropic isothermal Poisson's ratio for NaClO$_3$ (according to Voigt's data for c_{ij}) appeared to be negative, $\rho_{\langle 100 \rangle}$ being the most negative.

The diagram of the baric dependence of Poisson's ratios for cuprous chloride crystals (Figure 1, room temperature) is atypical. First of all, we note that all Poisson's ratios at the structure transition point $P_c\,B3 \rightarrow B1$ experience a discontinuity, which is characteristic of a phase transition of the 1$^{\text{st}}$ kind. The dependence of the anisotropic Poisson's ratios $\rho_{\langle 100 \rangle}$, $\rho_{\langle 111 \rangle}$ and isotropic ρ on pressure is linear in both phases of CuCl. Isotropic Poisson's ratio under the critical pressure P_c in $B2$ phase of CuCl approaches its extreme positive value.
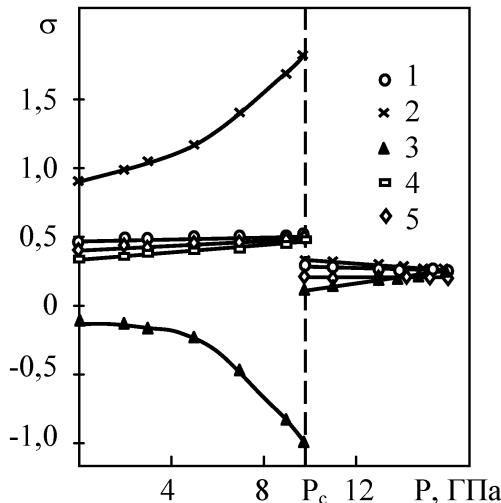
Figure 1: Changes of Poisson's ratios of CuCl crystal in the $B3 \rightarrow B1$ phases under pressure $1 - \rho_{\langle 100 \rangle}$, $2 - \rho_{\langle 110,001 \rangle}$, $3 - \rho_{\langle 110,1\bar{1}0 \rangle}$, $4 - \rho_{\langle 111 \rangle}$, $5 - \rho$ (polycrystal)

Poisson's ratios have significant dependence in the phase of conditionally low pressure when $P < P_c$ only when CuCl crystals are strained along the face diagonal $\langle 110 \rangle$. At the same time, lateral strains for this direction have opposite signs and are almost symmetrical. In the high pressure phase ($P > P_c$) of CuCl ($B1$) the linear changes of Poisson's ratios lead to approximately identical values and thus, in the vicinity of $P = 15$ GPa cuprous chloride crystal becomes elastically isotropic (or, at least, nearly isotropic).

Conclusion: This work is devoted to the study of anisotropic $\rho_{\langle hkl \rangle}$ Poisson's ratios of 36 ion, ion-molecular and ion-covalent cubic crystals with the following lattice types: $B1$ (NaCl), $B2$ (CsCl), $B3$ (ZnS, sphalerite) and NaClO$_3$. The study was performed under room temperature and atmospheric pressure. Relatively high positive

Poisson's ratios were found in crystals with essentially non-central interaction between the ions (alkali cyanides, silver and copper halogenides). Four of the five isothermal (static) Poisson's ratios of the $NaClO_3$ crystal (according to c_{ij} of Voigt) were negative, while all the adiabatic (dynamic) Poisson's ratios of this crystal were found to be positive. The dependence of the Poisson's ratios on pressure for the CuCl crystal was significantly different in the $B3$ ($P < P_c$) phase and in the $B1$ ($P > P_c$) phase. As the pressure was increased in the $0 - P_c$ (9.75 GPa) interval, a non-linear increase of $\rho_{\langle 110,001 \rangle}$ (116%) and non-linear decrease of $\rho_{\langle 110,110 \rangle}$ (700%) was observed. The Poisson's ratio of isotropic CuCl under a pressure of P_c reached its maximum positive value ($\rho = 0.485$), which is close to the extreme. At $B3 \rightarrow B1$ all the Poisson's ratios experienced a discontinuity. In the $B1$ phase the Poisson's ratios vary approximately linearly and near the pressure of $P = 15$ GPa the CuCl crystal is almost elastically isotropic.

References

[1] W. Voigt, 1893 Annalen der Physik und Chemie **49** 719
[2] W. Voigt, 1910, 1928 Lehrbuch der Kristallphysik, Leipzig, Leipzig und Berlin
[3] V. Belomestnykh, E. Soboleva, 2010 V Intern. conf. on physics of disordered systems PDS 10 181.

Stresses and strains in an auxetic ultra-high-molecular-weight polythelene (UHMWPE)

S. K. Bhullar[1], J. L. Wegner[1], A. Mioduchowski[2]

[1]*Department of Mechanical Engineering, University of Victoria*
Victoria, B.C., Canada

[2]*Department of Mechanical Engineering, University of Alberta*
Edmonton, AB, Canada

Wear remains a limiting factor in the longevity of ultra-high-molecular-weight polythelene components (e.g. for total joint replacement) and the magnitude and location of the stresses can vary substantially (in particular, for total knee replacement). A two-dimensional, plane strain elasticity solution for auxetic UHMWPE is modeled as half space to study strain and contact stresses arising from flat-on-flat, curved-on-flat, and curved-on-curved geometries. As it has been generally assumed that the perfect conformity of flat-on-flat designs minimizes the contact stresses (e.g. between the tibial and femoral components), the strains and contact stresses arising from these contacts are compared for perfect conformity.

Application of auxetics to the built environment

S. B. Bonnici[1], A. Torpiano[1], R. Gatt[2], J. N. Grima[2,3]

[1] *Department of Civil and Structural Engineering*
Faculty for the Built Environment, University of Malta
Msida, MSD 2080, Malta

[2] *Department of Chemistry, Faculty of Science, University of Malta*
Msida MSD 2080, Malta

[3] *Metamaterials Unit, Faculty of Science, University of Malta*
Msida MSD 2080, Malta

Auxetics exhibit the unusual feature of becoming fatter when placed in tension, and narrower when placed in compression. Therefore, they exhibit a negative Poisson's ratio, a counterintuitive behaviour that can impart many beneficial effects to macro, micro and nanostructures. This behaviour is induced in a structure or material by virtue of a specific combination of both its geometry and deformation mechanism. Auxetic behaviour has been found to be scale-independent, and hence research on the micro and nano levels can be applied to structures which are not a continuum, i.e. structures on the macro-level. This study discusses various auxetic structures, systems and material, some of which have been proposed and designed to be auxetic and others that exhibit auxetic characteristics as a result of their fundability (tensegrity) mechanism. A detailed study of the novel auxetic structure will also be discussed. The application of the above to habitation-scale macro-structures in then studied. Further applications of auxetics to structural engineering are then considered.

On stent design and Poisson's ratios

A. R. Casha[1], R. Gatt[2], M. Gauci[1], H. Vella[3],
K. Busuttil[4], J. N. Grima[2,5]

[1]*Mater Dei Hospital*
Msida MSD 2090, Malta

[2]*Department of Chemistry, Faculty of Science, University of Malta*
Msida MSD 2080, Malta

[3]*HM RD Ltd.*
Mosta Road, Lija, LJA 9016, Malta

[4]*Tek-Moulds Precision Engineering Limited*
B12 A Bulebel Industrial Estate, Zejtun ZTN 3000, Malta

[5]*Metamaterials Unit, Faculty of Science, University of Malta*
Msida MSD 2080, Malta

Stents are artificial tubes which are inserted into natural passages in the body such as coronary vessels to prevent or counteract localized flow constriction. Here we discuss the characteristics of some of the more commonly used stents from a geometry-deformation mechanism point of view and show how our knowledge on the design of systems with tailor-made Poisson's ratio can be used to design superior stents.

The effect of defects and missing connections on the Poisson's ratios and other properties of cellular systems with particular reference to their auxetic potential

A. R. Casha[1], R. Gatt[2], J. N. Grima[2,3]

[1]*Mater Dei Hospital*
Msida MSD 2090, Malta

[2]*Department of Chemistry, Faculty of Science, University of Malta*
Msida MSD 2080, Malta

[3]*Metamaterials Unit, Faculty of Science, University of Malta*
Msida MSD 2080, Malta

Auxetics are systems which exhibit a negative Poisson's ratio, i.e. get fatter when stretched and thinner when compressed. This anomalous behaviour is manifested in several honeycombs and cellular structures and may be explained in terms of various geometry / deformation mechanism based models. In particular, it has been proposed that auxetic behaviour may be obtained from re-entrant honeycombs which deform through hinging and/or hinging of the cell walls [1], rotation of rigid units [2,3] as well as mechanisms which involve selective removal of ribs in conventional honeycombs (missing ribs model) [4]. This work investigates the effect that defects have in cellular systems, in particular, how the removal of some structural unit within an auxetic or conventional system affects the mechanical properties, in particular the Poisson's ratios.

References

[1] L. J. Gibson, M. F. Ashby, G. S. Schajer, C. I. Robertson, The mechanics of two dimensional cellular solids. Proc. R. Soc. Lond. A 382 (1982) 25–42
[2] J. N. Grima, K. E. Evans, Auxetic behavior from rotating squares, Journal of Materials Science Letters, 19 (2000) 1563–1565
[3] J. N. Grima, A. Alderson, K. E. Evans, Auxetic behaviour from, rotating rigid units, Physica Status Solidi B-Basic Solid State Physics, 242 (2005) 561–575 [4] C. W. Smith, J. N. Grima, K. E. Evans, A novel mechanism for generating auxetic behaviour in reticulated foams: Missing rib foam model, Acta Materialia, 48 (2000) 4349–4356

Auxetic biomedical devices

A. R. Casha[1], M. Gauci[1], R. Gatt[2], J. N. Grima[2,3]

[1]*Mater Dei Hospital*
Msida MSD 2090, Malta

[2]*Department of Chemistry, Faculty of Science, University of Malta*
Msida MSD 2080, Malta

[3]*Metamaterials Unit, Faculty of Science, University of Malta*
Msida MSD 2080, Malta

This paper deals with the applications of auxetic materials in the field of medical devices and looks at the application of auxetics within patients or applied to patients and to devices that are used in the medical field.

In particular the use of auxetic materials with biomedical sensors, mattresses, surgical wire sutures, surgical non-slip braided suture material, dilator devices for coronary angioplasty, origami-type surgical stents, dental floss, smart filters, smart dressings, patches to release topical medication and auxetic artificial intervertebral discs is discussed.

The exponential increase in patents granted worldwide for applications of auxetic materials indicates that future developments in this field will be exciting especially in biomedical applications.

Acknowledgements

Influence of dielectric coverage on epitaxial thin films and photovoltaic conversion in solar cells obtained by epitaxial lateral overgrowth

K. Cieślak, S. Gułkowski, J. M. Olchowik

Lublin University of Technology
Nadbystrzycka 38, 20-618 Lublin, Poland

Thin film technologies which are based on silicon epitaxial lateral overgrowth (ELO) made by liquid phase epitaxy (LPE) are the main subject of this paper. This way of obtaining silicon layers can be easily used in photovoltaic applications. The main advantage of this method is a possibility of applying poor quality silicon growing substrates which decreases the costs of production, moreover liquid phase epitaxy apparatus does not require complicated systems which is also economical. All of these arguments lead to lowering the price of solar cells production.

We also made a special design of silicon epitaxial layers placed between two dielectric films – SiO_2 mask and anti-reflection coating causing light beam multi reflection from SiO_2-Si and SiN_x-Si surfaces and increasing the optical way of light inside the active layer. This increases the probability of absorption of light.

This work contains an analysis of the SiO_2 dielectric geometry influence on ELO thin films and solar photo-conversion efficiency. The layers used in our experiment were obtained in an LPE process in the same thermodynamical conditions: starting temperature of growth: $920°C$, temperature difference $\Delta T = 60°C$, ambient gas: Ar, metallic solvent: Sn+Al and in different cooling rates: $0.5°C/min$, $1°C/min$, $0.75°C/min$. We also used 4 dielectric masks with different geometry: grid opened in SiO_2 along $\langle 110 \rangle$ and $\langle 112 \rangle$ directions on a p+ boron doped (111) silicon substrate where silicon dioxide covers 65%, 68%, 75%, 80% of the silicon surface.

The results of our analyses show a correlation between efficiency and percentage of SiO_2 coverage on the obtained solar cells.

Molecular dynamics simulation study of liquid crystal phase in small mesogene cluster $(9CB)_{20}$

A. Dawid, Z. Gburski

Institute of Physics, University of Silesia
Uniwersytecka 4, 40-007, Katowice, Poland

We investigated a nano droplet composed of twenty mesogene molecules 4-n-alkyl-4'-cyanobiphenyl (9CB) using the molecular dynamics (MD) technique (Figure 1). The 9CB molecule geometry was calculated by the DFT method. We treated 9CB molecules as rigid bodies, the intermolecular interaction was taken to be the full site-site pairwise additive Lennard-Jones (LJ) potential. We calculated the radial and orientational distribution functions in the temperature range from 100 to 350 K, as well as the linear and angular velocity autocorrelation functions and their Fourier transforms. The 9CB molecules in the bulk material had the nematic liquid crystal phase in room temperature $T = 312$ K [1]. We observed liquid crystal ordering in the nanoscale system studied (Figure 2), up to its vaporization temperature.
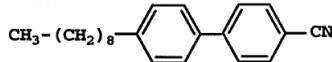
Figure 1: Chemical formula of 9CB (4-n-alkyl-4'-cyanobiphenyl) molecule
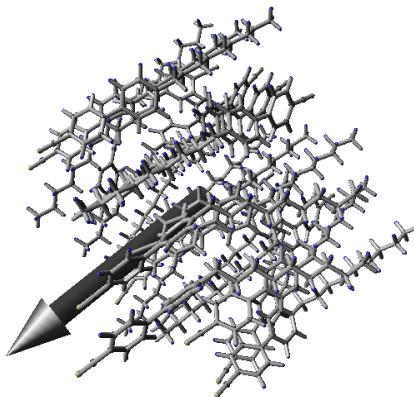
Figure 2: Instantaneous configuration of $(9CB)_{20}$ cluster at $T = 120$ K

References

[1] T. Manisekaran, T. K. Bamezai, N. K. Sharma, J. Shashidhara Prasad, Liquid Crystals, 1997, Vol. 23, No. 4, pp. 597–601

Spatial structure of thin 5CB mesogene layer between organoclay nanoplatelets: computer simulation study

A. Dawid[1], Z. Gburski[1], Ye. Shaydyuk[2]

[1]*Institute of Physics, University of Silesia*
Uniwersytecka 4, 40-007, Katowice, Poland

[2]*Institute of Physics, National Academy of Sciences of Ukraine*
46 Nauki Prosp., Kyiv 03022, Ukraine

Clays and organoclays are currently the subject of intensive study as they promise to play important roles in many areas of future technology ranging from medicine and molecular electronics to civil engineering. In this work nanocomposites of spatially confined liquid crystals between organo-clay nanoplatelets were investigated at temperatures between 293 and 310 K by a fully atomistic molecular dynamics simulation method. These nanomaterials may display unique properties intermediate between those of molecular and macroscopic regimes [1]. We simulated the structural and dynamical properties of 5CB molecules in nanoconfined space between organo-clay montmorillonite (MMT) nanoplatelets with a small inclusion of surfactant molecules octadecylbenzyldimethylammoniumchloride (B2) (Figure 1). We used the Van der Waals potential to calculate the forces acting on each site of the mesogene molecule.
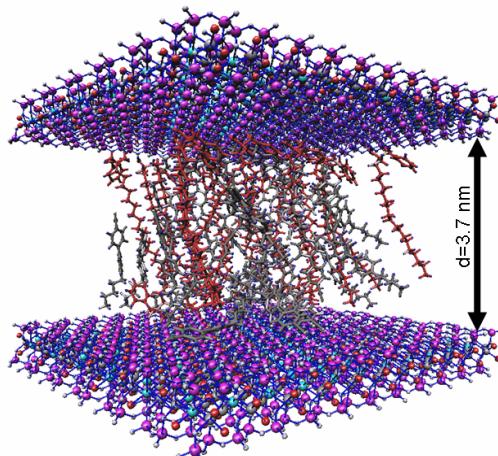
Figure 1: System instantaneous configuration at $T = 300$ K

P12

We calculated the linear and angular velocity autocorrelation function, radial distribution function, mean square displacement function, dipole moment correlation function and second rank order parameter. Although there are some experimental results of the system studied [2] the mechanism of molecular ordering in the layer is still unknown. Our work may contribute to these investigations.

References

[1] M. Kawasumi, et al. 1996 Mol Cryst. Liq. Cryst. 281, pp. 91–103

[2] I. Chashechnikova, L. Dolgov, T. Gavrilko, G. Puchkovska, Ye. Shaydyuk, N. Lebovka, V. Moraru, J. Baran, H. Ratajczak 2005 J. Mol. Struct. 744–747 , pp. 563–571

Influence of fullerenols $C_{60}(OH)_{24}$ on nitric oxide dynamics in water solvent: MD study

A. Dawid, K. Górny, Z. Gburski

Institute of Physics, University of Silesia
Uniwersytecka 4, 40-007, Katowice, Poland

The nitric oxide is known as one of the most important signaling molecules in a mammal's body. If only to mention that NO plays the key role in physiological processes as an intracellular and intercellular messenger [1]. In the current work we simulated the dynamics of NO molecules in pure water and also in a mixture of water and water soluble fullerenol molecules (Figure 1). The simulations were fully atomistic with intramolecular and intermolecular potentials. The striking difference between the dynamics of NO in pure water and in the mixture was observed by calculating the velocity autocorrelation function and the mean square displacement function of nitric oxide molecules.
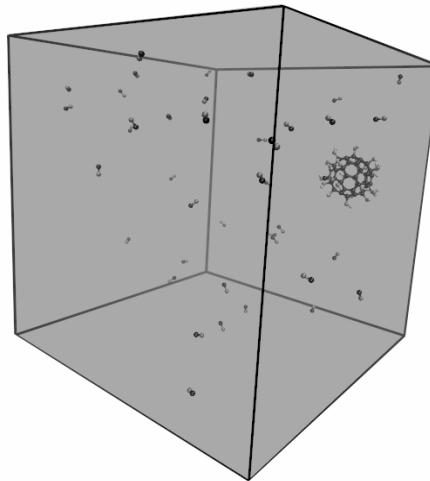
Figure 1: Snapshot of an instantaneous configuration of an ensemble consisting of fullerenol and NO molecules in water (water molecules are not shown for clarity)

References
[1] M. A. Tegenge, G. Bicker, J. Neurochem. 110 (2009) pp. 1828–1841

Dipolar relaxation of ethylene glycol confined in single walled carbon nanotube: computer simulation study

Z. Dendzik, K. Górny, Z. Gburski

Institute of Physics, University of Silesia
Uniwersytecka 4, 40-007 Katowice, Poland

The properties of molecules in nanoscale confinement are of great interest to biology, geology and materials science. Molecular systems embedded in carbon nanotubes are studied not only for fundamental reasons, but also for their potential importance in practical applications in energy storage, nanoelectronic devices, chemical biosensors, field emission displays and many others [1]. One important reason for studying water inside carbon nanotubes is that it is a biomime, a model for ion channels and mass transport through biological membranes [2]. The properties of water and other polar molecules embedded in carbon nanotubes have been intensively studied experimentally [3–5] and using computer simulation methods [3,6–10]. We performed all atom molecular dynamics simulations to study the geometrical confinement effect and interface interaction on the dynamical properties of ethylene glycol confined in single walled carbon nanotubes of different chirality.

References

[1] D. Mattia, Y. Gogotsi 2008 Microfluid. Nanofluid. 5 289
[2] F. Zhu, K. Schulten 2003 Biophysical Journal 85 236
[3] A. Kolesnikov, J. Zanotti, C. Loong, P. Thiyagarajan, A. Moravsky, R. Loutfy, C. Burnham 2004 Phys. Rev. Lett. 93 35503
[4] M. Rossi, H. Ye, Y. Gogotsi, S. Babu, P. Ndungu, J. Bradley 2004 Nano Lett. 4 989
[5] B. Kim, S. Sinha, H. Bau 2004 Nano Letters 4 2203
[6] Z. Dendzik, K. Gorny, Z. Gburski 2009 J. Phys.: Condens. Matter 21 425101
[7] J. Marti, MC. Gordillo 2002 J. Chem. Phys. 114 10486
[8] G. Garberoglio 2010 Eur. Phys. J. E 31 73
[9] Y. Lin, J. Shiomi, S. Maruyama, G. Amberg 2009 Phys. Rev. B 80 045419
[10] J. Kofinger, C. Dellago 2009 Phys. Rev. Lett. 103 080601

Numerical simulations of solitary waves in auxetic rods with quadratic nonlinearity

T. Bui Dinh[1], V. Cao Long[1], K. W. Wojciechowski[2,3]

[1]*Institute of Physics, University of Zielona Gra*
Prof. A.Szafrana 4a, 65-516 Zielona Gra, Poland

[2]*Institute of Molecular Physics, Polish Academy of Sciences*
Smoluchowskiego 17, 60-179 Poznań, Poland

[3]*President St. Wojciechowski PWSZ*
Nowy Świat 4, 62-800 Kalisz, Poland

Propagation of solitary waves in auxetic rods is studied by numerical simulations. Splitting of various initial pulses during propagation into a sequence of solitary waves is considered in the framework of a model in which the double dispersion equation (or Porubov's equation) [1–4] contains only the quadratic term. This work extends the results of a recent study described in [5]. The dependence of the amplitude and the velocity of the solitary waves on the Poisson's ratio is discussed in detail. Collisions between certain solitary waves obtained are also presented.

The simulation results are compared with certain exact analytical solutions – the latter reflect the balance between the nonlinearity and dispersion. The comparison indicates that the particular exact solutions are useful for describing more complicated wave fields obtained from numerical simulations.

References

[1] A. V. Porubov, G. A. Maugin, *Improved description of longitudinal strain solitary waves*, Journal of Sound and Vibration **310**, 694–701 (2008)

[2] A. V. Porubov, *Amplification of nonlinear strain waves in solids*, World Scientific, Singapore (2003)

[3] A. M. Samsonov, *Strain Solitons in Solids and How to Construct Them*, Chapman & Hall / CRC, New York (2001)

[4] V. I. Erofeev, N. V. Erofeeva, *Solitons and nonlinear periodic strain waves in rods, plates and shells (a review)*, Acoustical Physics **48**, 643–655 (2002)

[5] P. Kolat, B. M. Maruszewski, K. W. Wojciechowski, *Solitary waves in auxetic rods*, Physica Status Solidi B **248**, 148–157 (2011)

Electromagnetically induced transparency for system with double autoionizing levels

T. Bui Dinh, W. Leoński, V. Cao Long

Quantum Optics and Engineering Division
Institute of Physics, University of Zielona Góra
Prof. A. Szafrana 4a, 65-516 Zielona Góra, Poland

There are various papers concerning the problem of Fano resonance in nano-physics systems. For instance, in [1], a model of two indirectly coupled tiny resonators has been considered in the context of asymmetric Fano resonance. Similarly, the Fano effect on photon statistics for a quantum dot-metal nano-particle has been discussed in [2]. Moreover, as has been recently shown in [3], metamaterial with double continuum can exhibit the electromagnetically induced transparency (EIT) effect.

It has been the subject of much consideration since the first works concerning EIT (for instance, see the classical paper [4]). This phenomenon is a result of quantum interference between various transitions from one to other atomic levels. Such levels can be configured in various ways forming cascade (*ladder*), Λ or V configurations, whereas the transitions are induced by the *probe* and *strong* external fields. As a result of such interference, the absorption and refraction may be eliminated. The separate group of systems that can be a source of EIT phenomena are those involving continuum states. In particular, models with autoionizing (AI) levels can lead to various interesting interference effects. For instance, such interferences can lead to the *confluence of coherences* phenomenon discussed in [5,6].

Quite recently, Raczyński *et. al.* [7] have shown that the EIT effect can be observed for a Λ-like system, where the upper discrete level has been replaced by a structured Fano continuum. As has been shown in [8], such continuum is equivalent to the flat one interacting with a single AI level. In this communication, we concentrate on a case when two AI levels are involved. As has been shown in [6], an additional AI level can lead to quantum interferences that are absent for single AI level models. We also show that for EIT such interferences lead to new interesting effects. Particularly, an additional zero appears for the imaginary part of medium susceptibility χ – such a zero leads to the vanishing of the considered medium's absorption. We present derived analytical formulas that enable us to investigate the dependence of susceptibility on the parameters describing the AI system.

References

[1] Yun-Feng Xiao, Min Li, Yong-Chun Liu, Yan Li, Xiudong Sun, Qihuang Gong 2010 *Phys. Rev. A* **82** (6) 065804

[2] A. Ridolfo, O. Di Stefano, N. Fina, R. Saija, S. Savasta 2010 *Phys. Rev. Lett.* **105** (26) 263601

[3] C. Wu, A. B. Khanikaev, G. Shvets 2011 *Phys. Rev. Lett.* **106** (10) 107403

[4] S. E. Harris, J. E. Field, A. Imamoğlu 1990 *Phys. Rev. Lett.* **64** (10) 1107

[5] K. Rzązewski, J. H. Eberly, 1981 *Phys. Rev. Lett.* **47** (6) 408

[6] W. Leoński, Tanaś, S. Kielich, 1987 *J. Opt. Soc. Am. B* **4** (1) 72

[7] A. Raczyński, M. Rzepecka, J. Zaremba, S. Zielińska-Kaniasty, 2006 *Optics Commun.* **266** 552

[8] U. Fano, 1961 *Phys. Rev.* **124** (6) 1866

Noise reduction in Raman Ring Laser by two-telegraph pre-Gaussian pump

K. Doan Quoc, V. Cao Long, W. Leoński

Quantum Optics and Engineering Division
Institute of Physics, University of Zielona Góra
Prof. A. Szafrana 4a, 65-516 Zielona Góra, Poland

Laser lights are generally fluctuating in amplitude and phase. Due to the very complicated (in many cases even obscure) microscopic nature of all the relevant relaxation mechanisms, we model the laser lights by classical time-dependent random processes. The dynamical equations involved in the considered problem become stochastic differential equations. Except for some special cases, the obtaining of an exact solution for such stochastic equations is a very difficult task. One of the most useful stochastic models has been introduced by Wódkiewicz et al. [1–4] which is based on the so-called pre-Gaussian process. It is composed of a finite number of independent telegraph signals mentioned above. The strength of the pre-Gaussian formalism derives from the exact solubility of wide classes of stochastic equations.

In this communication, we will consider the Raman Ring Laser by using the stochastic equation given in [5]. In consequence, we will obtain the so-called noise reduction in this system: the Stokes output of this laser tends to stabilize under the influence of a broad-band two-telegraph pre-Gaussian pump. This phenomenon has been considered recently for the case of telegraph noise in [6].

References

[1] K. Wódkiewicz, B. W. Shore, J. H. Eberly 1984 *J. Opt. Soc. Am.* **B1** 398
[2] K. Wódkiewicz, B. W. Shore, J. H. Eberly 1984 *Phys. Rev.* **A30** 2390
[3] J. H. Eberly, K. Wódkiewicz, B. W. Shore 1984 *Phys. Rev.* **A30** 2381
[4] Cao Long Van, K. Wódkiewicz 1986 *J. Physics* **B19** 1925
[5] M. Lewenstein, K. Rzążewski, 1987 *Optics Comm.* **63** 174
[6] Cao Long Van, Doan Quoc Khoa, submitted to publication

The effect of solvents on polyurethane foams as applied to production of auxetic foam

R. Gatt[1], A. Buttigieg[1], J. N. Grima[1,2]

[1]*Department of Chemistry, Faculty of Science, University of Malta*
Msida MSD 2080, Malta

[2]*Metamaterials Unit, Faculty of Science, University of Malta*
Msida MSD 2080, Malta

Auxetics are counterintuitive materials which become fatter rather than thinner when uniaxially stretched. The first man-made auxetic was an auxetic foam which was prepared by converting a conventional foam to an auxetic one using a thermo-mechanical method [1]. Later, it was also proposed that a chemo-mechanical method could be used for the same conversion [2]. In this work, the interaction between a number of solvents and conventional polyurethane foam will be described. Such information is very significant as it can be used to improve the chemo-mechanical method used for the conversion of conventional foams to auxetic foams.

References
[1] R. S. Lakes, Foam structures with a negative Poissons ratio, Science 235 (1987) 1038–1040
[2] J. N. Grima, D. Attard, R. Gatt and R. N. Cassar, A Novel Process for the Manufacture of Auxetic Foams and for Their re-Conversion to Conventional Form, Advanced Engineering Materials, 11 (2009) 533–535

Kinetics on anatase-rutile phase transformation in single-modified TiO$_2$

M. Glen, B. Grzmil

Institute of Chemical and Environment Engineering
West Pomeranian University of Technology
Pułaskiego 10, 70-322 Szczecin, Poland

Hydrated titanium dioxide is calcined in order to obtain TiO$_2$ pigments in the sulfate process. Rutile is formed as a result of the polymorphous transformation. Different modifiers are introduced into the calcination suspension. Modifiers are added to obtain the required properties of the produced material, such as a suitable crystallite size of individual phases, proper values of optical properties and photostability.

In the present work the influence of small amounts of B$_2$O$_3$, CeO$_2$, Sb$_2$O$_3$, ZnO and ZrO$_2$ on the anatase-rutile phase transformation was determined. Solutions of modifiers were introduced to the starting material which was technical grade hydrated titanium dioxide (HTD). The prepared samples were calcined isothermally in the temperature range of 725–925°C. The phase transformation kinetics of the obtained samples was studied using XRD analysis. The activation energy of rutile crystallization was estimated on the basis of the Johnson-Mehl-Avrami-Kozolog (JMAK) equation.

Dipolar relaxation of glycerol nanodroplet in non-polar soft confinement: computer simulation study

K. Górny, Z. Dendzik, Z. Gburski

Institute of Physics, University of Silesia
Uniwersytecka 4, 40-007 Katowice, Poland

The behavior of water and other hydrogen bonded liquids in nanoscale porous media is of great interest to biology, geology and materials science and has been extensively investigated experimentally [1–6] and by means of computer simulations [7–12]. Molecular systems embedded in carbon nanotubes are interesting both from the scientific point of view and also because of their potential applications in energy storage, nanoelectronic devices, chemical biosensors, field emission displays and many others [13–15]. One important reason for studying water inside carbon nanotubes is that it is a biomime, a model for ion channels and mass transport through biological membranes [16]. We performed all atom molecular dynamics simulations for a glycerol nanodroplet confined in non-polar m-xylene soft confinement to study the effect of geometrical confinement and interface interactions.

References

[1] P. Pissis, D. Daoukaki-Diamanti, L. Apekis, C. Christodoulides 1994 J. Phys.: Condens. Matter 6 L325
[2] W. Gorbatschow, M. Arndt, R. Stannarius, F. Kremer 1996 Europhys. Lett. 35 719
[3] J. Swenson, G. Schwartz, R. Bergman, W. Howells 2003 Eur. Phys. J. E 12 179
[4] S. Cerveny, J. Mattson, J. Swenson, R. Bergman 2004 J. Phys. Chem. B 108 11596
[5] F. Kremer 2002 J. Non-Crystalline Solids 305 1
[6] M. Alcoutlabi, G. McKenna 2005 J. Phys.: Condens. Matter 17 R461
[7] P. Scheidler, W. Kob, K. Binder 2000 Europhys. Lett. 52 277
[8] P. Scheidler, W. Kob, K. Binder 2002 Europhys. Lett. 59 701
[9] I. Brovchenko, A. Geiger, A. Oleinikova, D. Paschek 2003 Eur. Phys. J E 12 69
[10] M. Rovere, P. Gallo 2003 Eur. Phys. J. E 12 77
[11] P. Raczyński, A. Dawid, M. Sokół, Z. Gburski 2007 Biomolecular Engineering 24 572
[12] A. Dawid, Z. Gburski 2007 J.Non-Crystalline Solids 353 4339
[13] A. Dillon, K. Jones, T. Bekkedahl, C. Kiang, D. Bethune, M. Heben 1997 Nature 386 377
[14] P. Chen, X. Wu, J. Lin, K. Tan 1999 Science 285 91
[15] J. Lu, J. Han 1998 Int. J. High Speed Electron. Syst. 9 101
[16] F. Zhu, K. Schulten 2003 Biophysical Journal 85 236

Dipolar relaxation of propylene glycol and ethylene glycol confined in ZSM 5 zeolite channels: computer simulation study

K. Górny, Z. Dendzik, P. Raczyński, Z. Gburski

Institute of Physics, University of Silesia
Uniwersytecka 4, 40-007 Katowice, Poland

We performed all atom computer simulations of molecular dynamics of propylene glycol and ethylene glycol confined in a ZSM 5 zeolite host matrix in order to study the dipolar relaxation process characteristic in this system and compare it to the recently published results for similar molecular systems confined in single walled carbon nanotubes [1,2]. There is some indication that a 1D chain of hydrogen bonded structured molecules confined inside sub 1 nm channels is exposing the pure Debye characteristic of dipolar relaxation [3,4], as opposite to more complex molecular structures confined inside channels of larger diameters [1,2,5], which retain the stretched exponential characteristic observed in bulk liquids. The structure of propylene glycol molecules inside the channels of a ZSM 5 host system are 1D chains of single molecules, it is also of interest to find out whether this system exhibits the pure Debye characteristic as in case of water chains confined inside carbon nanotubes or it retains its stretched exponential characteristic observed in the case of molecules confined inside channels of larger diameters. We focused on the influence of the geometric confinement inside ZSM 5 1D channels and interaction with the host system on the observed change in the character of deviation from exponential relaxation, as well as on the thermal activation characteristic of the process.

References

[1] Z. Dendzik, K. Górny, Z. Gburski 2009 J. Phys.: Condens. Matter 21 425101
[2] Z. Dendzik, K. Górny, W. Gwizdała, Gburski Z 2010 J. Non-Crystalline Solids 357 575
[3] J. Kofinger, C. Dellago 2009 Phys. Rev. Lett. 103 080601
[4] J. Kofinger, C. Dellago 2010 Phys. Rev. B 82 205416
[5] Z. Dendzik, M. Kosmider, M. Sokól 2008 J. Non-Crystalline Solids 354 4300

Metal oxide nanoparticle arrays formed in nanoreactors based on porous silicon

I. E. Gracheva, V. A. Moshnikov, A. S. Lenshin, V. V. Kuznetsov, Y. M. Spivak, M. G. Anchkov

Microelectronics Department, Saint-Petersburg State Electrotechnical University
5 Professora Popova Street, 197376 Saint-Petersburg, Russia

Sol-gel sintering [1–3] in nano-and microvolumes are in focus of high interest for theory as well as for application. Electrochemical methods could be used to obtain nanoreactors for such proposes.

In this paper sol-gel process [4–7] produced nanovolumes of porous silicon of a dendrite-type structure of pores. Samples of porous silicon [8] were obtained by electrochemical anodization of monocrystalline silicon in HF solutions. Solutions-sols based on semiconductors of n- type: metal oxides of Fe, Ni, Co, Sn, were introduced in nanoreactors of such kind.

Solutions-sols were obtained on the basis of binary heterochain inorganic polymers, whose atoms formed ion-covalent bonds between each other. The initial pre-courses used for preparation of solutions-sols are easily hydrolyzed components. Such components formed poly-molecules or poly-solvated groups due to interaction with water. Tetraethoxysilane (TEOS, $Si(OC_2H_5)_4$) was chosen to obtain nanostructured films of silicon dioxide. TEOS solutions helped to improve film-forming qualities and the ability to spread over the surface of porous silicon. Hydrolysis and polycondensation of TEOS in the presence of inorganic salts of iron, nickel, tin and cobaltwere carried out to obtain two-component oxide materials based on silicon dioxide.

The morphology study of porous silicon with embedded metal oxide nanoparticles (Figure 1) was carried out by atomic force microscopy (equipment Ntegra Terma (NT-MDT)). Porous silicon cross-sections were examined by scanning electron microscopy (Figure 2). Also, experimental data of luminescence spectra are discussed in this paper.

Studies of the electrical properties of nanomaterials based on porous silicon with the introduced metal oxide nanoparticles were performed by using impedance spectroscopy. The impedance spectra were registered in the frequency range from 1 Hz to 0.5 MHz at a combined installation using impedance meter «Z-500 P» (OOO «Elins»). This equipment allows nanostructures to be studied by impedance spectroscopy in changing gas environment and temperature of gas detection.
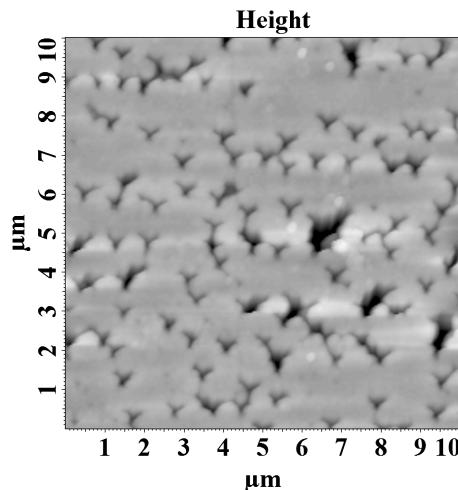
Figure 1: AFM image of porous silicon with embedded metal oxide nanoparticles
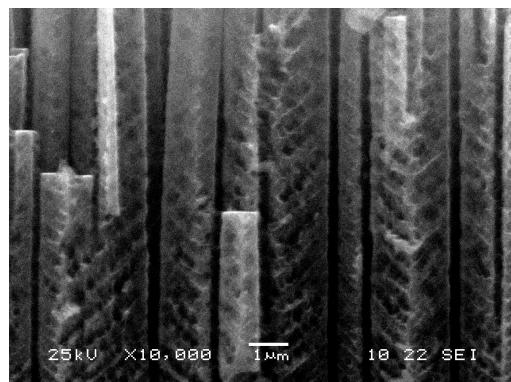
Figure 2: SEM image of porous silicon with embedded metal oxide nanoparticles

References

[1] Handbook of sol-gel science and technology: processing, characterization, and applications. Ed. Sumio Sakka. New York, 2004, V. 1–3

[2] R. Corriu, T. A. Nguyên, Molecular Chemistry of Sol-Gel Derived Nanomaterials. John Wiley & Sons, 2009

[3] A. I. Maximov, V. A. Moshnikov, Yu. M. Tairov, O. A. Shilova, Basics of sol-gel technology of nanocomposites. Second issue. "Tehnomedia". SPb.: "Elmor", 2008, p. 255

[4] V. A. Moshnikov, I. E. Gracheva, V. V. Kuznezov et al., Hierarchical nanostructured semiconductor porous materials for gas sensors, *Journal of Non-Crystalline Solids* 356, 2010, p. 2020–2025

[5] I. E. Grachova, A. I. Maksimov, V. A. Moshnikov, Analysis of structural features of tin dioxide-based fractal nanocomposites by atomic-force microscopy and X-ray diffraction, *Journal of Surface Investigation. X-ray, Synchrotron and Neutron Techniques* 3(5), 2009, p. 761–768

[6] I. E. Gracheva, Y. M. Spivak, V. A. Moshnikov, AFM techniques for nanostructures materials used in optoelectronic and gas sensors, *Eurocon-2009. International IEEE Conference*, May 18–2, 2009, Saint-Petersburg, Russia, 2009, p. 1250–1253

[7] I. E. Grachova, S. S. Karpova, V. A. Moshnikov, Gas-sensitive hierarchial porous nanostructuresz for multisensor systems, *Annual proceedings the Technical University of Varna*, 2010, p. 97–102

[8] S. Yu. Turishchev, A. S. Lenshin, E. P. Domashevskaya et al., Evolution of nanoporous silicon phase composition and electron energy structure under natural ageing. ıPhys. Status Solidi C 6(7), 2009, p. 1651–1655

Negative Poisson's ratios and negative compressibility in three dimensional structures

J. N. Grima[1,2], R. Caruana-Gauci[2], D. Attard[2], R. Gatt[2]

[1]*Metamaterials Unit, Faculty of Science, University of Malta*
Msida MSD 2080, Malta

[2]*Department of Chemistry, Faculty of Science, University of Malta*
Msida MSD 2080, Malta

A model of the elongated hexagonal dodecahedron, considered to be a three dimensional cellular system [1] is studied in detail. It is shown that this system may be made to exhibit some very unusual mechanical properties, including negative Poisson's ratio, zero Poisson's ratio and negative linear and area compressibility. Such behaviour of the system may be obtained from particular conformations of the model and is scale independent. Results predicted from the derived analytical model compare well to those obtained from numerical modelling showing that this 3D system can exhibit zero Poisson's ratios in one of its planes and positive or negative Poisson's ratios in other planes, depending on the geometry of the model.

Acknowledgements

References
[1] K. E. Evans, M. A. Nkansah, I. J. Hutchinson, Acta Metallurgica et Materialia, 42 (1994) 1289–1294

Negative Poisson's ratios
in the aluminophosphate APD

J. N. Grima[1,2], M. Zammit[1], R. Gatt[1], D. Attard[1]

[1] *Department of Chemistry, Faculty of Science, University of Malta*
Msida MSD2080, Malta

[2] *Metamaterials Unit, Faculty of Science, University of Malta*
Msida MSD2080, Malta

Auxetic materials exhibit the unusual property of becoming fatter when stretched. This phenomenon has been predicted and/or discovered in various materials, including zeolites. In this work, force-field based simulations are used to analyse the mechanical properties and deformation mechanism for the aluminophosphate APD. In particular, the crystal structure of APD is modelled using different force-fields which suggest that this aluminophosphate may be auxetic in its (100), (010) and (001) plane, with maximum auxeticity being predicted in its (010) plane for loading at 45° off-axis. The nanolevel deformations occurring in APD at different stress levels were also simulated and it is shown that a rotating quadrilateral mechanism is likely to be responsible for the predicted auxetic behaviour in the (010) plane.

Modelling of liquid crystalline polymers with anomalous mechanical properties

J. N. Grima[1,2], Ch. Zerafa[1], A. C. Griffin[3]

[1]*Department of Chemistry, Faculty of Science, University of Malta*
Msida MSD2080, Malta

[2]*Metamaterials Unit, Faculty of Science, University of Malta*
Msida MSD2080, Malta

[3]*School of Materials Science and Engineering, Georgia Institute of Technology*
801 Ferst Drive, Atlanta, GA 30332-0295 USA

In recent years, considerable advances have been made in the field of liquid crystalline polymers (LCPs), particularly those exhibiting a negative Poisson's ratio. This property arises from a mechanism that involves re-orientation of laterally attached rod-like units which are aligned along the direction of the main polymer chain in the unstressed state, and then rotate to the orthogonal direction in the stressed state. This deformation mechanism gives rise to a lateral expansion due to an increase in the inter-chain distance when the polymer is stretched. Here we present the results of molecular mechanics and molecular dynamics simulations performed using the PCFF force-field on such polymeric systems. These simulations suggest that when such polymers are stretched along the direction of the main chain, the systems are conventional at small strains but auxetic in some planes at higher strains. It was also found that certain polymers got thicker in certain planes but narrower in others.

Studies on obtaining of aluminum calcium phosphates

B. Grzmil, K. Łuczka

Institute of Chemical and Environment Engineering
West Pomeranian University of Technology
Pułaskiego 10, 70-322 Szczecin, Poland

Borates, molybdates, phosphites and phosphates have been widely tested as anti-corrosive fillers in organic coatings. Currently, zinc phosphate is the most commonly used anticorrosive phosphate filler. Nevertheless, few mentions about the harmfulness of zinc phosphate on the natural environment (mainly on naval organisms) have been made. These are reasons for intensive research on chemical modification of the mentioned phosphate mainly with Al, Ca and/or Fe.

The objective of these studies was to develop a preparation method of aluminum calcium phosphate nanoparticles with the use of inorganic compounds as precursors. Analytical-grade reagents were used. Phosphates were prepared by reaction of various substrates either in an aqueous solution or in a suspension. The influence of process parameters (molar ratio of substrates, concentration, temperature, pressure) on the phase composition and properties of products was determined. The phase composition of the obtained samples was studied using XRD analysis.

Simulations of interface evolution during epitaxial growth on partially masked substrate

S. Gułkowski, J. M. Olchowik, K. Cieślak

Lublin University of Technology
Nadbystrzycka 38, 20-618 Lublin, Poland

High quality thin Si layers obtained from the liquid phase by the Epitaxial Lateral Overgrowth (ELO) method can play a crucial role in photovoltaic applications. Laterally overgrown parts of a layer are characterized by lower dislocation density than the substrate. The layer thickness and width depend on the technological conditions of the LPE process, basically the growth temperature, the cooling rate and geometry of the system (mask filling factor). Therefore, it is very important to find an optimal set of growth parameters for obtaining very thin structures with maximum width (high aspect ratio).

This paper presents a two-dimensional computational study of the epilayer interface evolution for different conditions. The solute concentration in the Si-Sn solution was determined after each time step in order to calculate the interface motion. A new interface position was obtained by calculating the growth rate normal to the interface. The growth rate was computed from the concentration gradients near the growing surface. The Finite Element Method was used to solve the mass transport problem.
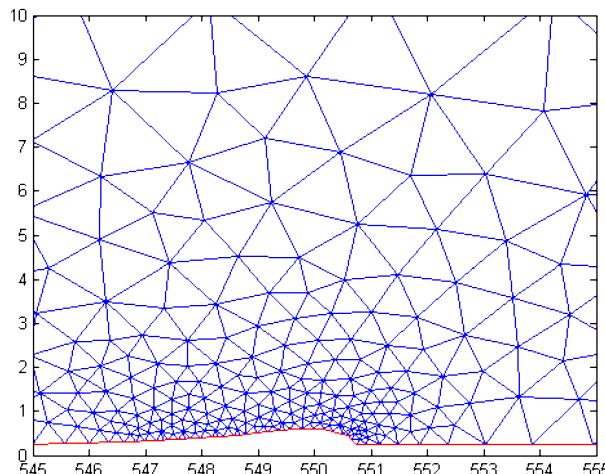

Figure 1: Adaptive mesh used to calculate concentration of Si in Si-Sn solution near growing layer edge

Simulations were carried out to obtain growth rates in the lateral and normal direction and the aspect ratio of epilayer for given conditions. The calculation results were compared with the experiments.
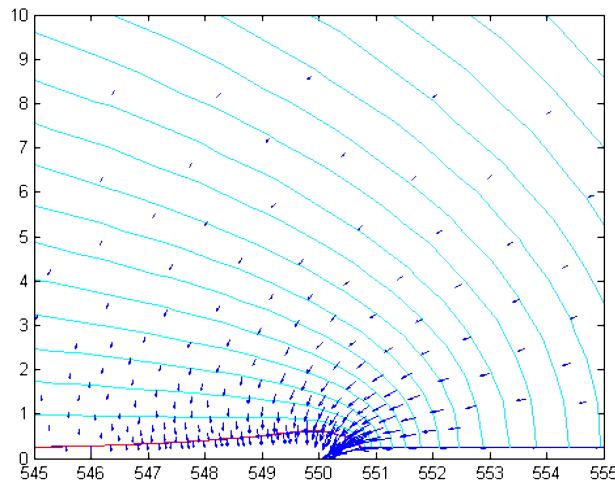

Figure 2: Solute transport in solution near growing layer interface edge

Spin reorientation processes in 0.95MnO/0.05ZnO nanocrystalline system studied by FMR

N. Guskos[1,2], M. R. Dudek[3], G. Żołnierkiewicz[2], J. Typek[2], A. Guskos[2], D. Sibera[4], U. Narkiewicz[4]

[1]*Solid State Section, Department of Physics, University of Athens*
Panepistimiopolis, 15 784, Greece

[2]*Institute of Physics, West Pomeranian University of Technology*
Al. Piastów 48, 70-311 Szczecin, Poland

[3]*Institute of Physics, University of Zielona Góra*
Szafrana 4a, 65-069 Zielona Góra, Poland

[4]*Institute of Chemical and Environmental Engineering*
West Pomeranian University of Technology
Al. Piastów 17, 70-310 Szczecin, Poland

A nanocrystalline $0.95(Mn_2O_3)/0.05ZnO$ sample was prepared by coprecipitation and calcination processes. The phase composition, determined by X-ray diffraction, was dominated by the Mn_3O_4 phase, but a very low concentration of $ZnMn_2O_4$ phase was also identified. The ferromagnetic resonance (FMR) investigation of the obtained sample was carried out in the temperature range from liquid helium to room temperature (RT). The presence of an asymmetrical and very intense magnetic resonance line was recorded in two different temperature ranges: one from 4 K up to 20 K, another significant shift of the line from RT down to 41 K towards lower magnetic fields with decreasing temperature was observed in both cases at low temperatures. A very good fitting by two Lorentzian functions was obtained which suggested the existence of anisotropy of magnetic interactions. The FMR spectra of the ferrimagnetic Mn_3O_4 phase dominated at low temperatures while strong magnetic interaction attributed to $ZnMn_2O_4$ was observed at high temperatures. The correlated spin system could transfer energy to the other spin system and the dipole-dipole broadening processes could account for the disappearance of the FMR spectra of Mn_3O_4 below 41 K. A large shift of the FMR resonance line arising from $ZnMn_2O_4$ ferrite suggested the existence of a strongly coupled spin system. A theoretical model was constructed to explain the experimental results. It was based on the stochastic version of the Landau-Lifshitz equation for system magnetization.

Influence of concentration of magnetic nanoparticles on blocking temperature in $0.05Fe_2O_3/0.95ZnO$ and $0.10Fe_2O_3/0.90ZnO$

N. Guskos[1,2], S. Glenis[1], G. Żołnierkiewicz[2], J. Typek[2],
D. Sibera[3], U. Narkiewicz[3]

[1]*Solid State Section, Department of Physics, University of Athens*
Panepistimiopolis, 15 784, Greece

[2]*Institute of Physics, West Pomeranian University of Technology*
Al. Piastów 48, 70-311 Szczecin, Poland

[3]*Institute of Chemical and Environmental Engineering*
West Pomeranian University of Technology
Al. Piastów 17, 70-310 Szczecin, Poland

Samples of $0.05Fe_2O_3/0.95ZnO$ and $0.10Fe_2O_3/0.90ZnO$ were prepared and investigated using the ferromagnetic resonance (FMR) method. The samples were characterized by the XRD method [1]. Figures 1 and 2 present the FMR spectra taken at different temperatures for both samples. The temperature dependence of parameters describing the FMR spectrum for both samples is shown in Figures 3–5. The FMR parameters were calculated using the procedure described in [2]. Strong temperature dependence was observed for three important parameters: apparent resonance field (H_r), linewidth (ΔH_{pp}) and amplitude. Essential differences between both samples were recorded in the low temperatures range which could be accounted for by differences in concentration of magnetic nanoparticles. Strong differences observed for the
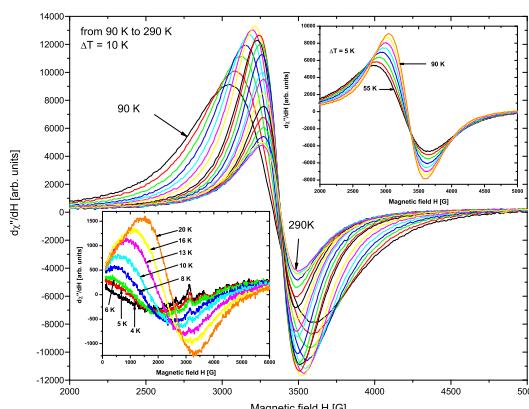

Figure 1: FMR spectra of $0.05Fe_2O_3/0.95ZnO$ registered at different temperatures

resonance amplitude signal (Figure 5) in both samples were attributed to differences in the blocking temperature of the a superparamagnetic state: $T_b = 150$ K for the sample with a lower concentration, and $T_b = 170$ K for sample with a higher concentration of magnetic nanoparticles.
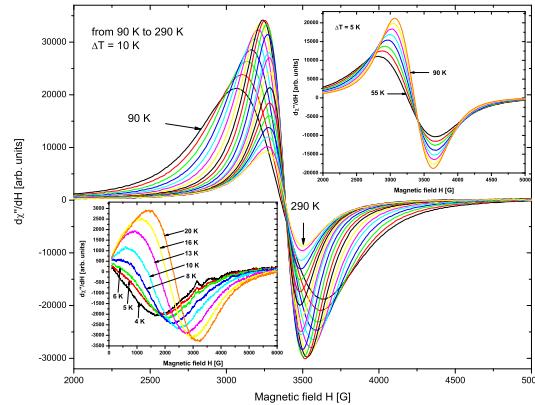
Figure 2: FMR spectra of $0.10Fe_2O_3/0.90ZnO$ registered at different temperatures

mm
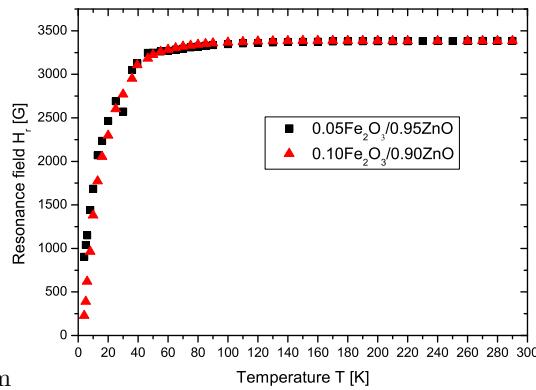
Figure 3: Temperature dependence of FMR resonance fields of $0.05Fe_2O_3/0.95ZnO$ and $0.10Fe_2O_3/0.90ZnO$ samples

References
[1] N. Guskos, J. Typek, M. Maryniak, U. Narkiewicz, W. Arabczyk, I. Kucharewicz 2005 *J. Phys.: Conference Series* **10** 151
[2] Yu. A. Koksharov, S. P. Gubin, I. D. Kosobudsky, M. Beltran, Y. Khodorkovsky, A. M. Tishin 2000 *J. Appl. Phys.* **88** 1587
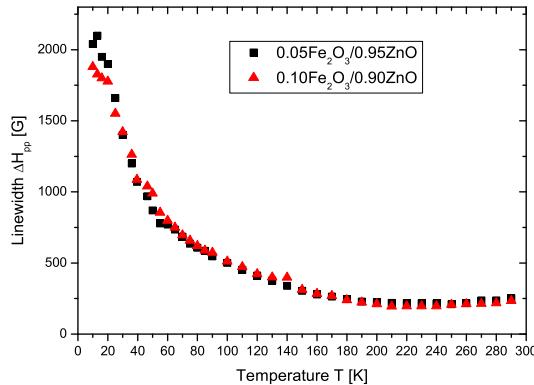
Figure 4: Temperature dependence of FMR linewidths of $0.05Fe_2O_3/0.95ZnO$ and $0.10Fe_2O_3$ /0.90ZnO samples
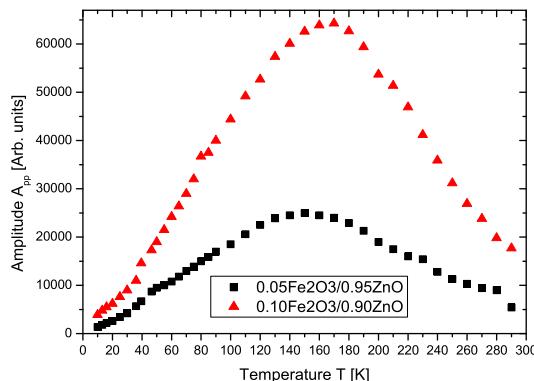
Figure 5: Temperature dependence of FMR signal amplitudes of $0.05Fe_2O_3/0.95ZnO$ and $0.10Fe_2O_3/0.90ZnO$ samples

Electrical transport properties
of $Ni_2MV_3O_{11}$ ($M^{(II)} = Cr$ and Fe)
and $M_3Fe_4(VO_4)_6$ ($M^{(II)} = Mg$, Zn and Mn)

N. Guskos[1,2], J. Typek[2], K. Karkas[1], A. Błońska-Tabero[3], M. Bosacka[3]

[1]*Department of Physics, University of Athens*
Panepistimiopolis 15 784 Zografos, Athens, Greece

[2]*Institute of Physics, West Pomeranian University of Technology*
Al. Piastów 48, 70-311 Szczecin, Poland

[3]*Department of Inorganic and Analytical Chemistry*
West Pomeranian University of Technology
Al. Piastów 17, 70-310 Szczecin, Poland

Transport properties of multicomponent vanadate oxides $Ni_2MV_3O_{11}$ ($M^{(II)} = Cr$ and Fe) and $M_3Fe_4(VO_4)_6$ ($M^{(II)} = Mg$, Zn and Mn) were investigated by electrical conductivity measurements.

All investigated compounds exhibited semiconducting behaviour. The two samples of $Ni_2MV_3O_{11}$ exhibited conducting properties that were two orders of magnitude (a factor of 10^5, at room temperature) better than those of the three $M_3Fe_4(VO_4)_6$ samples (see Figure 1). Substitution of magnetic $Fe^{(III)}$ ions for magnetic $Cr^{(II)}$ cations
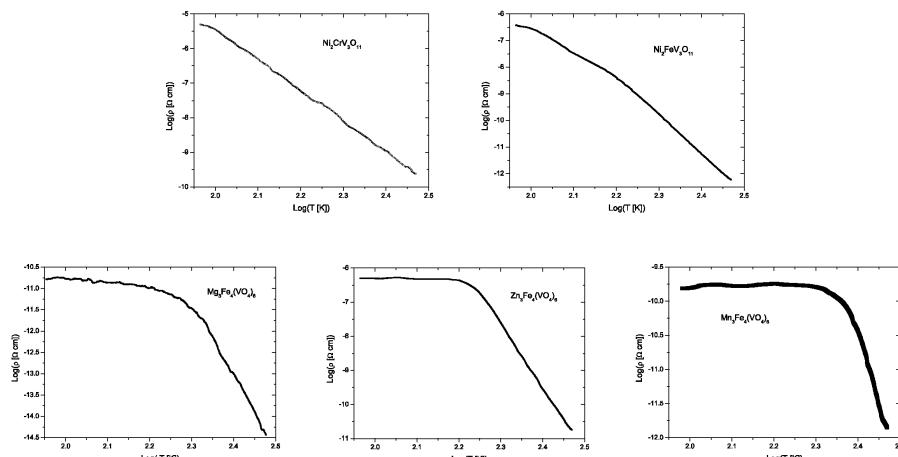
Figure 1: Log-log plot of the temperature dependence of resistivity for the five investigated multicomponent vanadate oxides

in $Ni_2MV_3O_{11}$ resulted in a significant improvement of its electrical conductivity at room temperature and led to a change in the activation energy. Very low conductivity was registered for the $M_3Fe_4(VO_4)_6$ samples in which the substitution of the magnetic $Mn^{(II)}$ ion for the non-magnetic $Mg^{(II)}$ ion led to a significant decrease in conductivity. $M_3Fe_4(VO_4)_6$, which contains various sublattices with magnetic ions involved in competing magnetic interactions could provide a good opportunity for a drastic change of $M_3Fe_4(VO_4)_6$ transport properties.

Angle dependence of FMR spectra
for S-phase obtained by PVD method

N. Guskos[1,2], G. Żołnierkiewicz[1], P. Berczyński[1], J. Typek[1],
J. Baranowska[3], S. Fryska[3]

[1] *Institute of Physics, West Pomeranian University of Technology*
Al. Piastów 48, 70-311 Szczecin, Poland

[2] *Solid State Section, Department of Physics, University of Athens*
Panepistimiopolis, 15 784 Zagrafos, Athens, Greece

[3] *Institute of Materials Science and Engineering*
West Pomeranian University of Technology
Al. Piastów 17, 70-310 Szczecin, Poland

S-phase coatings are hard and corrosion resistant and can be obtained by various technological methods. The tested coatings were deposited by the reactive magnetron sputtering method on a silicon substrate at 200°C and 2 mTorr (~ 0.26 Pa). The tested coatings were about 500 nm in thickness. Coatings with different textures can be produced depending on the deposition parameters. The most typical one is a texture in which S-phase columnar grains grow in the [100] direction perpendicular to the substrate, as was the case in the present study (Figure 1). The S-phase demonstrates magnetic properties which can be of high importance for its practical applications. Figure 2 presents the FMR spectra of expanded austenite (S-phase) at room temperature registered for different angles of a magnetic field external to the sample surface. The first spectrum was registered perpendicularly to the sample surface. Strong asymmetric resonance lines were recorded and strong angle dependence was observed. For
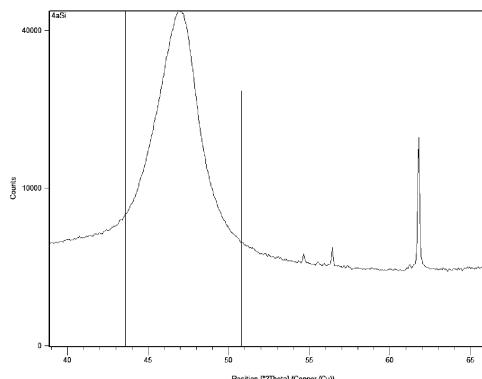
Figure 1: XRD spectrum of investigated sample
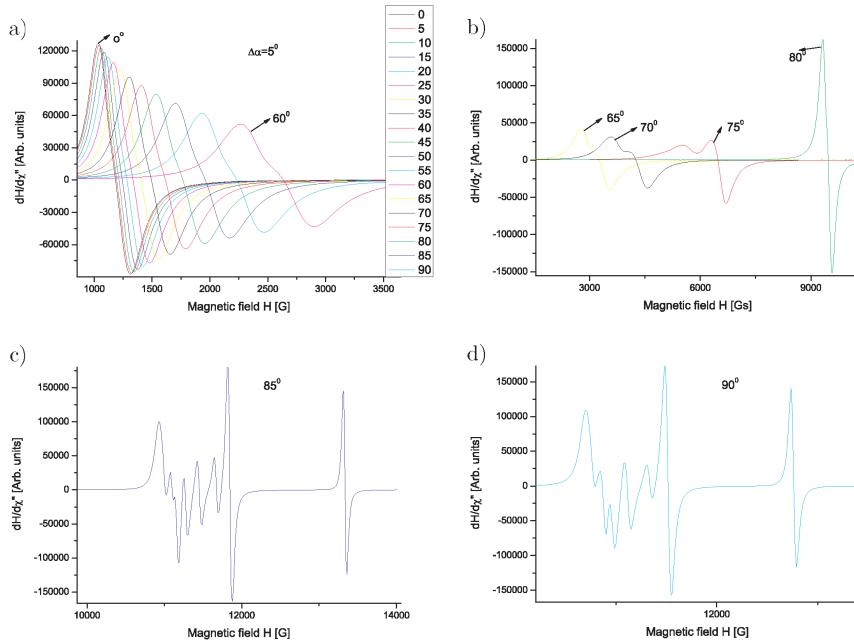
Figure 2: FMR spectra taken at different angles of magnetic field external to sample surface: (a) $0° \leqslant \theta \leqslant 60°$, (b) $65° \leqslant \theta \leqslant 80°$, (c) $\theta = 85°$, (d) $\theta = 90°$

the angle $0°$ the resonance line was shifted toward the direction of the lower magnetic field applied. This phenomenon is characteristic for magnetic nanoparticles small in size. An opposite effect was observed for greater angles. Additional lines appeared in the FMR spectra for a magnetic field forming an angle between $80°$ and $90°$.

FMR study of influence of carburization levels by methane decomposition on nanocrystalline iron

A. Helminiak[1], W. Arabczyk[1], G. Żołnierkiewicz[2],
N. Guskos[2,3], J. Typek[2]

[1]*Institute of Chemical and Environmental Engineering*
West Pomeranian Uniwersity of Technology
Al. Piastów 17, 70-311 Szczecin, Poland

[2]*Institute of Physics, West Pomeranian Uniwesity of Technology*
Al. Piastów 48, 70-311 Szczecin, Poland

[3]*Solid State Section, Department of Physics, University of Athens*
Panepistimiopolis, 15 784 Zagrafos, Athens, Greece

Methane decomposition on nanocrystalline iron promoted with small amounts of calcium, aluminum and potassium oxides was studied. Iron nanocrystallites were bridged by promoters. The carburization process was carried out in a differential tubular reactor with thermogravimetric measurement of mass changes. The carburization was investigated for a reduced iron catalyst with pure methane at the temperature of 650°C under atmospheric pressure during several different carburizing levels. The carburized samples contained nanocrystalline forms of iron carbide (Fe_3C), iron and graphite, what was evidenced by XRD measurements. Ferromagnetic resonance (FMR) spectra of Fe_3C were recorded at room temperature for samples subjected to different carburization levels (see Figure 1). The FMR spectra strongly depended on the concentration of graphite and stronger magnetic interaction was observed for smaller concentrations of graphite.
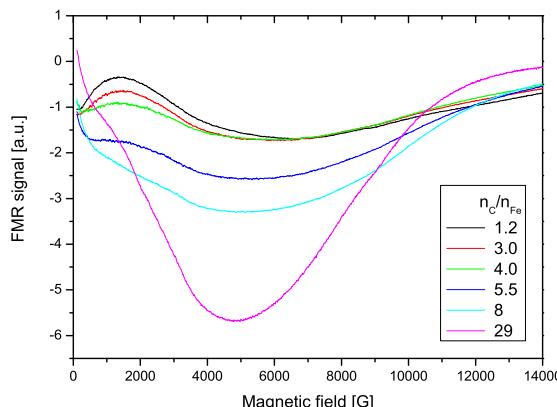
Figure 1: FMR spectra of Fe_3C/C for samples with different concentrations of graphite

Microscopy of auxetic particulate filled polymers

T. A. M. Hewage, K. L. Alderson, A. Alderson

University of Bolton, Institute for Materials Research and Innovation
Deane Road, Bolton BL3 5AB, UK.

In previous work we have performed modelling and experimental investigations into the effect of incorporating negative Poisson's ratio particulate fillers on the mechanical properties of polymeric materials. The studies showed that the effective properties of the filled systems could be enhanced in terms of Young's or shear moduli when auxetic fillers were employed. Similarly, for high modulus auxetic fillers the potential of developing filled systems with a negative effective Poisson's ratio was also shown to be achievable for realistic filler concentrations when a filler with a sufficiently large negative Poisson's ratio is employed. In order to reconcile the experimental and theoretical mechanical responses it is important to understand the microstructure of the real systems employed in the tests. This paper will, then, report on a recent microscopy study, including element mapping, of an epoxy polymer filled with α-cristobalite (auxetic silica) particles at a range of filler concentrations.

Negative thermal expansion of multifunctional Bi-perovskite

P. Hu[1], X. Peng[1], J. Chen[1], <u>X. Xing</u>[1,2]

[1]*Department of Physical Chemistry, University of Science and Technology Beijing*
Metallurgic Build 913#, 30 Xueyuan Road, Beijing 100083, China

[2]*State Key Laboratory for Advanced Metals and Materials*
University of Science and Technology Beijing
Metallurgic Build 913#, 30 Xueyuan Road, Beijing 100083, China

Negative thermal expansion was achieved and tuned in the multifunctional Bi-perovskites. The ferromagnetism-enhanced compounds $(1-x-y)$PbTiO$_3$-xBi(Ni$_{1/2}$Ti$_{1/2}$)O$_3$-yBiFeO$_3$, exhibiting zero thermal expansion, were developed by controlling the chemical composition. The appropriate content of dopants Bi(Ni$_{1/2}$Ti$_{1/2}$)O$_3$ and BiFeO$_3$ allowed one to control the thermal expansion and led to high thermal stability in a wide temperature range. Ferromagnetism was improved by adding BiFeO$_3$, and the ferroelectric and piezoelectric properties were well retained in the solid solution compound by doping Bi(Ni$_{1/2}$Ti$_{1/2}$)O$_3$. The ceramics exhibited good mechanical properties, such as high hardness and satisfactory fracture toughness due to Bi(Ni$_{1/2}$Ti$_{1/2}$)O$_3$ stabilizing the structure and reducing the internal stress. Various desirable properties make this material multifunctional and promising for multiple applications.

Modelling auxetic seat structures with progressive elastic characteristics

M. Janus-Michalska[1], D. Jasińska[1], J. Smardzewski[2]

[1]*Institute of Structural Mechanics, Cracow University of Technology*
Warszawska 24, 31-155 Kraków, Poland

[2]*Department of Furniture Design, Poznań University of Life Science*
Wojska Polskiego 28, 60-637 Poznań, Poland

Auxetic structures are increasingly finding application in engineering systems on account of their unique mechanical properties. As an example, we present seat structures, which reduce contact stress concentrations [2] owing to global auxeticity, providing the sensation of physical comfort . Their advantageous properties also include effective packaging, and gentle energy absorption. Applications generally involve large structural deformations, and are designed for either static or dynamic response regimes.

The seat skeleton is composed of 'springs', which are based on auxetic frame structures designed similarly to the microstructure of auxetic cellular materials [1]. The global mechanical seat properties are the result of spring geometry and its constituent material. This geometry should ensure global spring stability and the possibility of large deformations of its structure.

The structure is designed to work in two consecutive stages. At first, as an elastic response at small deformations, the network deforms fairly uniformly. Then, under increasing loading, local elastic collapse occurs, leading to an increased bending in
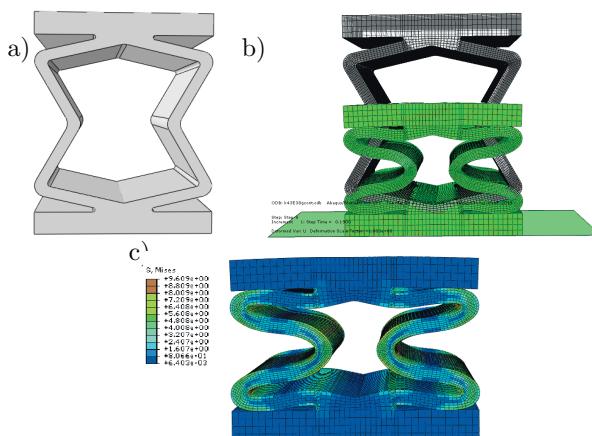

Figure 1: (a) Spring geometry, (b) deformation, (c) Mises stress map [MPa]

the network. As the structural configuration evolves, new weak points are created and high degrees of bending propagate throughout the structure, which results in large deflections. Finally, the network collapses onto itself and self-contact between frame elements results in a stiffening of the structure.

Computer simulations of the seat structure under typical static and dynamic loading exerted by the human body were performed by means of ABAQUS FEA. The considered auxetic spring is shown in Figure 1. The structure is made of elastic polyamide with the following material data: Young's modulus $E = 38$ MPa, rupture modulus $R = 36$ MPa, density $\rho = 1.11$ g/cm^3.

Deformation and stress map for maximal uniform pressure load $p_{\max} = 0.072 \times 10^6$ N/m^2 is illustrated in Figure 1, panels (b), (c). Geometric nonlinear analysis leads to load displacement paths presented in Figure 2.
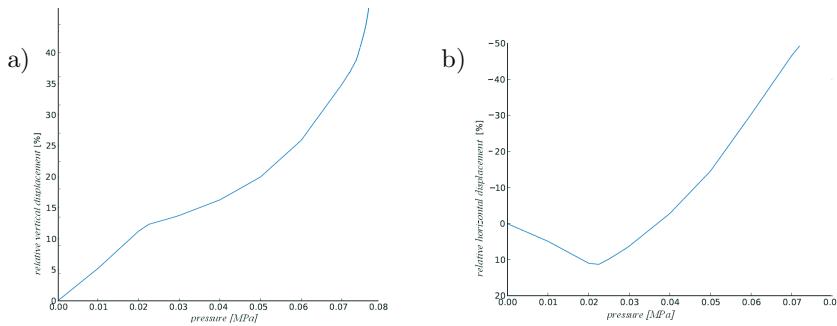
Figure 2: (a) load displacement curve, (b) auxetic behaviour of the compressed spring

The spring exhibits progressive elastic characteristics. Macroscopic pressure displacement curves agree qualitatively with experimental results.

References

[1] M. Janus-Michalska, "Micromechanical Model of Auxetic Cellular Materials", Journal of Theoretical and Applied Mechanics (JTAM), 4, vol. 47, 2009

[2] D. Jasińska, M. Janus-Michalska, "Material design of anisotropic elastic cellular bodies with respect to contact problem" – Engineering Transactions, vol. 3, 2008

[3] D. Jasińska, M. Janus-Michalska, J. Smardzewski, "A study on the design of auxetic structure of seat skeleton", in preparation for Journal of Mechanical Science and Technology, Springer

Mutual information parameter as an indicator of quantum-chaotic behavior

J. K. Kalaga[1], W. Leoński[1], A. Kowalewska-Kudłaszyk[2], V. Cao Long[1]

[1]*Quantum Optics and Engineering Division*
Institute of Physics, University of Zielona Góra
Prof. A. Szafrana 4a, 65-516 Zielona Góra, Poland

[2]*Department of Physics, Adam Mickiewicz University*
Umultowska 85, 61-614 Poznań, Poland

[3]*Institute of Physics of AS CR, Joint Laboratory of Optics*
17. listopadu 50a, 772 07 Olomouc, Czech Republic

In this communication, we show how the mutual information parameter (MIP) can be applied as an indicator of quantum chaos. This parameter was defined in an analogous way as in [1]. It can be expressed on the basis of the classical Wehrl entropy [2]

$$S[\alpha_1, \alpha_2] = -\int d\alpha_1 \, d\alpha_2 \, Q(\alpha_1, \alpha_2) \ln Q(\alpha_1, \alpha_2)$$

where the $Q(\alpha_1, \alpha_2)$ Husimi Q-function given by $Q(\alpha) = \pi^{-1} \langle \alpha | \rho | \alpha \rangle$. In fact, this function is coherent state representation of the density matrix ρ, and the coherent state is characterized by the complex parameter $\alpha = \alpha_1 + i\alpha_2$. The entropy having been defined in such a way, it is possible to derive the MIP in the following form

$$I[\alpha_1, \alpha_2] = S[\alpha_1] + S[\alpha_2] - S[\alpha_1, \alpha_2],$$

where

$$S[\alpha_i] = -\int d\alpha_i \, Q(\alpha_i) \ln Q(\alpha_i)$$

is related to the function

$$Q(\alpha_i) = \int d\alpha_j \, Q(\alpha_1, \alpha_2) \quad \text{with} \quad i, j = 1, 2 \quad j \neq j.$$

It is possible to extend this formalism to cases where more variables are used. In particular, instead of one-mode coherent state, $|\alpha\rangle$, a two-mode one, $|\alpha, \beta\rangle = |\alpha\rangle \otimes |\beta\rangle$ is used, and hence, two complex parameters, α and β are considered. Such a generalization gives us various possibilities to define the MIP parameters depending on the choice of the variable used in the integration. Quantum chaotic behavior of systems with a greater degree of freedom can be investigated. Hence, by comparing the time evolution of quantum systems and their classical counterparts we are able to extend our considerations to quantum hyper-chaotic systems. We believe that this is

a considerable extension of the previous investigations of quantum chaos phenomena where the fidelity [3,4] or Wigner function [5] were applied.

References

[1] K. Piątek, W. Leoński 2001 *J. Phys A: Math. Gen.* **34** (23) 5951
[2] A. Wehrl 1978 *Rev. Mod. Phys.* **50** (2) 221
[3] Y. S. Weinstein, S. Lloyd, C. Tsallis 2002 *Phys. Rev. Lett.* **89** (21) 214101
[4] A. Kowalewska-Kudłaszyk, J. K. Kalaga, W. Leoński 2009 *Phys. Lett. A* **2009** (15) 1334
[5] A. Kowalewska-Kudłaszyk, J. K. Kalaga, W. Leoński 2008 *Phys. Rev. E* **78** (6) 066219

Tests of polyurethane foams
with negative Poisson's ratio

S. Kłysz, J. Lisiecki, T. Błażejewicz, P. Reymer, G. Gmurczyk

Air Force Institute of Technology
Księcia Bolesława 6, 01-494 Warszawa, Poland

Polyurethane foams are materials that can be found in most areas of life. They are valued for their elasticity, durability and insulation properties. Foamed plastics have versatile applications due to their being waterproof, lightweight, chemically neutral, and exhibiting excellent damping properties.

By modifying the cellular structure of a foam, it can be transformed into an auxetic. Such materials are characterized by higher utility than traditional foam materials currently used in transportation and automotive industry. These materials can potentially increase safety in the case of a disaster and improve comfort during normal operation. The differences in performance are caused by their basic physical property, i.e. their negative Poisson's ratio. Traditional foam polymer materials used nowadays are characterized by a Poisson's ratio ranging from 0.1 to 0.4. For auxetic foams,
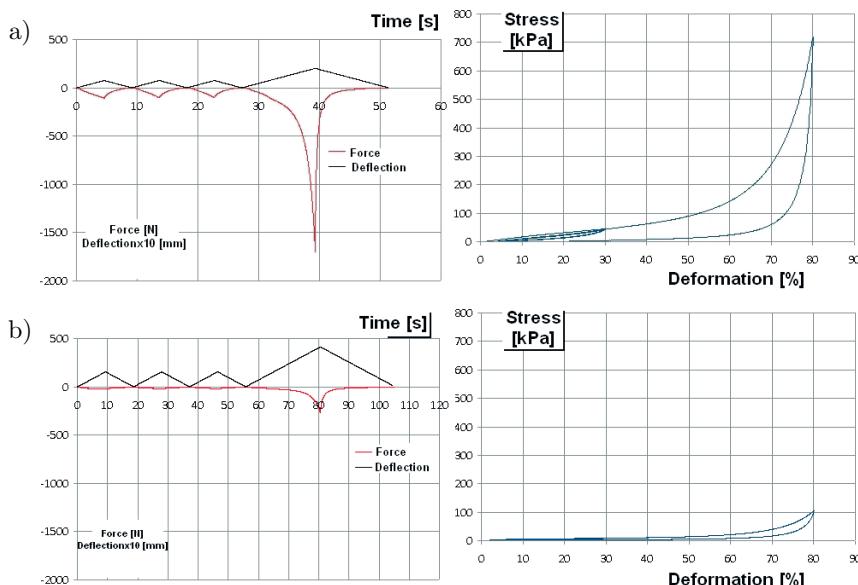

Figure 1: Results of compression tests (80%), comparison of auxetic (a) and conventional (b) foams
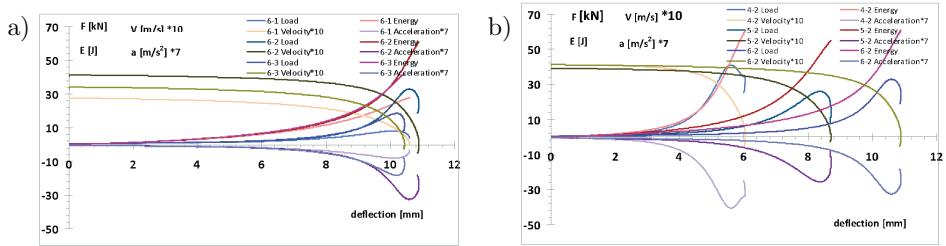
Figure 2: Damping characteristics of polyurethane foam samples: (a) N90HD (curves 6) density 90 kg/m^3; (b) comparison of the damping characteristics of the foam samples for an impact velocity of 4 m/s; S28190 (curves 4), NVE65 (curves 5)

the Poisson's ratio is usually within the range of -0.1 to -0.7. Due to this feature, auxetic foams tend to expand in the transverse direction while under tension, and to contract in the transverse direction while under compression. However, they exhibit many other interesting properties that need to be examined.

Since there are plans to apply auxetic foams to crew and passengers seats in military helicopters, their material characteristics under compression, as well as their dynamic damping properties must be carefully examined. In order to obtain test specimens, the Air Force Institute of Technology manufactured auxetic foams from conventional open-cell foams available on the market, based on the methods known from the literature. Also, the fatigue endurance test stand (MTS 810.23) was modified for testing the stress-strain characteristics of obtained auxetic foams under compression. The abovementioned tests were conducted on both auxetic and conventional foams of identical relative density (Figure 1). In the context of protecting military crews against the consequences of air accidents, we carried out additional tests of the dynamic damping properties of these foams (Figure 2). For this purpose, we used an INSTRON chute stand for impact testing at the Motor Transport Institute in Warsaw. This article describes the test program, our assumptions and goals, as well as interesting results.

Nanostructures in sulfonated block copolymers studied by Monte Carlo simulations

P. Knychała, M. Banaszak

Faculty of Physics, Adam Mickiewicz University
Umultowska 85, 61-614 Poznań, Poland

We investigated the phase behavior of copolymers consisting of three types of segments A, B and S [1]. This simple model can be used to examine the self assembly process in poly(styrenesulfonate-block-methylbutylene) (PSS-PMB) block copolymer melts [2]. The sulfonated copolymers can be applied as, for example, composite membranes that transport ions in energy-related applications such as batteries and fuel cells. Thermodynamic incompatibility of the ionic and nonionic species leads to microphase separation, resulting in the spontaneous assembly of conducting and nonconducting domains. The purpose of this work was to investigate this process in terms of the sulfonation level, length of chain and symmetry of copolymers [3]. In our simulations we used the Monte Carlo lattice simulations with the Cooperative Motion Algorithm and both the standard Metropolis algorithm and the Parallel Tempering method. We compared the simulations results with the experimentally observed nanostructures reported by Balsara and co-workers [2,3]. Finally, we outlined the phase diagrams for symmetric and asymmetric copolymers in terms of the volume fraction of S segments and temperature for different chain lengths and also in terms of the volume fraction of a sulfonated subblock and temperature for a constant sulfonation level.

Acknowledgements

References

[1] P. Knychała, M. Banaszak, M. J. Park, N. P. Balsara 2009 *Macromolecules* **42** (22) 8925
[2] M. J. Park, N. P. Balsara 2008 *Macromolecules* **41** (10) 3678
[3] X. Wang, S. Yakovlev, K. M. Beers, M. J. Park, S. A. Mullin, K. H. Downing, N. P. Balsara 2010 *Macromolecules* **43** (12) 5306

Structure and magnetic properties of Mg-Zn nanocrystalline ferrites

A. V. Kopayev[1], B. V. Padlyak[2,3], I. P. Yaremiy[1], V. S. Bushkova[1], A. Drzewiecki[2]

[1] *Physical-Technical Faculty, Vasyl Stefanyk PreCarpathian National University*
Shevchenko Str. 57, 76-000, Ivano-Frankivsk, Ukraine

[2] *Division of Spectroscopy of Functional Materials*
Institute of Physics, University of Zielona Góra
Prof. Szafrana Str. 4a, 65-516 Zielona Góra, Poland

[3] *Sector of Spectroscopy, Institute of Physical Optics*
Dragomanov Str. 23, 79-005, Lviv, Ukraine

Bulk Mg-Zn ferrites ($Mg_xZn_{1-x}Fe_2O_4$) reveal very interesting physical properties and are widely used in microwave devices. The magnetic structure and properties of Mg-Zn ferrites essentially depend on their chemical composition and cationic distribution caused by the technological conditions of the synthesis of samples. This especially concerns Mg-Zn ferrite nanoparticles which have not been satisfactory investigated to date.

The ferrite nanoparticles of the $Mg_xZn_{1-x}Fe_{2\pm y}O_4$ ($x = 0$, 0.5, 0.532, 0.56, 0.588; $y = 0$, 0.033) composition were obtained using the process of nanotechnology by the sol-gel auto-combustion method. According to the results of the X-ray analysis, the obtained powders of Mg-Zn ferrites consisted of one phase with a spinel structure. The technological conditions of synthesis of Mg-Zn nanoferrites led to changes in the nanoparticles size. The size of particles in the obtained Mg-Zn ferrite powders measured using the Scherrer's formula was in the range of 20–40 nm. The difference thermal analysis (DTA) did not show any phase transitions in the obtained samples of Mg-Zn ferrites at heating up to $1000°C$. The lattice parameters of the obtained nanocrystalline Mg-Zn ferrites were lower than in nanopowders with the same composition, obtained using the ceramic method. In particular, $a = 0.8407$ nm for the $Mg_{0.5}Zn_{0.5}Fe_2O_4$ sample obtained by the sol-gel auto-combustion method, whereas $a = 0.8420$ nm for the same sample, obtained by the ceramic method.

Using the XANES (X-ray Absorption Near Edge Structure) method it was shown that iron was incorporated into the crystal lattice of the Mg-Zn ferrite nanoparticles in the trivalent state. The magnetic structure parameters of the Mg-Zn ferrite nanoparticles were investigated using Mössbauer spectroscopy. Particularly, it was shown that the area and parameters of the $^{57}Fe^{3+}$ paramagnetic doublet, observed in the background of the $^{57}Fe^{3+}$ sextet of magneto-ordered phase, depended on the technological conditions of nanopowders preparation.

The magnetic properties of Mg-Zn ferrite nanoparticles were investigated using magnetic susceptibility measurements at low frequencies and ferromagnetic resonance

(FMR) spectroscopy in the microwave range. The magnetic susceptibilities of all Mg-Zn nanocrystalline ferrites showed a linear dependence on the reciprocal values of the external magnetic field. The temperature dependencies of the magnetic susceptibility and magnetization of the Mg-Zn ferrite nanoparticles were qualitatively similar to the corresponding temperature dependencies of the bulk Mg-Zn ferrite samples. The parameters (giromagnetic ratio, peak-to-peak derivative linewidths) and lineshapes of the observed FMR signals were determined and analyzed in comparison with other nanocrystalline and bulk ferrite samples. The magnetic properties and FMR spectra were interpreted and discussed in the framework of modern theory of nanosized antiferromagnetics.

Acknowledgements

Sudden death of entanglement
for qutrit-qutrit nonlinear coupler system

A. Kowalewska-Kudłaszyk[1], W. Leoński[2], J. Peřina Jr.[3]

Department of Physics, Adam Mickiewicz University
Umultowska 85, 61-614 Poznań, Poland

[2]*Quantum Optics and Engineering Division*
Institute of Physics, University of Zielona Góra
Prof. A. Szafrana 4a, 65-516 Zielona Góra, Poland

[3]*Institute of Physics of AS CR, Joint Laboratory of Optics*
17. listopadu 50a, 772 07 Olomouc, Czech Republic

Models that involve quantum nonlinear oscillators are very often the subject of papers concerning nano-systems. For instance, it has been shown that a nano-resonator with a moving mirror can be a source of various quantum states [1]. In particular, as has been discussed in [2,3], such systems behave as quantum nonlinear oscillators. Quite recently, investigations concerning nano-resonators have also involved models with carbon nano-tubes (discussed for instance in [4,5]).

In this communication, we discuss a system of two quantum nonlinear oscillators. They are coupled with each other and excited by an external parametric two-mode process. This model differs considerably from that described in [6] where the system is excited by external coherent field and the oscillators are coupled by internal nonlinear coupling.

We show that if the external excitation is sufficiently weak, as we compare it with the nonlinearity parameters, the system behaves as *nonlinear quantum scissors* [7,8]. In consequence, the system's evolution remains practically contained within a finite set of n-photon states. For the case discussed here, we can restrict our considerations to vacuum, one-photon and two-photon states only. In fact, using the quantum information theory language, the system behaves as a *qutrit-qutrit* one.

We show that if the system is initially in the vacuum state in modes corresponding to both oscillators, generalized Bell states (GBS) [9] can be generated. Those states can be expressed in a Fock basis as:

$$|\Psi_{mn}\rangle = \frac{1}{\sqrt{D}} \sum_{k=0}^{D-1} e^{2\pi i k m/D} |k\rangle \otimes |(k-n)\bmod D\rangle.$$

They belong to the group of *maximally entangled states* and play a crucial role in the quantum information theory.

If damping processes are included in our model, those states can be destroyed by decoherence effects. In this communication we concentrate on this problem. We show that such processes can lead to *sudden entanglement death* (SED) [10,11] and *sudden*

entanglement birth (SEB) [12,13] effects. This means that the entanglement vanishes (SED) after a finite period of time during the system's evolution and then rebuilds again (SEB).

References

[1] B. Jacobs, 2007 *Phys. Rev. Lett.* **99** (11) 117203

[2] S. Mancini, V. I. Man'ko, P. Tombessi 1997 *Phys. Rev. A* **55** (4) 3042

[3] J. Bose, K. Jacobs, P. L. Knight 1997 *Phys. Rev. A* **56** (5) 4175

[4] I. Wilson-Rae, C. Galland, W. Zwerger, A. Imamoglu 2009 *arXiv:0911.133v1* [cond-mat.mes-hall]

[5] Jin-Jin Li, Wei He, Ka-Di Zhu 2011 *Phys. Rev. B* **83** (11) 115445

[6] A. Kowalewska-Kudłaszyk, W. Leoński 2006 *Phys. Rev. A* **73** (4) 042318

[7] A. Miranowicz, W. Leoński 2004 *J. Opt B* **6** (3) S43

[8] A. Miranowicz, W. Leoński 2006 *J. Phys B: At. Mol. Opt. Phys.* **39** (7) 1683

[9] C. H. Bennett, G. Brassard, C. Crepeau, R. Jozsa, A. Peres, W. Wootters 1993 *Phys. Rev. Lett.* **70** (13) 1895

[10] K. Życzkowski, P. Horodecki, M. Horodecki, R. Horodecki 2001 *Phys. Rev. A* **65** (1) 012101

[11] T. Yu, J. H. Eberly 2004 *Phys. Rev. Lett.* **93** (14) 140404

[12] Z. Ficek, R. Tanaś 2006 *Phys. Rev. A* **74** (2) 024304

[13] A. Kowalewska-Kudłaszyk, W. Leoński 2009 *J. Opt. Soc. Am. B* **26** (7) 1289

Band structure of new ErFeAsO superconductors

S. P. Kruchinin[1], A. A. Zolotovsky[2]

[1] *Bogolyubov Institute for Theoretical Physics, NASU*
Kiev, 03143, Ukraine

[2] *Lashkaryov Institute of Semiconductor Physics*
Kiev, 03028, Ukraine

We investigated the band structure of Fe-based superconductors using the first-principle method of the density-functional theory. We calculated the band structure and the density of states at the Fermi level for ReFeASO (Re = Sm, Dy, Ho, Er) superconductors. Our calculations indicated that the maximum critical superconducting transition temperature, T_c, would be observed for compounds with Sm and Er.

Nanofabric nonwoven mat for filtration of smoke and nanoparticles

M. Lackowski, A. Krupa, A. Jaworek

Institute of Fluid-Flow Machinery, Polish Academy of Sciences
Gdańsk, Poland

The process of production of filtration mats of various thickness by the electrospinning method is presented in the paper. PVC and PVDF were used as the material for production of the nanofibrous mat. The physical background of electrospinning lies in utilization of electrical forces for generating shear stress on the surface of a viscous liquid, usually a polymer solution, flowing from a capillary nozzle. Under this stress, the jet becomes thinner, and finally thin fiber is formed after solvent evaporation. The electrospinning method has been applied for production of nanofibrous mats made from polymer material.

The filtration of nanoparticles and submicron particles is an important problem in industry and health protection in most of the air-conditioning and ventilation systems. Application of nonwoven fibrous filters made of a nonwoven nanofibrous filtration mat is a promising way which could solve this problem. The experimental results of investigation of mechanical properties of nanofibrous filtration mats and the removal efficiency of submicron-particles from gas are also presented, showing potential application in air-conditioning systems and/or ventilation ducts. One of the media to be removed in the presented experimental results is cigarette smoke. Cigarette smoke particles are about 1 μm in diameter. Particles of this size are particularly difficult to remove from the flow by a conventional method, for example, by a cyclone or an electrostatic precipitator. The efficiency of removal of cigarette smoke submicron particles and TiO2 nanoparticles from flowing air was measured in a small laboratory channel. The efficiency was calculated from the concentration of particles measured at the inlet and the outlet of the channel. The concentration was determined by the optical microscope technique (for submicron particles) and the nanofibrous mat was examined under scanning electron microscope EVO 40 produced by ZEISS.

The experimental results presented in the paper show that a nonwoven nanofibrous filtration mat has good filtration efficiency for nano-and submicron particles, by a pressure drop similar to HEPA filters.

Influence of oxygen partial pressure on optical properties of vanadium oxide thin films

<u>M. Łapiński</u>[1], V. Kambilafka[2], B. Kościelska[1]

[1] *Department of Solid State Physics, Gdańsk University of Technology*
Narutowicza 11/12, 80-233 Gdańsk, Poland

[2] *Institute of Electronic Structure and Laser*
Foundation for Research and Technology-HELLAS
P.O. Box 1527, 71110 Heraklion, Crete, Greece

Vanadium has various oxidation states. It is the reason why vanadium can produce a number of oxide forms, like VO, VO_2, V_2O_3, V_2O_5 and others. It can also exist as a mixture of different forms of oxides [1,2]. A variety of forms and interesting technological applications are the reason why vanadium oxides have been widely studied in recent years. It is especially V_2O_5 that is an oxide form with interesting electrical and optical properties in the field of optical filters, electrochromic and photocatalysis applications [2,3].

In this paper structural and optical properties of vanadium oxides thin films, as-deposited and post-annealed in air (at 673 K), are presented. Thin films with 200 nm in thickness were deposited from a vanadium target on fused silica substrates by the microwave-assisted magnetron sputtering method. The samples were deposited in plasma containing a mixture of $Ar-O_2$ gases at three different partial pressures of oxygen: $3 \cdot 10^{-4}$ Torr, $5 \cdot 10^{-4}$ Torr and $9 \cdot 10^{-4}$ Torr. The gas mixture total pressure was in the range from $4.2 \cdot 10^{-3}$ Torr to $4.8 \cdot 10^{-3}$ Torr.

The structural properties of the films were obtained using X-ray diffraction and Raman spectroscopy. It was shown that thin films were amorphous directly after deposition. After 2 hours of the annealing process at 673 K, the results of measurements revealed the V_2O_5 crystalline phase. Optical measurements showed low transmission (lower than 10 %) in the visible spectra range for as-deposited samples prepared under low oxygen partial pressure. The dark brown color indicates that the as-deposited samples were oxygen deficient. As a result of thermal treatment at 673 K the transmission increased up to 20 % and 35 % at 650 nm wavelength for the samples prepared under $3 \cdot 10^{-4}$ Torr and $5 \cdot 10^{-4}$ Torr of oxygen partial pressure, respectively. The change in the optical transmission after the annealing process was not evident in case of the sample prepared under the highest oxygen pressure. The optical band gap and refractive index were calculated based on the transmission and reflectance measurements. The correlation between structural and optical properties of thin films and oxygen pressure during deposition is discussed.

References

[1] L. J. Meng, R. A. Silva, H. N. Cui, V. Teixeira, M. P. dos Santos, Z. Xu 2006 *Thin Solid Films* **515** 195
[2] S. B. Wang, S. B. Zhou, X. J. Yi 2004 *Vacuum* **75** 85
[3] C. V. Ramana, O. M. Hussain, S. Uthanna, Srinivasulu Naidu B. 1998 *Optical Materials* **10** 101

Structural investigations of sol-gel derived lithium titanate thin films

M. Łapiński, B. Kościelska, W. Sadowski

Department of Solid State Physics, Gdańsk University of Technology
Narutowicza 11/12, 80-233 Gdańsk, Poland

$Li_{1+x}Ti_{2-x}O_4$ systems have been recently widely studied due to interesting practical applications. It is especially the superconducting properties of the $Li_{1+x}Ti_{2-x}O_4$ spinel system that are very interesting and have been the subject of numerous investigations [1,2]. Nowadays much attention is also focused on a new field of applications such as electrodes for rechargeable lithium-ion batteries [3,4].

In this paper structural investigations of lithium titanate thin films are presented. Thin films 800 nm in thickness were deposited by the sol-gel method on quartz glass substrates. Lithium acetate, tetrabutyl titanate, etanol and glycol were used as reagents for sol-gel synthesis. Smooth thin film was obtained using spin coater equipment. After deposition the samples were dried at $100°C$ for 10 hours and then calcined at different temperatures in the range of $500°C – 800°C$. Both the drying and calcinating processes were conducted in argon atmosphere.

The structures of the manufactured thin films were investigated using X-ray diffraction. The measurements showed a nanocrystalline structure of the films. The most visible lithium titanate phase was obtained for 20 hours annealing at $550°C$. Increasing the temperature above $600°C$ revealed the appearance of a rutile phase. A correlation between the temperature and time of calcination and the structure of manufactured films is shown.

References

[1] R. K. B. Gover, J. T. S. Irvine, A. A. Finch 1997 *Journal of Solid State Chemistry* **132** 382
[2] E. G. Moshopoulou 1999 *Journal of the American Ceramic Society* **82** 3317
[3] A. Kuhn, M. Martin, F. Garcia-Alvardo 2008 *Zeitschrift für anorganische und allgemeine Chemie* **634** 880
[4] J. Yang, J. Zhao, Y. Chen 2010 *Ionics* **16** 425

Synthesis and characterization of cobalt catalysts for ammonia decomposition

Z. Lendzion-Bieluń

Institute of Chemical and Environmental Engineering
West Pomeranian University of Technology
Pułaskiego 10, 70-322 Szczecin, Poland

The reaction yield of catalytic ammonia decomposition depends on many factors, such as gas phase composition, morphology and composition of the catalyst surface.

The aim of the present study was to prepare cobalt catalysts doped with chromium and to examine the influence of the dopants on the specific surface area, thermostability of the catalysts under reduction conditions and their activity in ammonia decomposition. The catalysts were characterized by ICP, H_2-TPR, BET and XRD. Ammonia decomposition was preceded by reduction at 600°C under atmospheric pressure. Catalytic ammonia decomposition was investigated under the atmosphere of a ammonia-hydrogen mixture and atmospheric pressure. Ammonia concentrations, and thus nitriding potentials, were varied gradually from 0 to 100% at the inlet of the reactor. The temperature was varied in the range of 450–600°C.
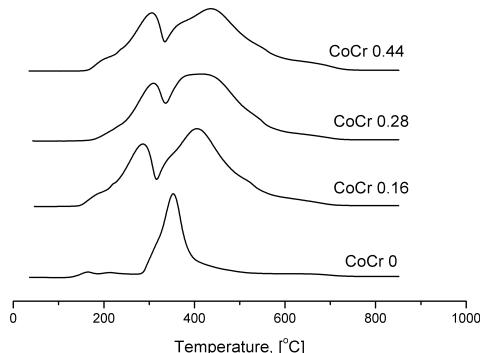

Figure 1: H_2-TPR profiles of cobalt catalysts modified with chromium

A small addition of chromium led to an increase in the reduction temperature of cobalt catalysts, cf. Figure 1.

Acknowledgements

Characteristics of blue organic light-emitting diodes with emitting layers of different thicknesses

Ch. Li[1], W. Huang[1], T. Tsuboi[2]

[1]*Key Laboratory for Organic Electronics & Information Displays*
and Institute of Advanced Materials
Nanjing University of Posts and Telecommunications
Wenyuan Road 9, Nanjing 210046, China

[2]*Faculty of Engineering, Kyoto Sangyo University*
Kamigamo, Kita-ku, Kyoto 603-8555, Japan

The efficiency of multilayer organic light-emitting diodes (OLEDs) depends on the layer thickness. The external quantum efficiency, power efficiency, and luminous efficiency of OLEDs, as well as their operational voltage and operational current density strongly depend on the thickness of the emitting layer (EML) and of the hole injection layer (HIL). The EML of the investigated OLED consisted of blue-emitting DSA-ph (1-4-di-[4-(N,N-di-phenyl)amino]styryl-benzene) as a dopant (5 wt.%) and diphenyl-lanthracene derivative 9,10-di(2-naphthyl)anthracene (ADN) as host. The hole injection layer (HIL) was 2-TNATA doped with F4-TCNQ, the hole transport layer (HTL) was 10 nm-thick NPB, and the electron transport layer (ETL) was 20 nm-thick Alq_3. The thickness of the EML varied between 15, 25, 35, 50, and 70 nm, whereas the thickness of the HIL varied between 95, 85, 75, 60, and 40 nm, while the thickness of the other layer (HIL and EML, respectively) was kept constant at 110 nm. Low operating voltage was obtained from the OLED with 15 nm-thick EML. The threshold voltage increased with an increase in the thickness of the EML layer. The highest luminous efficiency (14 cd/A) was obtained for 35 nm-thick EML, whereas the lowest (11 cd/A) was obtained for both the 15 and 70 nm-thick EMLs. The highest external quantum efficiency of 6.2% was obtained for 35 nm-thick EML, whereas the lowest (4.2%) was obtained for 70 nm-thick EML. The highest power efficiency of 8 lm/W was obtained for the 15 nm-thick EML, whereas the lowest power efficiency was obtained for both 70 nm-thick EML.

Effective micromechanical model for auxetic honeycombs

Z. Lu, Q. Liu

Institute of Solid Mechanics, Beihang University
Xueyuan Road 37, Beijing, 100191, China

An effective micromechanical model is formulated to reveal the macroscopic mechanical properties of auxetic honeycombs. We assumed that macroscopic mechanical behavior can be inferred from the deformation response of a representative volume element, where the cell struts are idealized as beams. The complementary energy of the unit cell was calculated by applying a uniform stress tensor to the beam skeleton. The effective flexibility matrix of auxetic honeycombs was thus obtained by averaging the energy in the equivalent continuum. Furthermore, the yield strength of auxetic honeycombs was also derived on the basis of the modified plastic hinge theory, which is also dependent on the axial stress. A novel honeycomb with auxetic behavor was finally constructed in order to verify the efficiency of the present model. The effective mechanical constants of the theoretical model, such as the Young's modulus, shear modulus, Poisson's ratio and the shear strength were in agreement with the predictions of the finite element method.

Nanostructured materials obtained in conditions of hierarchical self-assembly and modified by derivative forms of fullerenes

V. A. Moshnikov, O. A. Alexsandrova, I. E. Gracheva,
N. I. Alekseyev, V. V. Kuznetsov, K. N. Semenov, E. V. Maraeva

Microelectronics Department, Saint-Petersburg State Electrotechnical University
5 Professora Popova Street, 197376 Saint-Petersburg, Russia

The main point of a hierarchical self-assembly [1,2] is synthesis of initial constructive "blocks" of different sizes and shapes and their further integration. A hierarchical self-assembly can be a multilevel one, when the integrated blocks are basic elements for larger consolidations (with a larger interaction radius).

In this work the possibility of creation of hierarchical porous nanocomposites by self-assembly in sol-gel processes in conditions of spinodal decomposition and phase separation is shown. Three pore types created during the process – macropores, mesopores and micropores – can have different functions (nanoreactors with different capillary phenomena, canals for reaction products delivery and withdrawal, adsorption centers etc.). It is determined that self-assembly managing in sol-gel-processes [3,4] allows one to control the structure and gas-sensitive properties of hierarchical porous nanostructures based on metallic oxides.

Sol-gel processes were supplemented with template synthesis methods. Hierarchical porous nanocomposites were modified with water-soluble fullerene derivatives – fullerenols $C_{60,70}(OH)_n$ [5] – which were burnt later. We used fullerenol-d obtained by direct synthesis in which hydroxyl groups (OH) and a small quantity of other groups (e.g., $[C_n(OH)_X O_Y](ONa)_Z$) can exist, for insertion into semiconductor nanomaterials based on metallic oxides with a hierarchical porous structure. We investigated the sensitivity of adsorption-type gas sensors based on nanocomposites, obtained by the sol-gel method, due to insertion of fullerenols as a modifying additive.

The surface morphology diagnostics of nanomaterials synthesized from sol solutions in presence of a precursor based on tetraethoxysilane was conducted with the use of atomic force microscopy. Probes with cantilever as a beam with a rectangular section were used for the diagnostics of patterns surface in this work.

Nanocomposites specific surface area measurements were taken with the use of a Sorbi analytical instrument by the thermal desorption method. A thermal conductivity sensor was a detector of the gas mixture composition. The thermal conductivity sensor signal is a desorption curve; its area is proportional to the volume of gas being desorbed. The specific surface area of porous nanocomposites was calculated according to the model of Brunauer, Emmett, and Teller.

The diagnostic method for structures obtained in the conditions of hierarchical self-assembly and modified by fullerenols was suggested. The method concludes in

variable frequency electrical action [6] applying to nanomaterials in conditions of gas-reagent and detecting temperature changing. Preliminary investigations show the increasing reaction of modificated structures on water vapors in comparison with non-modified materials.

It was determined that semilogarithmic frequency dependences of the current-voltage phase shift for hierarchical nanocomposites illustrated two maximums with two closely spaced relaxation times. Two peaks which have various forms depending on gas environment and detecting temperature are evidence of the presence of a various-dimension pore system in nanomaterials that offers a challenge for the diagnostics of systems with a hierarchical structure.

Acknowledgements

References

[1] G. A. Ozin, K. Hou, B. V. Lotsch et al., Nanofabrication by self-assembly, *Materials Today* V. 12, Issue 5 (2009), p. 12–23

[2] V. A. Moshnikov, I. E. Gracheva, V. V. Kuznezov et al., Hierarchical nanostructured semiconductor porous materials for gas sensors, *Journal of Non-Crystalline Solids* 356 (2010), p. 2020–2025

[3] C. J. Brinker, G. W. Scherer, Sol-Gel Science. The Physics and Chemistry of Sol-Gel Processing. San Diego: Academic Press (1990), p. 908

[4] Handbook of sol-gel science and technology: processing, characterization, and applications, Ed. Sumio Sakka. New York (2004), V. 1–3

[5] J. Li, A. Takeuchi, M. Ozawa, M. Li, K. Saigo, K. Kitazawa, C_{60} Fullerenol Formation catalysed by Quaternary Ammonium Hydroxides. *J. Chem. Soc. Commun.* 23 (1993), p. 1784–1788

[6] I. E. Gracheva, V. A. Moshnikov, Disturbing variable frequency electrical action as a new perspective for sensitivity and selectivity increasing in "electron-nose" systems, Izvestiya of Herzen State Pedagogical University of Russia; *Natural science and exact sciences. Physics* 11, Issue 79 (2009), p. 100–107

Liquid phase epitaxy of strained layers of $Zn_xCd_{1-x}Te$

P. P. Moskvin[1], L. V. Rashkovetskyi[1], M. Antonov[1], J. M. Olchowik[2]

[1] *Zhytomyr State Technological University*
Chernyakhovsky 103, Zhytomyr, 10005, Ukraine

[2] *Technical University of Lublin*
Nadbystrzycka 38D, 20–618 Lublin, Poland

Thin films of $Zn_xCd_{1-x}Te$ solid solutions of the thickness of ca. 1 μm are used in the production of X-ray detectors. The strong dependence of the parameters of the crystal lattice of these compounds on their composition leads, however, to the formation of mechanical tensions in their heterostructure. Figure 1 shows a $Zn_{0.1}Cd_{0.9}Te$ layer on a CdTe(111)B substrate with $\Delta a/a_{CdTe} = 0.55\%$. This picture shows a network of dislocation lines, crossing at an angle of 60°, oriented on the (010) surface. These lines are the results of the relaxation of mechanical tensions in the interface.
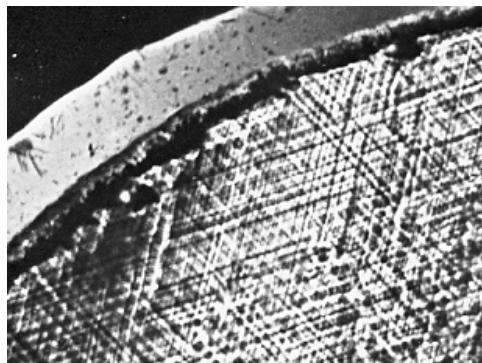
Figure 1: Topology of a $Zn_{0.1}Cd_{0.9}Te/CdTe$ heterostructure surface

In this study, we perform the analysis of phase equilibrium in a $Zn_xCd_{1-x}Te/CdTe$ heterostructure. Also, we present the analysis of the kinetics of growth of such layers. The theoretical description of the surface growth process takes into account the analysis of thermodynamical equilibrium with respect to the spring deformation of the interface and polyassociative compounds of the liquid phase [1,2]. The process of mass transfer in the direction of the interface follows the diffusion-limited crystallization model – both with and without the conditions of preserving of phase equillibrium. Figure 2 presents the experimental data as a function of the mole composition of $Zn_xCd_{1-x}Te$ layer (1) taking into account the deformation energy and (2) neglecting the deformation energy.
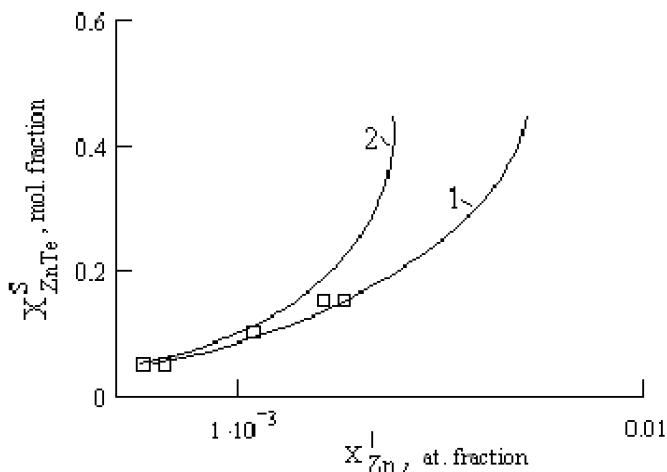
Figure 2: Experimental data and the results of mole composition modeling of $Zn_x Cd_{1-x} Te$ layer (1) with the deformation energy and (2) without the deformation energy

The results of our computations and experiments were obtained at a crystalization temperature of $T = 550°C$ and the supercooling of solution of $\Delta T = 100°C$. Better agreement between the theory and experiment was observed when the elastic deformation of the interface was taken into account.

References

[1] P. Moskvin, L. Rashkovetskyi, V. Khodakovsky, Russian J. Physical Chemistry A, 83, Issue 1 (2009), p. 20

[2] P. Moskvin, V. Khodakovsky, J. Olchowik, A. Zdyb, et al., J. Non-Crystalline Solids, 354 (2008), p. 4407

Influence of yttrium content on luminescent properties of microwave-hydrothermal synthesized ZrO_2:Tb,Y

U. Narkiewicz[1], J. Kaszewski[1], I. Pełech[1],
S. Yatsunenko[2], M. Godlewski[2]

[1]*Institute of Chemical and Environmental Engineering*
West Pomeranian University of Technology
Pułaskiego 10, 70-322 Szczecin, Poland

[2]*Institute of Physics of the Polish Academy of Sciences*
Al. Lotników 32/46, 02-668 Warsaw, Poland

Yttrium is a typical phase stabilizer in zirconia materials. The content of yttrium determines the phase composition and influences the luminescent properties, as well as the yttrium to rare-earth metal ratio [1]. Terbium was chosen from the rare earths owing to its ability to form the Tb^{3+} ion, the luminescence emission of which is in the visible spectral range [2]. Systematic research is necessary in order to find which part of the excitation energy is transferred to Tb^{3+} luminescence centers. Enhancing the luminescence intensity of doped zirconia materials will pave the way for a new generation of semiconductor light sources. Powders exhibiting a narrow grain size distribution were synthesized and their luminescence intensity was investigated. The concentration of terbium was fixed at 0.5, and the concentration of yttrium varied from 0 to 10 molar percent. Yttrium content was correlated with luminescent properties. We found the composition corresponding to the brightest luminescence and the optimal excitation wavelength for obtaining the highest intensity. The phase composition of the powders varied in a common way, as a function of yttrium content. The mean crystallite size decreased with an increase in the concentration of the stabilizer in a very narrow range from 5 to 8 nm.

References
[1] Nakajima H., Mori T. 2009 *J. Appl. Phys.* **97** (2) 503
[2] Reisfeld R., Zelner M. and Patra A. 2000 *J. Alloys Compd.* **300–301** 147

Oxidation of SO_2 on Pt/CNT catalyst

U. Narkiewicz, A. Pietrasz, I. Pełech, E. Borowiak-Paleń

Institute of Chemical and Environmental Engineering
West Pomeranian University of Technology
Pułaskiego 10, 70-322 Szczecin, Poland

Sulphur dioxide is emitted mainly as a component of exhaust gases from vehicles, and industrial and power plants. In order to reduce the emissions of this toxic gas, various absorption, adsorption and catalytic methods are applied. Catalytic methods are the most useful, because they generate a useful commercial product – sulphuric acid.

In this work we study the elimination of sulphur dioxide from gases on modified nanocarbons (carbon nanotubes containing platinum).

A nanocarbon product containing iron carbide crystallites, carbon nanotubes and amorphous carbon was synthesised using chemical vapor deposition (CVD) through the catalytic decomposition of ethylene on nanocrystalline iron. After hydrogen treatment of the pristine material, we obtained multi-walled carbon nanotubes with crystallites of metallic iron. Reduction under hydrogen resulted in the removal of amorphous carbon and the decomposition of iron carbide to iron and methane. The next step was to decorate the carbon nanotubes with platinum in order to obtain NCHPt (catalyst).

This process was carried out by passing 10 dm^3/h of a gas mixture of SO_2, O_2, N_2, containing 1.0 vol.% SO_2 at 300–400°C. The flow of the gas mixture was fixed
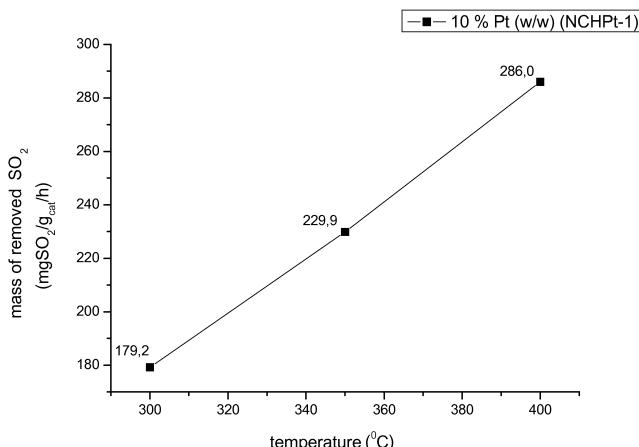
Figure 1: Temperature dependence of the mass of the SO_2 removed on the Pt/CNTs catalyst

at 10 dm^3/h using a mass flow meter. The glass reactor was heated in an electric furnace, where the volume of the sample was 5 ml and the height of the catalyst bed was ca. 12 mm.

Figure 1 shows the dependence of the mass of the removed SO$_2$ on temperature. The inlet concentration of SO$_2$ was 1.0 vol.%. Between 300 and 400°C, the efficiency of the process increased with temperature, and the best results were obtained at 400°C.

Con-flow monolithic silica microreactor functionalized with gold nano-particles

K. Odrozek[1], W. Pudło[1], A. B. Jarzębski[1,2], J. Malinowski[1],
K. Maresz[1], J. Mrowiec-Białoń[1,2]

[1]*Departament of Chemical Engineering, Silesian University of Technology
M. Strzody 7, 44-100 Gliwice, Poland*

[2]*Institute of Chemical Engineering, Polish Academy of Sciences
Bałtycka 5, 44-100 Gliwice, Poland*

The application of microreactors in synthesis of fine chemicals appears to be a very effective technical approach. In addition to the clear advantages of diminished sizes in microchannel devices the surface-to-fluid volume ratio of the fluid entity may even be increased 500 times and this greatly improves productivity, saves energy and expensive catalysts [1,2].

Here we propose a new microreactor made of monolithic silica, functionalized with gold nano-particles (NPs) for application in selective oxidation reactions and demonstrate its good performance in glucose oxidation to the gluconic acid.

The reactor was constructed by embedding seven rods (3×40 mm) into a polymeric cylinder, connected to headers with suitable ports. The silica rods featured an extensive system of meso (20 nm) – and flow-through macropores (ca. 30 μm) and they were synthesized by combining the liquid crystal templating method and phase separation [3]. Gold NPs were introduced onto the silica surface using a colloidal-deposition method [4]. The surface of the monoliths was modified with thiol/amine groups and/or alumina before deposition.

The con-flow monolithic microreactor performances were compared with those obtained by crushing monoliths and functionalizing the powder obtained in the same way.

The structural and chemical characteristics of the materials obtained were investigated using nitrogen adsorption at 77 K, transmission and scanning electron microscopy, dynamic light scattering and X-ray diffraction.

References
[1] W. Ehrfeld, V. Hensel, H. Löwe, Microreactors, Wiley-VCH, Weinheim (2000)
[2] A. Sachse, A. Galarneau, B. Coq, F. Fajula, New J. Chem. 35 (2011) 259
[3] A. Burkat-Dulak, V. Pashkova, W. Pudło, E. Włoch, A. Jarzębski, M. Derewiński, Pol. J. Chem. 9 (2008) 1809
[4] S. Biella, F. Porta, L. Prati, M. Rossi, Catal. Lett. 90 (2003) 23

Functionalization of multi-walled carbon nanotubes by chlorination in the gas phase

I. Pełech[1], U. Narkiewicz[1], D. Moszyński[1], R. Pełech[2]

[1] *Institute of Chemical Technology and Environmental Engineering*
West Pomeranian University of Technology
Pułaskiego 10, 70-310 Szczecin, Poland

[2] *Institute of Organic Technology, West Pomeranian University of Technology*
Pułaskiego 10, 70-310 Szczecin, Poland

Carbon nanotubes (CNTs) have potential applications in many fields, e.g. as electron emitters in field of emission displays, scanning probe microscopy tips and sensors. These materials can also be applied as fillers in polymer composites, since the addition of CNTs to the polymer matrix improves the mechanical properties of the composite. Pristine nanotubes are insoluble in many liquids, such as water and most solvents, therefore, they are difficult to disperse in the polymer matrix. To make nanotubes more easily dispersible in liquids, functionalization is performed. This process consists in attaching molecules or functional groups to the sidewalls of carbon nanotubes.

For oxidative modification of CNTs, gas or liquid-phase oxidation can be applied. Various acids can be used as oxidants in the liquid phase. Oxidation generates functional groups, such as $-COOH$, $-OH$, $-C=O$ and eliminates metal particles. Another method for the functionalization of carbon nanotubes consists in modifying the surface of CNTs with halogens: fluorine or chlorine.

In this paper, we present the modification of carbon nanotubes by chlorination, which enables the purification of multi-walled nanotubes (MWNTs) from metal impurities and the functionalization of the surface of carbon nanotubes. The raw material was obtained by decomposition of ethylene on nanocrystalline iron or iron-cobalt catalyst at 700°C. Chlorination was performed in the gas phase for 2 h. X-ray photoelectron spectroscopy (XPS) confirmed the presence of chlorine species on the surface of the chlorinated samples. The quantitative analysis of the content of metal impurities was confirmed by thermogravimetric analysis. The phase composition of the samples was determined by X-ray diffraction and the morphology of carbon nanomaterials was studied by transmission electron microscopy.

Purification of multi-walled carbon nanotubes by microwave-assisted acid digestion

I. Pełech, U. Narkiewicz, K. Owodziń

Institute of Chemical Technology and Environmental Engineering
West Pomeranian University of Technology
Pułaskiego 10, 70-310 Szczecin, Poland

Carbon nanotubes (CNTs) can be synthetized by chemical vapor deposition (CVD). CVD consists in the catalyst-assisted decomposition of carbon-containing compounds. This is the most popular method and can produce carbon nanotubes on a large scale. The product of the synthesis contains not only carbon nanotubes but also numerous impurities, e.g. amorphous carbon and metal particles.

In order to purify CNTs from carbon impurities, oxidation must be carried out under air or steam atmosphere or using oxidizing agents, e.g. nitric acid, potassium permanganate or hydrogen peroxide. The separation of carbon nanotubes from catalyst traces is usually carried out using the acid reflux method in the presence of acids. An alternative method of purifying CNTs from metal particles is by microwave heating.

In this work, we present an approach which uses microwave-assisted acid digestion for the purification of multi-walled carbon nanotubes obtained by the decomposition of ethylene at 700°C on a bimetallic iron-cobalt catalyst. The carbon material was immersed in a Teflon vessel filled with nitric or hydrochloric acid, either directly after the synthesis or after subsequent treatment under air atmosphere. Subsequently, the entire content was placed in a microwave-heated reactor. Experiments were carried out under pressures ranging from 15 to 30 at for 15 min. We investigated the influence of the type of acid, its concentration, pressure in the reactor and the preliminary treatment of the raw sample on the degree of removal of catalyst particles.

The phase composition of the samples was studied by X-ray diffraction. Transmission electron microscopy was applied to determine the morphology of carbon. The amount of catalyst particles in the samples after purification was determined by thermogravimetric analysis.

Configurational temperature and Monte Carlo simulations

S. Pieprzyk[1], S. Maćkowiak[2], A. C. Brańka[1]

[1] *Institute of Molecular Physics, Polish Academy of Sciences
Smoluchowskiego 17, 60-179 Poznań, Poland*

[2] *Technical Physics Faculty, Poznań University of Technology
Nieszawska 13a, 60-965 Poznań, Poland*

In stochastic calculations, such as Monte Carlo simulations, only positions or configurations of particles are generated and therefore the kinetic temperature (the average kinetic energy per degree of freedom) cannot be calculated. In this case, the temperature is often an input quantity, which cannot be verified directly during the simulations. The concept of configurational temperature may offer a solution to this problem.

In the presentation, the expressions for the configurational temperature will be investigated from the point of view of their utility as a diagnostic tool for Monte Carlo (MC) simulations. The simulations were performed for systems of spherically symmetric particles in the bulk, and in a narrow channel geometry. Different densities and system sizes were considered. It is shown that the configurational temperature based on the ratio of two averages of the force functions can serve as a suitable method for calculating the temperature for an MC simulation. Furthermore, it is demonstrated that this configurational temperature can signal the presence of random number correlations and can serve as a cross-check formula in the studies of strongly confined systems. The possible utility of the configurational temperature in the studies of small particle clusters will also be mentioned.

Modeling of branching and gelation in living copolymerization of monomer and divinyl cross-linker atom transfer radical polymerization (ATRP): simulation studies

P. Polanowski[1], J. K. Jeszka[2,3], K. Matyjaszewski[4]

[1] *Department of Molecular Physics, Technical University of Lodz*
Żeromskiego 116, 90-924 Łódź, Poland

[2] *Centre of Molecular and Macromolecular Studies, Polish Academy of Sciences*
90-365 Łódź, Poland

[3] *Department of Man-Made Fibres, Technical University of Lodz*
Żeromskiego 116, 90-924 Łódź, Poland

[4] *Department of Chemistry, Carnegie Mellon University*
4400 Fifth Avenue, Pittsburgh, Pennsylvania 15213, US

Technological progress requires new advanced polymeric materials with precisely defined complex architectures. The synthesis of such materials is challenging and requires a better understanding of the polymerization processes. One of the most powerful methods for the synthesis of well-defined polymer materials with complex architectures is controlled radical polymerization (CRP), and atom transfer radical polymerization (ATRP) in particular. Compared with conventional radical copolymerization, where initiation is slow and chain growth is very fast, CRP processes allow better control of molecular architecture and yield gels with preserved chain-end functionality and more homogeneous structure.

In this work, we use the dynamic lattice liquid model (DLL) in order to simulate ATRP copolymerization of a monomer and a divinyl cross-linker. We present the structural properties of randomly cross-linked polymers obtained for various initial cross-linker/monomer ratios in bulk polymer and diluted ATRP systems. During different ATRP experiments we found that this simple model allows to predict the gel point, which was in good agreement with experimental data. Moreover, it is able to predict the effect of the solvent dilution on the gel points. Molecular weights, polydispersities and the effect of intramolecular cyclization can be modeled as a function of time and monomer conversion. We also discuss the source of the discrepancy between the results obtained with the DLL method and the mean-field theory.

LPE growth and characterization of CdZnTe films

L. V. Rashkovetskyi[1], P. P. Moskvin[2], J. M. Olchowik[3]

[1] *V. Lashkaryov Institute of Semiconductor Physics*
41, prospect Nauki, Kiev, 03028, Ukraine

[2] *Zhytomyr State Technological University*
Chernyahovsky str., 103, 10005 Zhytomyr, Ukraine

[3] *Lublin University of Technology*
Nadbystrzycka 38D, 20-618 Lublin, Poland

At present the requirements concerning the quality of single crystals and epitaxial layers of CdZnTe which are widely used as active elements of IR and optoelectronic devices as well as radiation dosimetry are sufficiently increased. Thus, the efforts of technologists are directed towards the development and updating of crystallization methods of high quality materials with the required parameters.

$Cd_{1-x}Zn_xTe$ films of the solid phase content of $x = 0.015$–0.15 mol.fr. and thickness of > 10 μm were grown in a closed vacuum system in the 480–580°C temperature interval from a tellurium solution (more than 98% of Te) by liquid phase epitaxy (LPE). The supercooling temperature range was 15–50°C. The growth time was 30–60 min. Chemically polished (surface roughness of less than 0.1 μm) single-crystalline CdTe plates, 20 mm in diameter, orientation (111), were used as substrates. When the growth of the epitaxial films had ended, a special procedure of removing the growth solution was used. Experiments were carried out to select the liquid phase composition in order to obtain CdZnTe films of the abovementioned composition in the given interval of growth temperatures. The point when there was no substrate melting in contact with the growth solution was chosen as the correct crystallization onset temperature whereby planar growth of the layer was achieved.

The kinetic model of layer crystallization was based on the diffusion-limited crystallization model. The kinetics analysis results were data on interconnections of the growth temperature compositions of the liquid and solid phases, the super-cooling values and the layer growth rates. Based on the theoretical and experimental data, taking into account the stresses arising in CdZnTe/CdTe heterostructures due to the mismatching of the layer-substrate crystal lattice parameters, the surface of a coherent diagram of the Cd-Zn-Te system in the tellurium angle was constructed.

The degree of perfection of the grown Cd-Zn-Te layers was investigated using X-ray diffraction methods (the Berg-Barrett method and reflection which were obtained in (111) symmetrical geometry of diffraction for CuKα-radiation). The analysis of the results showed that the grown films were single-crystalline, following the substrate orientation, and the rocking curve halfwidth (FWHM) was monotonically increased from 40 arcsec (0.015 Zn mol.fr.) up to 200 arcsec (0.1 Zn mol.fr.). In topographs (reflection 422) the appearance of the 60°" network of dislocation mismatching was

clearly seen which was determined by the presence of mechanical stresses in the system which led to the tension of the lattice of crystalline layers.

The microhardness of the heterostructures in question was investigated for the first time by the Vickers method with the indenter loading of $P = 0.05$ N. A monotonic increase in the microhardness from 360 (0.015 Zn mol.fr.) up to 3.90 MPa (0.1 Zn mol.fr.) was observed. The obtained microhardness data were different from the reference data on the microhardness of the initial components, i.e. CdTe and ZnTe single crystals and solid solutions made on their base [1].

In our case the crystal lattice strengthening effect during the introduction of zinc was explained by the microstress effect near the film-substrate interface.

The dopant-defect influence on the parameters of the freshly-grown CdZnTe films, in comparison to the substrates, was investigated by the Auger spectroscopy method and by low temperature (of 5 K) photoluminescence method. A laser was used as the source of excitation of photoluminescence in the 1.5–1.7 eV energy interval He-Ne.

It was only one dominating line that was observed in the photoluminescence spectra. The line was connected with the annihilation of excitons which were bound to deep donors (D°X) and acceptors (A°X). Its intensity was almost 20 times higher than that for other lines and its halfwidth (FWHM) −2.5 meV which was observed for the best bulk crystal and for film samples obtained by the different methods (HPB, MBE).

References

[1] S. N. Ekpenuma, C. W. Myles, *J. Vac. Sci. Technol. A.* 10 (1), 208 (1992)

Modeling of high-magnetic-field and high-frequency (HMF-EPR) spectroscopy data for Fe^{2+} ($S = 2$) ions in $FeM*_{Z*}HO$ ($M* = F_2$, Cl_2, $(NH_4)_2$, (SO_4) and $Z* = 4$, 6) compounds

C. Rudowicz, D. Piwowarska

Modeling in Spectroscopy Group, Institute of Physics
West Pomeranian University of Technology
Al. Piastów 17, 70-310 Szczecin, Poland

Conventional electron magnetic resonance (EMR) techniques utilize magnetic fields $B \leq 1.5$ T and microwave frequencies $\nu \leq 36$ GHz, which are suitable for transition ions exhibiting small or moderate zero-field splitting (ZFS) [1–3]. These techniques can hardly be applied to spin systems exhibiting large ZFS, e.g. $3d^4$ (V^+, Cr^{2+}, Mn^{3+}, Fe^{4+}) and $3d^6$ (Mn^+, Fe^{2+}, Co^{3+}, Ni^{4+}) ions with spin $S = 2$ in crystals [4]. Instead of conventional X/Q-band EMR, these ions require novel high-magnetic-field and high-frequency EMR (HMF-EMR) techniques [5–8], e.g. employing swept fields up to 25 T combined with multiple sub-THz frequencies [5]. Due to rapid progress in HMF-EMR techniques in the last decades, a vast amount of experimental data has been accumulated, which still awaits theoretical explanation.

The orthorhombic spin Hamiltonian (SH) parameters have recently been determined [5] for Fe^{2+} ions in ferrous ammonium sulfate hexahydrate $Fe(NH_4)_2(SO_4) \cdot 6H_2O$ [FASH]. This system belongs toa series of compounds with the chemical formula $FeM*_{Z*}H_2O$, where $M* = F_2$, Cl_2, $(NH_4)_2(SO_4)$, and $Z* = 4$, 6. Theoretical explanation of experimentally observed spectroscopic properties of Fe^{2+} ($S = 2$) ions in these systems was provided by crystal-field (CF) theory and the microscopic spin Hamiltonian (MSH) theory [1–3]. The MSH approach [9,10] was applied to correlate HMF-EMR data with the microscopic parameters, i.e. spin-orbit coupling λ, spin-spin coupling ρ, energy level splittings Δ_i, and mixing coefficients $q(s)$. Comprehensive modeling of ZFS parameters (in the extended Stevens notation, b_k^q, and in conventional notation, D, E) and Zeeman electronic g_i-factors was carried out using the MSH/VBA (Visual Basic for Applications) computer package. This package is capable of plotting the values of the ZFS parameters versus the input values λ, ρ, Δ_i [9]. The variation of the ZFS parameters was studied taking into account the reasonable ranges of the microscopic ones suitable for Fe^{2+}:FASH and related systems. Our analysis indicates the importance of fourth-rank ZFS terms and spin-spin coupling contributions. Modeling of SH parameters may aid the theoretical interpretation as well as the simulation of HMF-EMR experimental data for these complexes.

References

[1] A. Abragam, B. Bleaney, Electron Paramagnetic Resonance of Transition Ions, Clarendon Press, Dover, 1986

[2] J. R. Pilbrow, Transition-Ion Electron Paramagnetic Resonance, Clarendon, Oxford, 1990

[3] F. E. Mabbs, D. Collison, Electron Paramagnetic Resonance of d Transition-Metal Compounds, Elsevier, Amsterdam, 1992

[4] C. Rudowicz, H. W. F. Sung, J. Phys. Soc. Japan 72 Supplement B (2003) 61

[5] J. Telser, et al., Magn. Reson. Chem. 43 (2005) S130

[6] L. C. Brunel, in: O. Grinberg and L. J. Berliner (Eds.), Biological Magnetic Resonance, vol. 22, Very High Frequency (VHF) ESR/EPR, Kluwer Academic Publishers, Netherlands, 2004, Chapter 14, p. 466

[7] M. Motokawa, Rep. Prog. Phys. 67 (2004) 1995

[8] J. Telser, J. Braz. Chem. Soc. 17 (2006) 1501

[9] C. Rudowicz, H. W. F. Sung, Manual for the package MSH/VBA (2004) – *Internal CityU Report*

[10] C. Rudowicz, H. W. F. Sung, Physica B 337 (2003) 204

Size effect of triglycine sulphate nanocomposites

E. Rysiakiewicz-Pasek, A. Ciżman, J. Komar, T. Marciniszyn,
R. Poprawski, A. Sieradzki

Institute of Physics, Wrocław University of Technology
W. Wyspiańskiego 27, 50-370 Wrocław, Poland

The influence of the size-effect on phase transitions in ferroelectrics has acquired a great impetus in the last two decades resulting from the technological need for smaller and faster devices. The experimental techniques in the search of nanostructured ferroelectrics rely on the ability to create new types of structures. A well known method among different methods of nanosized ferroelectric fabrication is introducing ferroelectric materials into porous matrices [1, 2].

Triglycine sulphate TGS nanocomposites of different sizes (24 to 624 nm in diameter) were prepared by the simple water solution method which relies on filling nanovoids in porous matrices by a ferroelectric material [3]. After crystallization the sample surfaces were polished mechanically to remove small TGS crystals. The dielectric properties of nanometer-sized TGS samples were investigated in the wide frequency range from 0.1Hz to 3MHz, and the temperature range including the ferroelectric phase transition. The pyroelectric measurements were carried out after earlier polarization by an external electric field. The pyroelectric current measurements in a wide temperature range were performed during the heating process. On the basis of dielectric and pyroelectric measurements a phase diagram (the phase transition temperature vs. the reverse mean value of the ferroelectric size) was created. The results showed that the ferroelectric phase transition temperature of TGS was strongly affected by the size of nanocrystals. It was observed that size effect was strongly non-linear and in agreement with the theoretical predictions for crystals with polarization rising at surface (negative extrapolation length) [4,5]. It is worth noting that such dependence has been observed experimentally for the first time.

References

[1] E. V. Colla, A. V. Fokin, Yu. Kumzerov, 1997 Sol. State Comm. 103, 127–130
[2] R. Poprawski, E. Rysiakiewicz-Pasek, A. Sieradzki, A. Ciman, J. Polanska, 2007 J. Non-Cryst Sol. 353, 4457–4461
[3] E. Rysiakiewicz-Paser, R. Poprawski, J. Polaska, A. Sieradzki, E. B. Radojewska, 2005 J. Non-Cryst Sol. 351, 2703–2709
[4] W. L. Zhong, Y. G. Wang, P. L. Zhang, B. D. Qu, 1994 Physical Review B 50, 698–703
[5] E. V. Charnaya, A. L. Pirozerskii, Cheng Tien, M. K. Lee, 2007 Ferroelectrics 350, 75

Dielectric properties of nanostructured potassium nitrate

E. Rysiakiewicz-Pasek[1], E. Koroleva[2,3], E. Berman[3],
A. Naberezhnov[2,3], A. Sysoeva[2]

[1] *Institute of Physics, Wroclaw University of Technology*
W. Wyspianskiego 27, 50-370 Wrocław, Poland

[2] *Ioffe Phys.-Tech. Institute RAS*
Polytechnicheskaya 26, 194021, St.-Petersburg, Russia

[3] *St.-Petersburg State Polytechnical University*
Polytechnicheskaya 29, 1952151, St.-Petersburg, Russia

The size effect leads to a change in the macroscopic physical properties of nanostructured materials (NSM). There are different methods of NSM preparation and one of them is embedding substances into the pores of various porous media, for example, porous glasses. This contribution is devoted to a study of the dielectric response of NSM on the base of porous glasses containing embedded potassium nitrate (KNO_3).

We used porous glasses with average pore diameters of 320 (PG320), 46 (PG46) and 7 (PG7) nm as the matrix. The dielectric properties were studied in the frequency range of 0.1–10 MHz and in the temperature interval of 273–590 K. The rectangular flat plates of porous glasses were filled by melted KNO_3. After filling, the surfaces of the samples were cleaned to remove the bulk material and dried at 370 K for 2 hours to remove any possible remnant water. Sputtered gold was used as electrodes. The temperature dependences of dielectric permittivity, ε', on heating and cooling
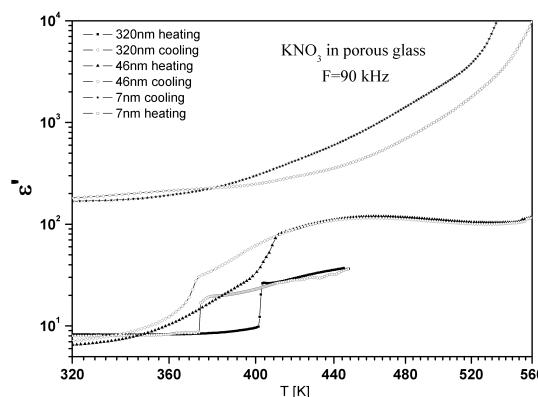
Figure 1: Temperature dependencies of ε' for KNO_3 within PG320, PG46 and PG7

at 90 kHz for all types of samples are presented in Figure 1. It is shown that ε' for NSM is essentially higher than for the bulk and increases more than 10 times with the decreasing pore diameter. The phase transition (PT) temperatures increase for KNO_3 from the low-temperature to high-temperature paraelectric phase within PG46 and PG7 on heating.

The phase transition temperatures decreased for KNO_3 from the ferroelectric phase to the low-temperature paraelectric phase within PG46 and PG7 on cooling. We did not observe any anomalies in ε' corresponding to the transition from the high-temperature paraelectric phase to the intermediate ferroelectric phase on cooling for all samples, but preliminary neutron diffraction studies of the crystal structure evolution of these NSM showed that this PT was realized. A decrease in the average pore diameters led to essential smearing of all the observed PT. The temperature dependencies of the parameters of relaxation processes and the input of DC conductivity were determined from an analysis of the dielectric response. The existence of a relaxation process with an anomaly of dielectric strength in the region of the ferroelectric PT was shown. The analysis confirmed the supposition that the giant effective dielectric response was due to nonhomogeneous conductivity. The activation energies of relaxation processes were estimated.

References

[1] U. Kawabe, T. Yanagi, S. Sawada, 1965 J. Phys. Soc. Japan 20, 2059

Carbon microflowers

A. T. Sobczyk[1], A. Jaworek[2], Z. Sobisz[3]

[1]*Institute of Fluid Flow Machinery, Polish Academy of Sciences*
Fiszera 14, 80-952 Gdańsk, Poland

[2]*Institute of Physics, Pomeranian Academy*
Arciszewskiego 22B, 76-200 Słupsk, Poland

[3]*Institute of Biology and Environment Protection, Pomeranian Academy*
Arciszewskiego 22B, 76-200 Słupsk, Poland

Micro- or nanoflower is a self-organized planar or 3D microstructure resembling a macroscopic biological form known as the flower. In recent years, microflowers have drawn the attention of scientists not only due to their aesthetic features, but also because of powerful potential applications owing to their high specific surface area. The term "nanoflower" was probably used for the first time by Yan Qiu Zhu et al. in their papers published in 1998 and 1999, although "cauliflower-like" structures had been mentioned in many earlier papers. Microflowers can be formed by using various standard methods applied in microfabrication or in nanotechnology and built from almost all metal, ceramic or polymer materials as incomplete growth or as a part of a bulk product. As each flower has its own structure and no two of them are identical (like two snowflakes) the microflower building process cannot be exactly reproducible but the general form of the structure remains the same for the same material and for the same process parameters.

In the paper we analyzed the morphology of carbon flower-like microstructures produced in electrically generated plasma in a mixture of cyclohexane with argon as the carrier gas. The supply voltage used for plasma generation ranged from 5 to 25 kV, and the discharge current, from 1 to 5 mA. The physical properties of carbon structures were analyzed with scanning electron microscopy, Raman spectroscopy, and X-ray diffraction.

The Raman spectrum emitted in the range from 1000 cm^{-1} to 1700 cm^{-1} revealed the following peaks: 1192 cm^{-1}, 1309 cm^{-1}, 1486 cm^{-1} and 1598 cm^{-1}, corresponding to carbon Dand G-bands that indicate a hexagonal graphite-lattice structure and the existence of a large quantity of carbonaceous impurities. The X-ray diffraction measurements showed that the carbon structures obtained during the discharge were partially crystalline and partially amorphous. The values of $26.5°$, $28.5°$, $32.3°$, $47.5°$ were recorded in peaks at 2θ. An XRD peak at $2\theta = 26.5°$ corresponds to the 002 plane of graphite which is in good agreement with the Raman spectroscopy investigations. Other peaks at $2\theta = 35.7°$ and $38.4°$ correspond to Si (which was the detector substrate), and the peak of $2\theta = 32.3°$ is of unknown origin. The elemental analysis was used to identify the weight percentage of carbon and hydrogen in synthesized deposit. The analysis confirmed that carbon was the dominant element in the product, with C – 98.7 wt.% and H – 0.9 wt.%, the rest was N and O absorbed from the

atmosphere (comparing to cyclohexane of C – 85.7 wt.%, H – 14.3 wt.%). It is therefore evident that highly carbonized products can be obtained from decomposition of cyclohexane in electrically generated plasma.

For aesthetic reasons the produced microflowers were referred to the actual biological species. An example of a carbon microflower similar to the Red Peacock (*Brassica oleracea*) is presented in the Figure 1.
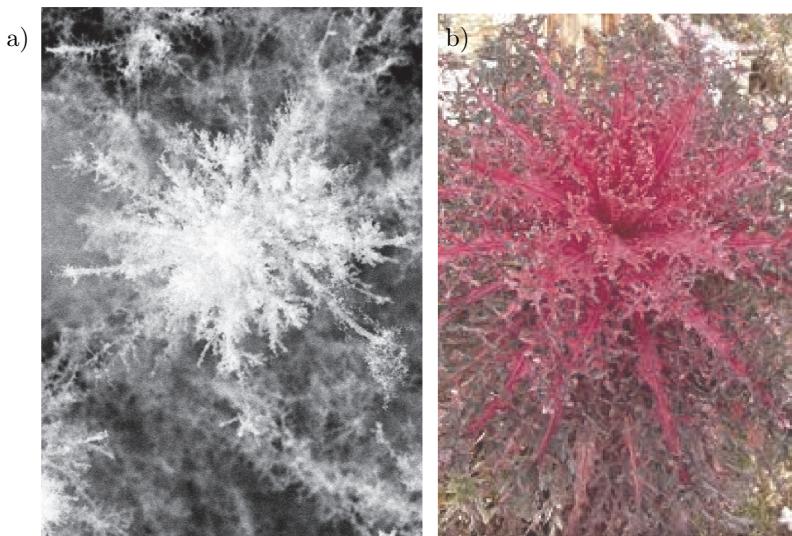
Figure 1: (a) Soot deposit on stainless steel substrate, discharge current 4 mA, cyclohexane concentration 4 wt.%; (b) Red peacock (*Brassica oleracea*) [www.jungleseeds.com/images/]

Ferromagnetic resonance study
of carbon coated nickel and cobalt nanoparticles

M. Soboń[1], I. E. Lipiński[2]

[1] *The Faculty of Management and Economic of Services, University of Szczecin*
Cukrowa 8, 71-004 Szczecin, Poland

[2] *Institute of Physics, Faculty of Mechanical Engineering and Mechatronics*
West Pomeranian University of Technology
Al. Piastów 17, 70-311 Szczecin, Poland

Two types of samples of agglomerated cobalt and nickel magnetic nanoparticles coated with carbon dispersed in a paraffin matrix were studied. The temperature dependence of the FMR (ferromagnetic resonance) spectra was recorded in the temperature range from 100 K to 300 K.

Both the samples showed a very intense and broad asymmetric FMR resonance line arising from cobalt and nickel nanoparticles. However, for the nickel sample, in spite of a structure similar to the cobalt sample, a quite different FMR spectrum and temperature dependence were obtained. In order to calculate the values of magnetic resonance fields and linewidths, the FMR spectra were fitted by summing up Lorentz curves representing absorption and dispersion functions. The differences in the recorded FMR spectra and their temperature dependence were explained by an analysis of magnetic interactions as well as taking into account the influence of the paraffin matrix on active ionic displacements.

Magnetic resonance study
of γ-Fe$_2$O$_3$-betaine-MnCl$_4$ system

J. Typek[1], N. Guskos[1,2], G. Żołnierkiewicz[1], D. Petridis[3], K. Wardal[1]

[1]*Institute of Physics, West Pomeranian University of Technology*
Al. Piastów 48, 70-311 Szczecin, Poland

[2]*Solid State Section, Department of Physics, University of Athens*
Panepistimiopolis, 15 784 Zografos, Greece

[3]*Institute of Materials Science, NCRS "Demokritos"*
153 10 Aghia Paraskevi, Attikis, Athens, Greece

A novel class of compounds combining molecular magnets with ferrimagnetic iron oxide nanoparticles was synthesized. The purpose was to examine the effect of the magnetic properties of γ-Fe$_2$O$_3$ on the magnetic properties of its partner. In this report we describe the magnetic resonance behaviour of Mn^{2+} bound as an MnCl$_4$$^{2-}$ anion to γ-Fe$_2$O$_3$ through a betaine (Me$_3$N$^+$-CHCOO$^-$) spacer. Nanosize γ-Fe$_2$O$_3$ was prepared according to the precipitation method using FeCl$_3$.6H$_2$O and FeSO$_4$.7H$_2$O in the 2:1 mole ratio. After isolation and washing the γ-Fe$_2$O$_3$ nanoparticles were dispersed in water and treated with betaine. The solid γ-Fe$_2$O$_3$-betaine was dispersed in ethanol containing a few drops of HCl. MnCl$_2$ was added to this solution.

The obtained sample was investigated by using an X-band electron paramagnetic resonance (Bruker E 500) spectrometer in the 90-300 K temperature range. The registered spectra are presented in Figure 1.
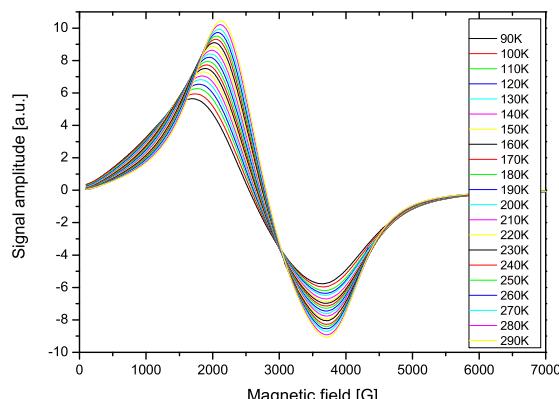
Figure 1: Magnetic resonance spectra of the investigated sample registered at different temperatures in the 90–300 K range

The spectral lines were slightly asymmetric and they were attributed to the γ-Fe_2O_3 nanoparticles in a superparamagnetic state. Following the method proposed by Kliava [1] the registered spectra were fitted by two lines with lineshapes obtained from the solution of the Landau-Lifshitz equation. These two component lines were a result of magnetic anisotropy of the γ-Fe_2O_3 nanoparticles. As an example, a comparison of the experimental and fitted spectra at $T = 120$ K is presented in Figure 2. The fitting allowed s to determine the intrinsic resonance fields, linewidths and integrated intensities for both spectral components at different temperatures. The two obtained resonance fields (280 and 345 mT) did not vary in the studied temperature range. This behaviour was in contrast to the usually observed decrease in the resonance field with lowering temperature for typical nanoparticles embedded in a non-magnetic matrix [2]. On the other hand, two linewidths showed a pronounced temperature variation (Figure 3). On lowering the temperature the linewidths increased significantly.
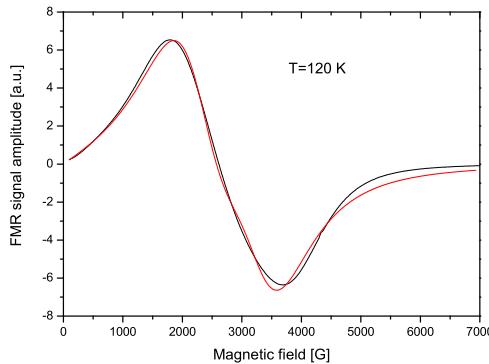
Figure 2: Experimental (black) and fitted (red) spectra of the investigated sample at $T = 120$ K
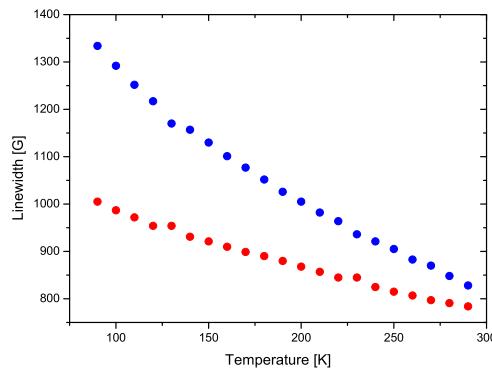
Figure 3: Temperature dependence of linewidths of two fitted components

The temperature dependence of integrated intensity (calculated as an area under the absorption curve) displayed the Curie-Weiss-type of behaviour, $I(T) = C/(T - T_0)$, with $T_0 = -33.2$ K. This indicates the existence of strong antiferromagnetic interactions in the studied sample.
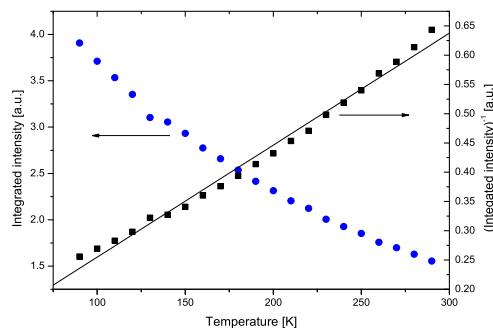
Figure 4: Temperature dependence of integrated intensity (left axis) and reciprocal of integrated intensity (right axis) for investigated sample

References

[1] S. P. Gubin (Editor) 2009 *Magnetic nanoparticles*, Wiley-VCH, Chapter 7: Janis Kliava – Electron Magnetic Resonance of Nanoparticles: Superparamagnetic Resonance, pp. 255–302

[2] N. Guskos, M. Maryniak, J. Typek, A. Guskos, R. Szymczak, E. Senderek, Z. Rosłaniec, D. Petridis, K. Aidinis 2008 *J. Non-Cryst. Solids* **354** (35–39) 4401

Magnetic resonance study
of new compound Nb_2SbVO_{10}

J. Typek[1], G. Żołnierkiewicz[1], A. Cyran[2], K. Wardal[1],
E. Filipek[3], M. Piz[3]

[1]*Institute of Physics, West Pomeranian University of Technology*
Al. Piastów 48, 70-311 Szczecin, Poland

[2]*Institute of Material Science, West Pomeranian University of Technology*
Al. Piastów 19, 70-310 Szczecin, Poland

[3]*Department of Inorganic and Analytical Chemistry*
West Pomeranian University of Technology
Al. Piastów 42, 71-065 Szczecin, Poland

In recent years, the research on multicomponent oxides systems has been intensified in order to obtain new materials with interesting electric, magnetic or catalytic properties. The basic studies on the ternary V_2O_5-Nb_2O_5-Sb_2O_4 system showed that oxides in the solid state in air formed an unknown compound with the formula $Nb_2\,SbVO_{10}$ [1]. This compound was obtained by heating the mixture $V_2O_5/Sb_2O_4/Nb_2O_5$ (in the molar ratio of 1:1:2) in air at temperatures up to 750°C according to the equation: $V_{2}O_{5(s)} + 2Nb_2O_{5(s)} + Sb_2O_{4(s)} + \frac{1}{2}O_{2(g)} = 2Nb_2SbVO_{10(s)}$. The compound Nb_2VSbO_{10} can be also obtained by heating an equimolar mixture of $SbVO_5$ and T-Nb_2O_5 according to the equation: $Nb_2O_{5(s)} + SbVO_{5(s)} = Nb_2\,SbVO_{10(s)}$ [2]. The new compound Nb_2VSbO_{10} was stable in air up to 880°C and then melted incongruently with a deposition of solid Nb_9VO_{25}. It crystallized in the orthorhombic system with the following unit cell parameters: $a = 0.328143$ nm, $b = 0.458946$ nm, $c = 1.22476$ nm, $(Z = 1)$ [2].

The electron paramagnetic resonance (EPR) study of Nb_2SbVO_{10} was carried out on a conventional Bruker E 500 X-band continuous wave equipped with a TE_{102} cavity with 100 kHz modulation. The temperature variation studies in the 7–300 K range were performed using an Oxford ESP300 continuous-flow helium cryostat. The EPR spectrum registered in the high temperature range is presented in Figure 1.

A comparative study with a standard $VOSO_4 \cdot 5H_2O$ sample with a known number of spins was performed to estimate the number of spins in the Nb_2SbVO_{10} sample participating in the resonance. Assuming that vanadium ions in the Nb_2SbVO_{10} compound could be only in 4+ (EPR active) or 5+ (EPR inactive) valence states it was calculated that only 5.2% of the vanadium ions were magnetic and thus in the 4+ valence state. This concentration of magnetic ions was much larger than in the previously studied $SbVO_5$ compound [3,4]. The knowledge of concentration of magnetic ions might be important in estimating the compound's catalytic activity as minority magnetic ions often play a dominant role in such activity.
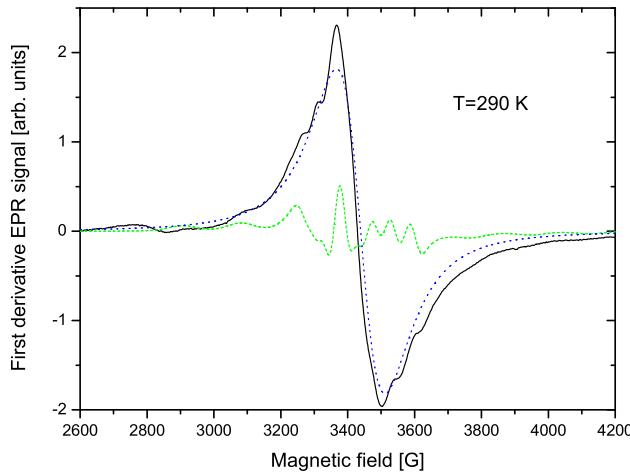
Figure 1: Observed spectrum of Nb_2VSbO_{10} (continuous line) at $T = 290$ K and its two main components: isolated V^{4+} ions (dashed line) and the broad line (dotted line)

The EPR spectrum of Nb_2SbVO_{10} in the high temperature range could be decomposed on three components: a broad signal in the range of $g \simeq 2$ without a hyperfine structure (hfs), partially resolved hfs lines typical of isolated vanadium ions in axial symmetry and a weak line near 2800 G. The broad line without hfs could be attributed to a mobile electron hopping along the V^{4+}-O-V^{5+} bond. The hfs could be substantially suppressed or even disappear due to various interactions of electronic spins with their surroundings. One such interaction occurs via a super-exchange through the oxygen bridge of an electron between aliovalent vanadium centers. The second component usually displays two sets of eight lines, partially overlapping, attributed to the interaction of electron spin ($S = 1/2$) with nucleus ^{51}V ($I = 7/2$, abundance 99.75%). This spectrum could be satisfactory described by an axial spin Hamiltonian of the form $H = \beta[g_{\parallel}B_zS_z + g_{\perp}(B_xS_x + B_yS_y)] + A_{\parallel}S_zI_z + A_{\perp}(S_xI_x + S_yI_y)$, where the symbols have their usual meaning. Fitting the registered spectrum by using the SimFonia program allowed us to obtain the following values of the spin Hamiltonian: $g_{\parallel} = 1.907$, $g_{\perp} = 1.947$, $A_{\parallel} = 164.6$ G, $A_{\perp} = 43.5$ G. These values did not show any significant temperature dependence. The third component displayed very anisotropic behavior. It shifted significantly with temperature, reaching the lowest resonance field of 2800 G at 200 K.

The temperature dependence of EPR integrated intensity of the whole spectrum was studied to reveal magnetic interactions in Nb_2SbVO_{11}. Figure 2 presents the reciprocal of integrated intensity *vs* temperature. Two temperature regimes are observed: in the high temperature range, ($T > 120$ K), this dependence is described by a Curie-Weiss law, $I_{EPR} = C/(T - T_{cw})$, with $T_{cw} = -82.8$ K. In the low temperature range (below 120 K) the same dependence is registered but with different Curie-Weiss temperature, $T_{cw} = -10.86$ K. As both T_{cw} are negative it follows that an effective antiferromagnetic interaction dominates in the magnetic system of Nb_2SbVO_{10}.
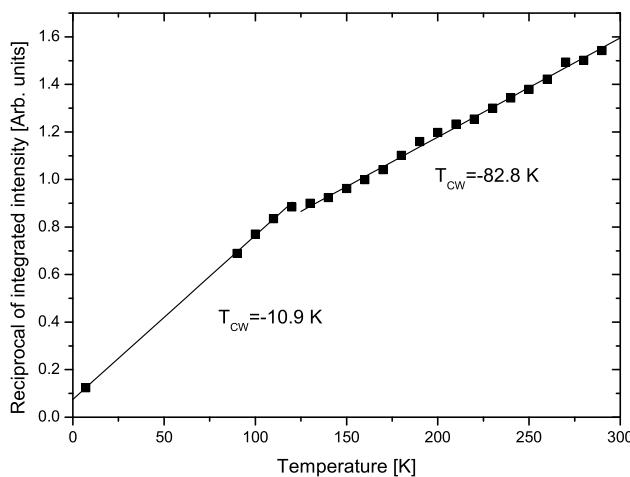
Figure 2: Temperature dependence of reciprocal integrated intensity of Nb_2SbVO_{11}; the straight lines are the least square fits for low and high temperature ranges

References

[1] E. Filipek, M. Piz, 2009 *Proc. 10th Conf. Calorium. Them. Anal. (Poland)* 41

[2] E. Filipek, M. Piz, 2010 *J. Therm Anal. Calorium.* **101** (2) 447

[3] J. Typek, N. Guskos, D. Buchowski, M. Wabia, E. Filipek, 2002 *Radiat. Eff. Defact. S.* **157** 1093

[4] J. Typek, E. Filipek, M. Maryniak, N. Guskos, 2005 *Mater. Sci-Poland* **23** (4) 1047

FMR and TGA study of Fe_2O_3/ZnO nanoparticles in PEN-b-PTMO polymer

K. Wardal[1], J. Typek[1], N. Guskos[1], G. Żołnierkiewicz[1],
E. Piesowicz[2], U. Narkiewicz[3], D. Sibera[3]

[1] *Institute of Physics, West Pomeranian University of Technology*
Al. Piastów 48, 70-311 Szczecin, Poland

[2] *Department of Polymer, West Pomeranian University of Technology*
Al. Piastów 19, 70-311 Szczecin, Poland

[3] *Institute of Chemical and Environmental Engineering*
West Pomeranian University of Technology
Al. Piastów 17, 70-311 Szczecin, Poland

Eight samples containing γ-Fe_2O_3/ZnO magnetic nanoparticles dispersed at concentrations of 0.05 and 0.1 wt.% in a PEN-b-PTMO multiblock copolymer were prepared and investigated using the DTA/DSC and FMR methods. The FMR spectra of the obtained samples were registered at room temperature (Figure 1). The FMR parameters (resonance field, linewidth, integrated intensity) were calculated (Table 1).
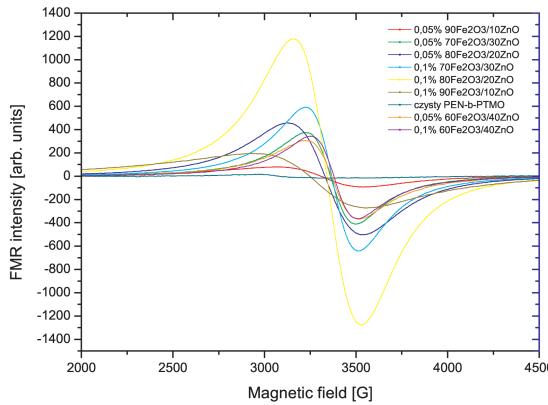
Figure 1: FMR spectra of all investigated samples at room temperature

A comparison with the previously studied similar nanocomposites [1,2] allowed drawing conclusions about the magnetic interactions of Fe_2O_3/ZnO nanoparticles in a PEN-b-PTMO polymer.

The resonance field shifted towards a smaller magnetic field with an increase in the Fe_2O_3 content in nanoparticles. A similar trend was observed for the linewidth which increased with an increase in the Fe_2O_3 content. The integrated intensity increased

Table 1: FMR parameters of investigated samples

Sample		Resonance field [G]	Linewidth [G]	FMR amplitude [arb. units]	Integrate intensity [arb. units]
Concentration in polymer [wt.%]	Nanoparticle				
0.05%	60%Fe2O3/40%ZnO	3375	250	700	1.094
	70%Fe2O3/30%ZnO	3335	330	800	2.178
	80%Fe2O3/20%ZnO	3305	456	950	4.938
	90%Fe2O3/10%ZnO	3300	510	174	1.131
0.10%	60%Fe2O3/40%ZnO	3375	260	690	1.166
	70%Fe2O3/30%ZnO	3335	394	1240	4.812
	80%Fe2O3/20%ZnO	3330	396	2470	9.683
	90%Fe2O3/10%ZnO	3208	750	410	5.766

initially with an increase in the Fe_2O_3 content, but a sharp drop was registered for the $90\%Fe_2O_3/10\%ZnO$ sample. This was connected with a decrease in the $ZnFe_2O_4$ content that produced the magnetic response of our samples.

Figures 2 and 3 present DSC thermograms and TGA response of an undoped PEN-b-PTMO polymer and this polymer with a 0.1 wt.% content of $80\%Fe_2O_3/20\%ZnO$. The melting temperature was slightly affected by a low concentration of magnetic
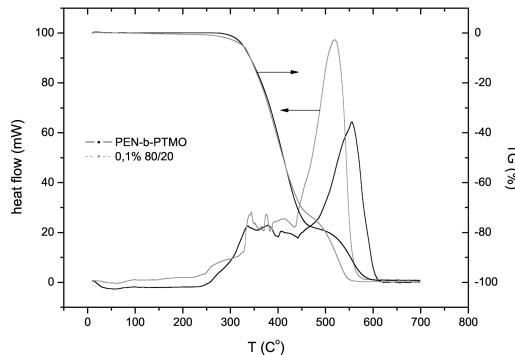
Figure 2: DSC scans of PEN-b-PTMO polymer containing 0.1% of $80\%Fe_2O_3/20\%ZnO$ (left axis) and TGA measurements in air (right axis)
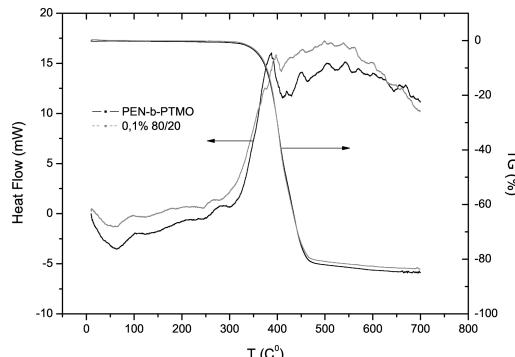
Figure 3: DSC scans of PEN-b-PTMO polymer containing 0.1% of $80\%Fe_2O_3/20\%ZnO$ (left axis) and TGA measurements in argon (right axis)

nanoparticles. The thermal and thermo-oxidative stability values of PEN-b-PTMO composites were examined by the TGA response in air and argon. Three distinct stages of degradation were observed in air, while only two steps were registered in argon.

References

[1] N. Guskos, M. Maryniak, G. Żołnierkiewicz, J. Typek, A. Guskos, E. Senderek, Z. Rosłaniec, D. Petridis 2008 *Appl. Magn. Reson.* **34** 175–181
[2] N. Guskos, J. Typek, G. Żołnierkiewicz 2010 *Current Topic in Biophysics* **33 (suppl A)** 77–80

Vanadium local structure in VN-SiO$_2$ sol-gel derived thin films

A. Witkowska, B. Kościelska, L. Wicikowski

Department of Solid State Physics, Gdańsk University of Technology
Narutowicza 11/12, 80-233 Gdańsk, Poland

In recent years, much attention has been paid to nitride and oxynitride thin films, and to VN films in particular, due to their extreme hardness, wear resistance, excellent oxidative stability, corrosion resistance and high-temperature stability [1]. Moreover, VN exhibits interesting electrical and superconducting properties (transition temperature of ~ 9 K) [2] and can be used in several microelectronic applications. The addition of even a small amount of silicon oxide to VN films improves their superconducting properties [3]. For future applications, it is crucial to know whether and how the VN/SiO$_2$ molar ratio and the film thickness influence the properties of VN films.

This paper is devoted to the structural analysis of xVN-$(100-x)$SiO$_2$ ($x = 90, 80,$ 70, 60 mol%) thin films by means of X-ray absorption spectroscopy (XAS). Thermal nitridation with ammonia at 1200ºC of sol-gel derived xV$_2$O$_3$-$(100-x)$SiO$_2$ coatings was used as the preparation method of the films. The microporous structure of the coatings enabled both the significant incorporation of nitrogen and its homogeneous distribution in the film. After this process, we obtained regularly shaped VN nanocrystals dispersed in SiO$_2$ amorphous matrix (their average diameter dependent on the VN/SiO$_2$ ratio). For thus prepared VN-SiO$_2$ thin films (of various composition and thicknesses), we collected near-edge (XANES) and extended (EXAFS) X-ray absorption fine-structure spectra at V K-edge (5465 eV). The XAFS experiment was performed at XAFS 11.1 beamline station at ELETTRA. The measurements were carried out at liquid-nitrogen temperature and at room temperature using fluorescence geometry (thin films contained very small amounts of vanadium photoabsorbing ions and are supported on a 1mm-thick silica glass plate). A detailed structural information about the local vanadium environment in the samples and its correlation with the addition of SiO$_2$ and the film thickness was obtained by EXAFS data analysis using the GNXAS method [4]. Spectra of the reference samples (V foil and vanadium pentoxide) were also analysed in order to construct a proper model for the elaboration of the data for the thin films.

On the basis of reference measurements and the systematic study performed on a series of selected vanadium compounds described in [5], we determined that in the considered thin films, independently of their composition and thickness, VN is the dominating phase, and the vanadium oxide phase consists mainly of V^{+3} ions. Thus, the XANES analysis demonstrated that the electronic structure of vanadium was independent of composition and thickness, which is in agreement with the superconducting properties of the films. The considered 450nm-thick samples and 80VN-20SiO$_2$ films of various thicknesses exhibited a superconducting transition. The critical temperature

(T_{conset}) ranged from 7.0 K to 7.5 K, with the only exception being the 90VN-10SiO$_2$, 450 nm-thick sample. In this sample a small drop in resistivity was observed at about 6.7 K. However, small differences in the temperature dependence of the sheet resistivity of the films with various values of x and of various thicknesses were observed below T_{conset}. This can be related to the granular structure of the films, i.e. to the amount of intergranular phase and/or to the ordering of the intragranular structure.

References

[1] Kwon H, Choi S and Thompson L T 1999 *J. Catal.* **184** 236
[2] Gray K E, Kampwirth R T, Capone II D W, Vaglio R and Zasadzinski J 1988 *Phys. Rev. B* **38** 2333
[3] Kościelska B, Winiarski A and Jurga W 2010 *J. Non-Cryst. Solids* **356** 1998
[4] Filipponi A and Di Cicco A 1995 *Phys. Rev. B* **52** 15122; *ibid.* 15135
[5] Wong J, Lytle F W, Messmer R P and Maylotte D H 1984 *Phys. Rev. B* **30** 5596

Effect of nanoparticles on the physical properties of PET-PTMO reactive blends

J. Wojnowski[1], M. Kwiatkowska[1], I. Pełech[2], Z. Rosłaniec[1]

[1] *Institute of Materials Science and Engineering*
West Pomeranian University of Technology
Al. Piastów 19, 70-310 Szczecin, Poland

[2] *Institute of Chemical and Environment Engineering*
West Pomeranian University of Technology
Pułaskiego 10, 70-322 Szczecin, Poland

Recently, an increased interest in the subject of nanocomposites, and hybrid nanocomposites in particular, has been observed. Being distinct from common nanocomposites, hybrid nanocomposites tend to have better properties owing to the synergistic effect of two-filler compounds. The aim of this research was to obtain hybrid nanocomposites and to examine the influence of the nanoparticles on the behavior of the matrix. Nanocomposites based on poly(ether-ester) copolymers, containing commercial multi-walled carbon nanotubes (MWCNTs) and carbon/metal magnetic nanoparticles (MNPs) were prepared by *in situ* polycondensation.

Magnetic nanoparticles and conductive (metallic) multi-walled carbon nanotubes were combined in equal amounts of 0.3 wt%, but in different arrangements (MWCNT + MNP = cons.). Fe-based compounds were used as magnetic fillers.

The morphology and the dispersion of the nanoparticles in the polymer matrix were characterized by scanning electron microscopy (SEM). The mechanical properties and rubber elasticity in static and cyclic tensile tests have been investigated. The influence of the nanoparticles on the melt viscosity of nanocomposites was evaluated. It was observed that the elongation at break of nanocomposites depended on the filling degree but rubber elasticity (reversibility) of the materials was constant.

Crystallization of hard disks induced by temperature gradient

S. Wołoszczuk

Institute of Physics, A. Mickiewicz University
Umułtowska 85, 61-614 Poznań, Poland

While uniform temperature has no effect on the equilibrium properties of hard-core systems, its gradient might substantially change their behavior. In particular, in a hard-disk system which is subject to temperature difference ΔT, disks are repelled from the system's hot boundary and accumulate at the cold one. Using event-driven molecular dynamics simulations we show that crystal forms at the cold boundary for sufficiently large ΔT or coverage ratio $\rho*$.

In this spatially inhomogeneous system a significant decrease in the diffusivity of disks clearly marks the stationary interface between liquid and crystal. Such behavior is also supported through calculation of the radial distribution function and the bond order parameter. Simulations show that for this nonequilibrium system the equipartition of energy holds and velocity obeys the Boltzmann distribution.

Investigations of 1.2–1.4 μm emission properties of Tm:Y$_2$O$_3$ transparent ceramic

Q. Yi[1], T. Tsuboi[2], S. Zhou[1], Y. Nakai[1], H. Lin[1], H. Teng[1]

[1] *Key Laboratory of Materials for High Power Laser*
Shanghai Institute of Optics and Fine Mechanics, Chinese Academy of Sciences
P.O. Box 800-211, Shanghai 201800, China

[2] *Department of Information and Communication Science*
Faculty of Engineering, Kyoto Sangyo University
Kamigamo, Kita-ku, Kyoto 603-8555, Japan

6 at% Tm^{3+}-doped Y$_2$O$_3$ transparent ceramic was fabricated by sintering at 1800°C for 20 h under vacuum of $1 \cdot 10^{-3}$ Pa. 3 at% ZrO$_2$ was introduced as a sintering aid. The addition of Zr^{4+} ions decreased the O^{2-} vacancy concentration, which led to a subsequent decrease in the Y^{3+} interstitial concentration and thus to lower grain boundary mobility. Lower grain boundary mobility was beneficial for eliminating the pores on grain boundaries. Therefore, with the addition of ZrO$_2$, the microstructure was uniform with an average grain size of 22 μm. The optical transmittance of the ceramic reached 76.3% at 1 μm. Basing on the photoluminescence excitation (PLE) spectra at 12 K and 296 K, the PL spectra were investigated at various temperatures at RT-12 K under Xe light excitation at 361 nm, 485 nm, 683 nm and 795 nm. Both room-temperature and 12 K-PL spectra were measured. An emission band at ~ 1270 nm was observed under the excitation at 361 nm and 485 nm. An emission band at ~ 1450 nm was observed under all four excitation wavelengths. Both bands consisted of numerous sharp lines. The emission intensity on the high-energy side decreased with temperature decreasing from RT to 12 K and disappeared below ca. 100 K. The luminescence mechanism is discussed for the 1270 nm and 1450 nm bands.

Organic-inorganic hybrid materials doped with Eu^{3+}, Tb^{3+} rare earth and lithium ions

<u>E. Żelazowska</u>[1], E. Rysiakiewicz-Pasek[2], M. Borczuch-Laczka[3]

[1]*Institute of Ceramics and Building Materials*
Division of Glass and Building Materials in Cracow
Lipowa 3, 30-702 Kraków, Poland

[2]*Institute of Physics, Wroclaw University of Technology*
Wybrzeze Wyspianskiego 27, 50-370 Wrocław, Poland

[3]*Faculty of Materials Science and Ceramics*
AGH University of Science and Technology
Al. Mickiewicza 30, 30-059 Kraków, Poland

Silica-based organic-inorganic hybrid materials doped with terbium, europium (Eu^{3+}, Tb^{3+}) rare earth and lithium ions were produced by the sol-gel method. Tetraethyl orthosilicate (TEOS), poly(methyl methacrylate) (PMMA, M.W. 12 000), ethyl methacrylate, butyl methacrylate, ethyl acetyloacetate, $LaCl_3 \cdot 7H_2O$ and $TbCl_3 \cdot 6H_2O$, $EuCl_3 \cdot 6H_2O$, $LiClO_4$ were used as precursors and dopants, respectively. The materials obtained (ca 40% of organic parts) were aged at room temperature for at least three weeks and dried at the temperature of 125°C. Scanning electron microscopy equipped with energy dispersive X-ray spectroscopy (SEM/EDS, X-ray diffraction (XRD), Fourier transform infrared spectroscopy (FTIR, KBr technique), ^{29}Si MAS Magnetic Nuclear Resonance were used for morphology, composition and structure investigation. The excitation and emission luminescence spectra were recorded at room temperature, using a fluorescence spectrometer equipped with a pulsed xenon lamp as an excitation source. The influence of organic additives on the host material microstructure and the luminescence properties of the hybrid materials obtained was analyzed. All the materials revealed photoluminescence blue-green and red emission lines characteristic of terbium and europium ions.

Synthesis of carbon nanomaterials over Ni/ZMS-5 catalyst

J. Ziebro, B. Skorupińska, G. Kądziołka, B. Michalkiewicz

West Pomeranian University of Technology in Szczecin
Pułaskiego 10, 70-322 Szczecin, Poland

Catalytic chemical vapor deposition (CCVD) of hydrocarbons is a promising method for synthesis of carbon nanomaterials (CNM) such as carbon nanotubes (CNT), carbon nanocapsules (CNC), carbon nanofibers (CNF). The advantages are as follows: low cost, large-scale production, relatively low temperature used in the process.

The aim of the our work was to investigate carbon nanomaterials grown by catalytic decomposition of CH_4. The CNM were synthesized by CCVD using Ni supported on SiO_2 as the catalyst. The carbon deposited in the reaction was analyzed by Raman spectroscopy, thermogravimetric analysis (TGA), scanning electron microscopy (SEM) and transmission electron microscopy (TEM). The effects of the reaction temperature and Ni loading on the CNM formation were evaluated.

The catalyst with a high Ni concentration favored a high yield of CNM at lower temperatures. An increase in the temperature led to an increase in the yield of CNM but a very high temperature was a disadvantage to the carbon production. The kind of CNM was determined by the Ni concentration method and the conditions of synthesis.

Optical and magnetic properties
of ceramic nanoparticles

A. A. Zolotovsky[1], S. P. Kruchinin[2]

[1] *Institute of Semiconductor Physics of the National Academy of Sciences of Ukraine*
45, Prosp. Nauky, Kyiv 03028, Ukraine

[2] *Bogolyubov Institute for Theoretical Physics, NASU*
Kiev 03143, Ukraine

The mechanism of formation of electron pairs in ceramic nanoparticles is studied. The influence of second-order phase transitions in nanoparticles on the optical and magnetic properties are analyzed within the method of multielectron hybrid orbitals.

Translocation of elastic polymers through nanopores

<u>S. Żurek</u>, M. Kośmider, A. Drzewiński

Institute of Physics, University of Zielona Góra
Prof. Szafrana 4a, 65-516 Zielona Góra, Poland

Polymer translocation through a nanopore is a process that can be modeled with the Rubinstein-Duke [1,2] rules for hopping reptons on a lattice. The model provides insights into the chain dynamics, such as the average translocation time as a function of chain length.

An exact approach to the problem [3] requires the evaluation of sparse matrices of enormous sizes (Figure 1) and can be performed efficiently only for short chains (a dozen reptons). However, approximate Monte Carlo methods [4] enable the analysis of long chains and allowed us to perform useful analysis in the time domain. Our previous one-dimensional studies [5,6] showed that the mass-current (in terms of reptons threaded through a nanopore per time) was unsaturated in an extremely strong electric field. In this paper, we explain this discrepancy by examining the impact of chain flexibility on its behavior.
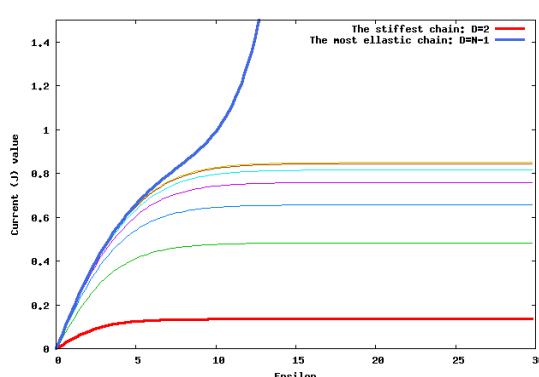
Throughput current as a function of applied bias; chain length is $N = 9$, hernia creation/annihilation rate is 0.5. The plotted data were calculated exactly by solving almost 10^6 linear equations. Infinitely elastic chain leads to a *short-cut* in current behavior
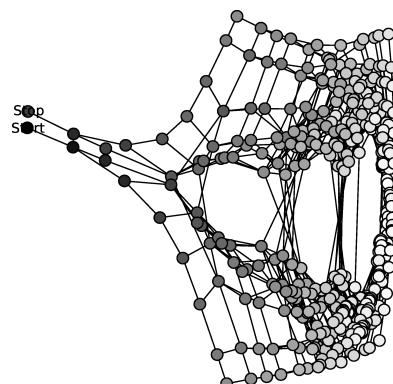
Graph of connections between chain states (the chain has 6 links); each connections represents a transition: there are 2562 transition linking 462 chain configurations in this plot

Figure 1: Exact analysis of chain translocation through a pore requires the evaluation of a stochastic matrix, which holds information on the transitions of chain states; each transition (the connection between two particular states) was assigned a probability rate and was used to evaluate the translocation process in terms of the throughput current

References

[1] M. Rubinstein 1987 *Phys. Rev. Lett.* **59**

[2] T. A. J. Duke 1989 *Phys. Rev. Lett.* **62**

[3] A. Drzewiński, J. M. J. van Leeuwen 2006 *Phys. Rev. E* **73**

[4] A. van Heukelum, G. T. Barkema 2003 *J. Chem. Phys.* **119**

[5] S. Żurek, A. Drzewiński, 2010 *Comp. Methods in Science and Technology* **16**

[6] S. Żurek, A. Drzewińsk, J. M. J. van Leeuwen 2011 *Journal of Statistical Mechanics: Theory and Experiment* **5**

Au/TiO$_2$ as Catalysts of Carbon Dioxide Reduction

G. Kądziołka, A. Morawski, B. Michalkiewicz

Institute of Chemical and Environment Engineering
West Pomeranian University of Technology
Pułaskiego 10, 70-322 Szczecin, Poland

The reduction of carbon dioxide to organic compounds received considerable attention in the last decade. One can find many reports on the reduction of carbon dioxide by chemical, electrochemical and photochemical methods.

We investigated the possibility of applying materials containing gold deposited on TiO$_2$ (P25). The catalysts were prepared by impregnating TiO$_2$ with HAuCl$_4$ 3H$_2$O. The excess solution was removed by evaporation or filtration. The obtained material was dried in air, in the absence or presence of light, respectively.

The process was performed at atmospheric pressure at 30°C. A glass reactor equipped with a lamp emitting UV/VIS radiation at wavelengths of 300–600 nm was used. The reaction was performed in water or in a solution of NaOH in water containing a suspension of catalyst. The catalyst concentration was 0.1 wt. %. Carbon dioxide was supplied periodically or continuously.

Subsequently, the presence of organic groups on the surface of catalysts was examined by FT-IR spectrometry. On the basis of FT-IR spectra, we found the presence of -CH, -CH$_2$, -CH$_3$ groups. The results showed that Au/TiO$_2$ materials are promising as catalysts in the reduction of carbon dioxide to organic compounds. The type and the number of products obtained depended on the preparation method of the catalyst.

INDEX OF AUTHORS